

0061465



NASA CONTRACTOR REPORT



NASA CR-2

LOAN COPY: RETURN TO
AFWL TECHNICAL LIBRARY
KIRTLAND AFB, N. M.

NASA CR-2667

EVALUATION OF STRUCTURAL DESIGN CONCEPTS FOR AN ARROW-WING SUPERSONIC CRUISE AIRCRAFT

I. F. Sakata and G. W. Davis

Prepared by

LOCKHEED-CALIFORNIA COMPANY

Burbank, Calif. 91520

for Langley Research Center

1. Report No. NASA CR-2667		2. Government Accession No.		3. Recipient's Catalog No.	
4. Title and Subtitle EVALUATION OF STRUCTURAL DESIGN CONCEPTS FOR AN ARROW-WING SUPERSONIC CRUISE AIRCRAFT				5. Report Date May 1977	
				6. Performing Organization Code D/75-72	
7. Author(s) I. F. SAKATA AND G. W. DAVIS				8. Performing Organization Report No. LR 27832	
				10. Work Unit No.	
9. Performing Organization Name and Address LOCKHEED-CALIFORNIA COMPANY DIVISION OF LOCKHEED AIRCRAFT CORPORATION BURBANK, CALIFORNIA 91520				11. Contract or Grant No. NAS1-12288	
				13. Type of Report and Period Covered Contract Report	
12. Sponsoring Agency Name and Address NATIONAL AERONAUTICS AND SPACE ADMINISTRATION LANGLEY RESEARCH CENTER HAMPTON, VIRGINIA 23665				14. Sponsoring Agency Code	
15. Supplementary Notes Langley Technical Representative: James C. Robinson Langley Alternate Technical Representative: E. Carson Yates, Jr. Final Report					
16. Abstract An analytical study was performed to determine the best structural approach for design of primary wing and fuselage structure of a Mach 2.7 arrow-wing supersonic cruise aircraft. Concepts were evaluated considering near-term start-of-design. Emphasis was placed on the complex interactions between thermal stress, static aero-elasticity, flutter, fatigue and fail-safe design, static and dynamic loads, and the effects of variations in structural arrangements, concepts and materials on these interactions. Results indicate that a hybrid wing structure incorporating low-profile convex-beaded and honeycomb sandwich surface panels of titanium alloy 6Al-4V were the most efficient. The substructure includes titanium alloy spar caps reinforced with boron-polyimide composites. The fuselage shell consists of hat-stiffened skin and frame construction of titanium alloy 6Al-4V. This report presents a summary of the study effort, and includes a discussion of the overall study logic, design philosophy and interaction between the analytical methods for supersonic cruise aircraft design.					
17. Key Words (Suggested by Author(s)) Design Concepts, Structural Design, Supersonic Airframe Technology, Arrow-Wing Supersonic Cruise Aircraft			18. Distribution Statement Unclassified - Unlimited Subject Category 39		
19. Security Classif. (of this report) Unclassified	20. Security Classif. (of this page) Unclassified	21. No. of Pages 137	22. Price* \$6.00		



0061465

FOREWORD

The following substantiating data report entitled: "Arrow-Wing Supersonic Cruise Aircraft Structural Design Concepts Evaluation," is available as NASA CR-132575, Vol. 1-4.

- Volume 1 - Sections 1 - 6: Structural Design Concepts; Baseline Configuration; Aerodynamics; Structural Design Criteria; Structural Design Loads; Structural Temperatures
- Volume 2 - Sections 7 - 11: Materials and Producibility; Basic Design Parameters; Structural Analysis Models; Vibration and Flutter; Point Design Environment
- Volume 3 - Sections 12 - 14: Structural Concept Analysis; Fatigue and Fail-Safe Analysis; Acoustics
- Volume 4 - Sections 15 - 21: Mass Analysis; Production Costs; Concept Evaluation and Selection; Design; Propulsion-Airframe Integration; Advanced Technology Assessment; Design Methodology.

CONTENTS

	Page
FOREWORD	iii
ILLUSTRATIONS	vii
TABLES	x
LIST OF SYMBOLS AND NOTATIONS	xiii
SUMMARY	1
INTRODUCTION	3
CONFIGURATION	3
Reference Configuration	4
Configuration Refinement	4
Passenger Accommodations	4
Main Landing Gear Concept	4
Propulsion System	4
Low-Speed Longitudinal Characteristics	6
Low-Speed Lift Capabilities	6
Final Configuration	6
DESIGN CRITERIA	9
STRUCTURAL DESIGN CONCEPTS	12
Wing Structure Concepts	12
Fuselage Structure Concepts	15
DESIGN METHODOLOGY	16
Aerodynamic Heating Analysis	16
Finite Element Model Analysis	17
Aeroelastic Loads Analysis	19
Vibration and Flutter Analysis	19
Point Design Analysis	22
DESIGN ENVIRONMENT	25
Mission Performance	25
Design Loads	25
Design Concepts Evaluation Loads	25
Engineering Design-Analysis Loads	27
Design Temperatures	29
Wing Panel Temperatures	29
Fuselage Panel and Frame Temperatures	29
Fuel Tank Temperatures	34
Acoustics	34
Isointensity Contours	34
Sound Pressure Levels	37
DESIGN CONCEPTS EVALUATION	37
Initial Screening Analysis	37
Chordwise-Stiffened Wing Concepts	39
Spanwise-Stiffened Wing Concepts	39
Monocoque Wing Concepts	39
Fuselage Shell Concepts	39
Detail Concept Analyses	42
Strength-Design Analyses	43
Chordwise-Stiffened Wing Arrangement	43
Spanwise-Stiffened Wing Arrangement	46
Monocoque Wing Arrangement	48

CONTENTS (Continued)

	Page
DESIGN CONCEPTS EVALUATION (Continued)	
Composite-Reinforced Chordwise-Stiffened Wing Arrangement	48
Fuselage Shell	54
Stiffness-Design Analyses	56
Vibration Analyses	56
Flutter Analyses	56
Flutter Optimization	63
Cost Analyses	64
Concept Selection	65
Constant Mass Aircraft	67
Constant Payload-Range Aircraft	70
Hybrid Design Concept	70
ENGINEERING DESIGN-ANALYSES	73
Wing Strength Analyses	74
Wing Ultimate and Fatigue Strength Analyses	74
Wing Sonic Fatigue Analyses	74
Wing Fail-Safe Analyses	74
Wing Box Mass	81
Fuselage Strength Analyses	81
Fuselage Ultimate and Fatigue Strength Analyses	83
Fuselage Sonic Fatigue Analyses	85
Fuselage Fail-Safe Analyses	85
Fuselage Shell Mass	85
Flutter Analyses	87
Roll Control Effectiveness	88
FINAL DESIGN AIRPLANE	93
Wing Structure Design	93
Fuselage Structure Design	97
Critical Design Conditions and Requirements	98
Final Design Airplane Mass Estimates	100
CONCLUSIONS	103
RECOMMENDATIONS	105
APPENDIX A - ADVANCED TECHNOLOGY ASSESSMENT	107
APPENDIX B - MACH 2.2 CRUISE SPEED ASSESSMENT	119
APPENDIX C - WING TIP THICKNESS ASSESSMENT	123
REFERENCES	125

ILLUSTRATIONS

Figure		Page
1	Reference Configuration	5
2	Final Airplane Arrangement	7
3	Design Flight Profile - International Mission (Mach 2.62 - Hot Day)	10
4	Structural Design Speeds	10
5	Wing Structure Concepts; (a) Monocoque (Biaxially- Stiffened), (b) Spanwise-Stiffened, (c) Chordwise- Stiffened, (d) Chordwise-Stiffened Composite- Reinforced Concepts	13
6	Fuselage Structural Arrangement - Skin-Stringer and Frame	15
7	Analytical Design Cycle	16
8	Finite-Element Structural Model for Design Concepts Evaluation	18
9	Finite-Element Structural Model for Detail Design- Analysis	18
10	Aerodynamic Influence Coefficient Grids; (a) Subsonic Aerodynamic Grid, (b) Supersonic Aerodynamic Grid	20
11	Load Panel Grid	21
12	Symmetric Degrees-of-Freedom for Vibration Analyses	21
13	Design Regions for Flutter Optimization; (a) Wing Design Regions, (b) Detailed Wing Tip Design Regions	23
14	Point Design Regions; (a) Wing Point Design Regions, (b) Fuselage Point Design Regions	24
15	Mission Segment Data	26
16	Mach Number/Trim Angle-of-Attack Profile	27
17	Design Loading Conditions - Design Concepts Evaluation	28
18	Design Loading Conditions - Engineering Design-Analyses	28
19	External Surface Isotherms - Mach 2.62 (Hot Day) Cruise	30
20	Chordwise-Stiffened Wing Panel Temperature Histories - 40322 Upper Surface	31
21	Chordwise-Stiffened Wing Panel Temperature Histories - 40322 Lower Surface	31
22	Bulk Fuel Temperatures in Wing Tanks	35
23	Near-Field Noise Contours - Reference Turbojet Engine	35
24	Overall Sound Pressure Level	36
25	Mass Trends of the Candidate Surface Panel Concepts - Chordwise-Stiffened Wing Arrangement - Initial Screening	40
26	Mass Trends of the Candidate Surface Panel Concepts - Spanwise-Stiffened Wing Arrangement - Initial Screening	40
27	Mass Trends of the Candidate Surface Panel Concepts - Monocoque Wing Arrangement - Initial Screening	41
28	Optimum Frame Spacing for the Candidate Fuselage Arrangements - Point Design Region FS 2500	41
29	Promising Structural Concepts	43
30	Component Mass for Chordwise-Stiffened Wing Arrangement at Point Design Region 40536	45
31	Optimum Spar Spacing for Chordwise-Stiffened Wing Arrangement	45

ILLUSTRATIONS (Continued)

Figure		Page
32	Component Mass Penalties for a Damaged Spar Cap - Chordwise-Stiffened Arrangement	46
33	Optimum Rib Spacing for Spanwise-Stiffened Wing Arrangement	47
34	Panel-to-Substructure Junction Designs - Monocoque Arrangement	49
35	Optimum Spar Spacing for the Monocoque Wing Mechanically Fastened Densified-Core Design	50
36	Monocoque Panel Damage Configurations	51
37	Mass Comparision of Candidate Composite Materials	52
38	Optimum Spar Spacing for the Composite Reinforced Wing Arrangements (Region 40536)	52
39	Symmetric Flutter Analysis for Chordwise-Stiffened Arrangement - Mach 0.60 - OEM	59
40	Flutter Speeds for Symmetric Bending and Torsion Mode - Chordwise-Stiffened Arrangement	59
41	Flutter Speeds for Symmetric Hump Mode - Chordwise-Stiffened Arrangement	60
42	Flutter Speeds for Symmetric Stability Mode - Chordwise-Stiffened Arrangement	60
43	Symmetric Flutter Analysis-Mach 0.90 - FFFP - Chrodwise-Stiffened Arrangement	61
44	Symmetric Flutter Analysis - Mach 0.90 - FFFP - Spanwise-Stiffened Arrangement	62
45	Symmetric Flutter Analysis - Mach 0.90 - FFFP - Monocoque Arrangement	62
46	Flutter Optimization - Chrodwise-Stiffened Arrangement	64
47	Hybrid Structural Approach	73
48	Fuselage Panel Identification	82
49	Flutter Speeds for Symmetric Bending and Torsion Mode - Strength-Design	89
50	Flutter Speeds for Strength + Stiffness Design	90
51	Design Variables for Mach 0.6 Flutter Optimization	91
52	Mach 1.85 Flutter Optimization (a) Design Variables (b) Surface Panel and Web Thickness	91
53	Mach 1.85 Flutter Optimization Results - Bending and Torsion Mode	92
54	Primary Roll Control Schedule	94
55	Supersonic Roll Power	94
56	Structural Arrangement of Final Design Airplane	95
57	Structural Details for Chordwise-Stiffened Surfaces	96
58	Structural Details for Fuselage Shell	98
59	Critical Design Requirements for the Wing Structure	99
60	Critical Design Conditions	101
61	Composite Material Wing Design Concepts	109
62	Advanced Technology Hybrid Structural Approach - 1990 Start-of-Design (Far-Term)	117

ILLUSTRATIONS (Continued)

Figure		Page
63	Lower Surface Isotherms - Mach 2.16 and 2.62 Hot Day Cruise	120
64	Airframe Mass Trends	121
65	Impact of Wing Tip Thickness Increase on Range	124

TABLES

Table		Page
1	Final Airplane Configuration Data	8
2	Final Engine Data	8
3	Design Loading Conditions Data	29
4	Temperature and Gradients for Fuselage Skin Panels	32
5	Temperature and Gradients for Fuselage Frames	33
6	Wing Panel Load/Temperature Environment - Initial Screening	38
7	Fuselage Panel Load Intensities - Initial Screening	38
8	Mass Trends of the Candidate Fuselage Panel Concepts - Initial Screening	42
9	Fuselage Point Design Environment for Detailed Concept Analysis	44
10	Point Design Mass Penalties for a Damaged Spar Cap - Chordwise-Stiffened Arrangement	47
11	Mass Trends of the Monocoque Wing Designs	50
12	Detailed Wing Box Mass for Beaded Panels with Composite Reinforced Spar Caps	53
13	Hat-Stiffened Fuselage Panel Geometry at FS 2500	55
14	Fuselage Mass Summary for Point Design Regions	55
15	Vibration and Flutter Analyses	57
16	Lower Frequency Symmetric Vibration Modes for the Chordwise-Stiffened Structural Arrangement	58
17	Lower Frequency FFFP Symmetric Vibration Modes for Structural Arrangements	58
18	Total Manhours - Materials and Tooling Costs	66
19	Summary of Production Costs	66
20	Wing Mass for Structural Arrangements	67
21	Fuselage Mass Estimates	68
22	Structural Arrangement Evaluation Data; (a) Constant Mass Aircraft, (b) Constant Payload-Range Aircraft	69
23	Concept Evaluation Summary - Constant Mass Aircraft	71
24	Concept Evaluation Summary - Constant Payload-Range Aircraft	71
25	Evaluation Data for Hybrid Structural Arrangement	72
26	Wing Point Design Environment - Mach 1.25 Symmetric Maneuver - Final Design	75
27	Convex-Beaded Panel Data	76
28	Honeycomb Sandwich Panel Data	76
29	Summary of Wing Spar Cap Data	77
30	Detail Wing Mass for the Hybrid Structural Arrangement	78
31	Summary of Wing Panel Sonic Fatigue Analyses	79
32	Summary of Wing Panel Fail-Safe Analyses	80
33	Wing Box Mass for Point Design Regions	82
34	Fuselage Point Design Environment - Mach 2.7 Start-of-Cruise	83
35	Fuselage Panel Geometry	84
36	Fuselage Panel Mass Data	84
37	Summary of Frame Geometry and Mass	85
38	Summary of Fuselage Sonic Fatigue Analyses	86
39	Summary of Fuselage Fail-Safe Analyses	86

TABLES (Continued)

Table		Page
40	Fuselage Shell Mass at Point Design Regions	87
41	Lower Frequency Symmetric Vibration Modes - Final Design	89
42	Summary of Mass Penalties for Flutter	92
43	Mass Estimate for Final Design Wing	102
44	Mass Estimates for Final Design Fuselage	103
45	Estimated Group Mass Statement for the Final Design Airplane	104
46	Wing Mass Comparision for Composite Designs	111
47	Fuselage Mass Comparison for Composite Designs	113
48	Wing Box Structure Mass Comparison	114
49	Fuselage Shell Structure Mass Comparison	114
50	Airplane Mass and Performance Comparison - Advanced Technology Aircraft	116

LIST OF SYMBOLS AND NOTATIONS

A	area
AR	aspect ratio
BL	buttock line
C	cents
C_r	root chord
C_t	tip chord
D	diameter
DOC	direct operating costs
FS	fuselage station
HR	hour
Hz	Hertz
M	Mach number
MS	margin of safety
N_x, N_y, N_{xy}	normal and shearing forces per unit distance in the middle surface of plate or shell
OASPL	overall sound pressure level
OEM	operating empty mass
R	radius
RT	room temperature
S	honeycomb core cell size, surface area
SM	seat-mile
S_{REF}	wing reference area
S_W	total wing area
T	temperature
$T_{av.}$	average temperature
TH	thermal
TOGM	takeoff gross mass
V	velocity
V_A, V_C, V_D, V_S	design maneuvering speed, design cruise speed, design dive speed, and design stall speed
\bar{V}_H	horizontal tail volume coefficient
\bar{V}_V	vertical tail volume coefficient
W	weight, mass
X	length
X,Y,Z; x,y,z	Cartesian coordinates
a,b	panel dimension between supported edges
b	span, spar spacing, width
b_s	stiffener pitch
\bar{c}, MAC	mean aerodynamic chord
dB	measure of the intensity of pressure fluctuations, decibels
f	stress, natural frequency
h,H	height
n_z	normal load factor ~ g's
t	thickness
\bar{t}	equivalent panel thickness
t_1, t_2	interior and exterior face sheet thickness of honeycomb-core sandwich panels
t_s	skin thickness
w	equivalent unit panel mass
Δ	incremental value(s)

EVALUATION OF STRUCTURAL DESIGN CONCEPTS
FOR AN ARROW-WING
SUPERSONIC CRUISE AIRCRAFT

by
I. F. Sakata and G. W. Davis
LOCKHEED-CALIFORNIA COMPANY

SUMMARY

An analytical study was performed to determine the best structural approach for design of the primary wing and fuselage structure of a Mach 2.7 arrow-wing supersonic cruise aircraft. The study encompassed an in-depth structural design of the NASA-defined baseline configuration, based on the specified design criteria and objectives, and consistent with the premise of near-term start-of-design. In addition, the study identified opportunities for structural mass reduction and resulted in recommendations for needed research and technology.

A spectrum of structural concepts that had been proposed or have found application for supersonic aircraft designs, such as the Anglo-French Concorde supersonic transport, the Mach 3.0-plus Lockheed YF-12 aircraft, and the proposed Lockheed L-2000 and Boeing B-2707 supersonic transports, were evaluated. The evaluation involved systematic multi-disciplinary studies encompassing: airplane configuration refinement (including propulsion-airframe integration); design/manufacturing/cost studies; and the complex interactions between airframe strength and stiffness, static and dynamic loads, flutter, fatigue and fail-safe design, thermal loads, and the effects of variations in structural arrangements, concepts and materials on these interactions. Due to the complex nature of these studies, extensive use was made of computerized analysis programs, including Lockheed-California's integrated NASTRAN-FAMAS structural analysis system.

The structural evaluation was conducted in two phases: (1) a design concept evaluation study wherein a large number of candidate structural concepts were investigated and evaluated to determine the most promising concepts, and (2) a detailed engineering design-analysis study of the selected structural approach to define the critical design parameters and the estimated structural mass of the final design airplane.

The results of the design concept evaluation indicated that a hybrid design using a combination of a primarily chordwise-stiffened wing structure arrangement, with a biaxially stiffened (monocoque) arrangement for the wing tip to satisfy flutter requirements, would be the most efficient from a mass and cost standpoint. The wing tip construction selected was aluminum-brazed titanium honeycomb-sandwich. For the remainder of the wing, low-profile convex-beaded surface panels of titanium alloy 6Al-4V were used, supported with discrete submerged spanwise titanium spar caps reinforced with boron-polyimide composite material. The fuselage was a Ti-6Al-4V hat-stiffened design with supporting frames.

The resultant final design airplane satisfies all the design objectives, including payload, service life and range, and meets or exceeds the commercial aircraft requirements of Federal Aviation Regulation, Part 25 (FAR 25). The wing structure was designed by a combination of strength, stiffness and minimum gage (foreign object damage) requirements, with no significant impact from the Mach 2.7 temperature environment. The fuselage structure was designed by a combination of strength and fatigue, including cabin pressurization and elevated temperature effects.

The study makes clear the importance of including realistic consideration of aeroelastic effects early in the design cycle for this type of aircraft. Significant structure, over and above that required for strength, was added in selected areas to remove flutter deficiencies. In addition, the potential of computer-aided design methods for reducing the manpower and design calendar time was amply demonstrated. Finally, the study described above and related supplementary investigations identified a major potential for structural mass reduction through the development and application of high temperature composite materials; and the need for further improvement of aerodynamic performance through the use of active control devices and other configuration development.

INTRODUCTION

For the past several years, the National Aeronautics and Space Administration (NASA) Langley Research Center has been pursuing a supersonic cruise aircraft research program to provide sound technical bases for future civil and military supersonic vehicles, including possible development of an environmentally acceptable and economically viable commercial supersonic transport.

The design of a satisfactory advanced supersonic cruise aircraft requires reduced structural mass fractions attainable through application of new materials and concepts, and advanced design tools. Configurations, such as the arrow-wing, show promise from the aerodynamic standpoint; however, detailed structural design studies are needed to determine the feasibility of constructing this type of aircraft with sufficiently low structural mass.

The investigation now being reported was conducted to subject promising structural concepts to in-depth analyses, including the more important environmental considerations that could affect the selection of the best structural approach for design of primary wing and fuselage structure of a given Mach 2.7 arrow-wing supersonic cruise aircraft, assuming a near-term start-of-design.

A spectrum of structural concepts were evaluated. The evaluation involved systematic multi-disciplinary studies encompassing: airplane configuration refinement, design/manufacturing/cost studies, and a structural evaluation involving the complex interactions between airframe strength and stiffness, static and dynamic loads, flutter, fatigue and fail-safe design, thermal loads, and the effects of variations in structural arrangements, concepts and materials on these interactions. The structural evaluation was conducted in two phases: (1) a design concept evaluation study wherein a large number of candidate structural concepts were investigated and evaluated to determine the most promising concepts, and (2) a detailed engineering design-analysis study of the selected structural approach to define the critical design parameters and the estimated structural mass of the final design airplane.

This report summarizes the study made by the Lockheed-California Company and discusses the design methodology and results. Detail descriptions of the analyses and substantiation of the results are presented in Reference 1. (An executive summary of the study was presented in Reference 2; and a summary of the producibility technology studies was presented in Reference 3.)

CONFIGURATION

The initial task was the evaluation and refinement of the reference aircraft configuration in terms of aerodynamic performance and design.

Reference Configuration

The reference configuration shown in Figure 1 is a discrete wing-body airplane with a low wing that is continuous under the fuselage and was derived from the NASA SCAT 15F configuration. The external shape of the airplane was defined at the design lift coefficient by a computer card deck supplied by NASA. As noted in the figure, the configuration is based on the use of four underwing turbojet engines, a horizontal tail volume coefficient of 0.055, and a wing tip sweep angle of 64.6-degrees (1.13-rad). The airplane incorporates vertical fins on the wing, but does not include a canard or inboard leading-edge devices. Pitch control and trim is provided by the horizontal tail.

Configuration Refinement

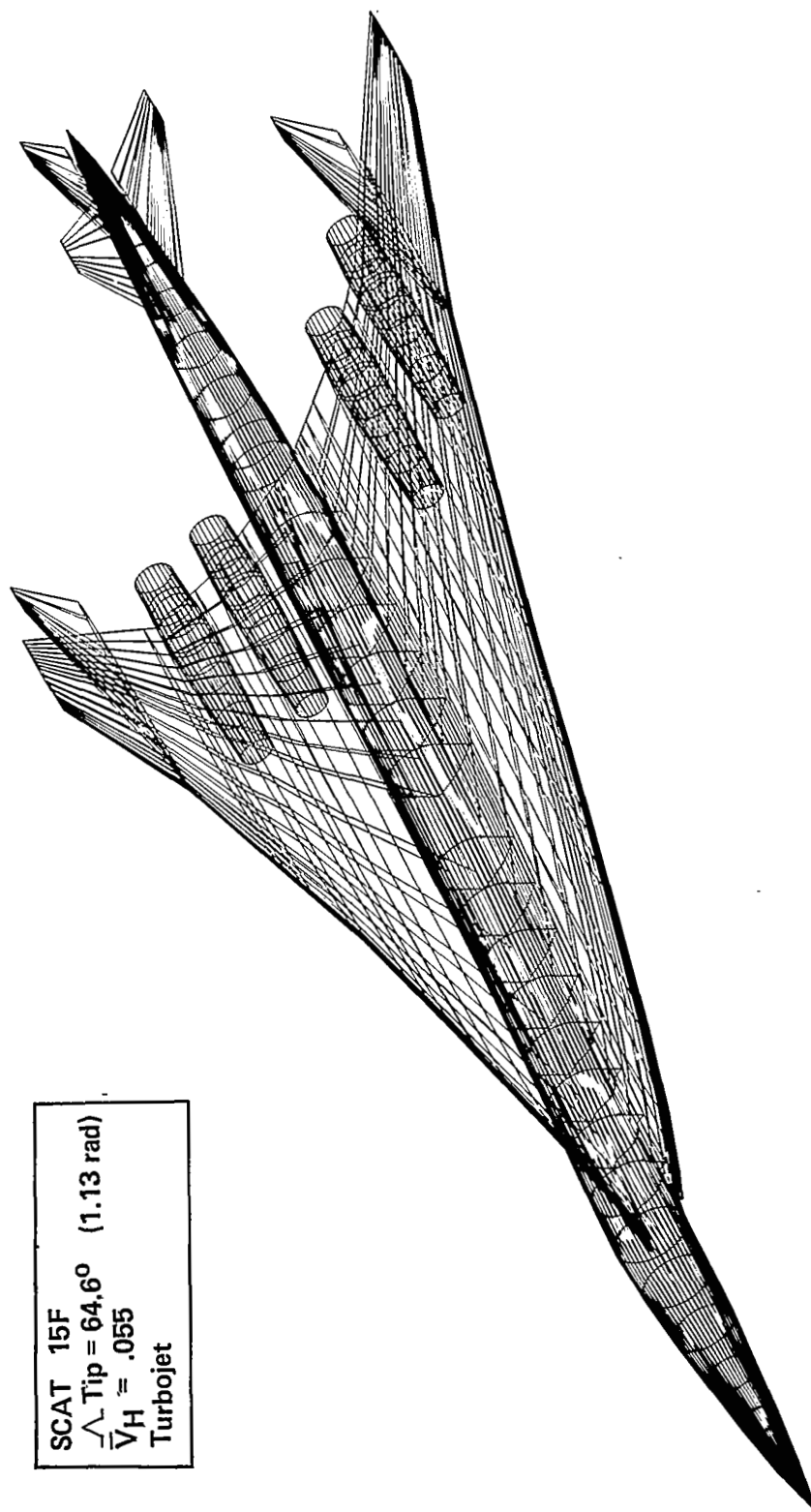
Several areas of concern were identified with regard to the reference configuration, and refinements to these areas were examined and appropriate changes incorporated into the design.

Passenger Accommodations.- Fuselage cross-section requirements were examined in light of the need to provide suitable passenger accommodations in terms of comfort, baggage storage, cargo and passenger services. From a passenger comfort standpoint, it was necessary to provide head room and to have a cabin width which would allow for wide seats and sufficient aisle widths. Below-the-floor volume was needed for cargo and baggage. At the same time, efficient use of the fuselage volume was needed in order to minimize the cross-sectional area and the associated cruise drag penalty. These objectives were met by increasing the fuselage depth using interior dimension standards established in earlier studies of the National SST Program. The pressure shell radius remained essentially unchanged from the reference configuration. A decrement in airplane lift-to-drag ratio equal to 0.10 resulted from this modification.

Main Landing Gear Concept.- A main landing gear concept was adopted which avoided the necessity for deviations from the NASA-supplied external contour. The gear is wing-stowed, forward retracting and has twelve tires per strut. The concept does not require a hump in the upper surface, thus avoiding a drag penalty and minimizing the complexity and mass of the wing structure.

Propulsion System.- The engine characteristics selected were based on the results of a parallel NASA-funded systems study (Reference 4). The selected engine is a duct-burning turbofan with an uninstalled sea level static thrust of 89,500-lbf (398,000-N). The engine is used with an axisymmetric mixed compression inlet and a variable convergent-divergent nozzle.

An engine-airframe integration study was made to explore the effects of engine size and location. This study revealed that the primary constraint on both increasing engine size, and spanwise movement of the engines, was the available wing trailing edge control surface of the arrow-wing configuration. At the same time, the inconclusive projected benefits of moving the engines forward led to retaining their original location with the exhaust 100-in (2.54-m) aft of the wing trailing edge. An inlet fence was required to prevent engine unstart due to mutual interference.



SCAT 15F
 \angle Tip = 64.6° (1.13 rad)
 $V_H \approx .055$
 Turbojet

Figure 1. Reference Configuration

Low-Speed Longitudinal Characteristics.- The low-speed pitch-up characteristics of the arrow-wing were examined using an interactive computer graphics technique that simulates, in real-time, the longitudinal behavior of the airplane response to control disturbances. The feasibility of using the horizontal tail as a pitch limiter to provide satisfactory longitudinal control while operating into the pitch-up region was investigated. Findings showed that if adequate control authority was provided, it was possible to provide automatic pitch limiting capability and good handling qualities. However, two requirements must be met: (1) a definite tail size to center-of-gravity relationship must be maintained, and (2) the pitch limiter system must be fail-operative. On the basis of these considerations, a tail volume coefficient of 0.07 is the minimum that would yield an acceptable center-of-gravity range; in conjunction, the airplane balance should be set so that the center-of-gravity is at 55-percent MAC at the maximum landing mass.

Low-Speed Lift Capabilities.- Configuration development studies explored application of leading and trailing edge devices with auxiliary trimming surfaces (canards and horizontal tail) to provide schemes for supplementing the low-speed lift capabilities of the arrow-wing planform. The objective was to maximize the usable lift at take-off attitudes considering in-ground effects. Methods of low-speed pitch stability improvement were also studied. This involved airplane balance, including the fuel system and its related tankage arrangement. On the final configuration a change in wing tip sweep from 64.6-degrees (1.13-rad) as defined by the NASA-supplied data to a 60-degree (1.05-rad) sweep was made. This change reduced the demands on the longitudinal stability augmentation system and permitted a more aft center-of-gravity location with the existing horizontal tail power.

Final Configuration

The final airplane arrangement is shown on Figure 2. Geometric characteristics are presented in Table 1. The airplane has a design gross mass of 750,000-lbm (340,000-kg). The fuselage accommodates 234 passengers in five-abreast seating. The overall length is 296.9-ft (90.5-m). This includes a 119-in (3.02-m) shortening of the fuselage to compensate for the structural mass increase associated with increasing the fuselage depth. The wing span is 132.6-ft (40.4-m). The leading edge sweep of the wing tip has been decreased to 60-degrees (1.05-rad). The wing-mounted main landing gear employs a three-wheel axle design and retracts into a well just outboard of the fuselage. The length of the gear strut has been increased 19-in (0.48-m) to accommodate the larger diameter of the selected engines.

The aircraft is equipped with a three-axis stability augmentation system (SAS) with adequate redundancy to be fail-operative. The primary control surfaces are indicated on Figure 2. An all-moving horizontal stabilizer with a geared elevator is used for pitch control. For yaw control, a fuselage mounted all-moving vertical tail with a geared rudder is provided. The tail volume coefficients for the horizontal stabilizer (\bar{V}_H) and the vertical tail (\bar{V}_V) are 0.07 and 0.024, respectively. The inboard wing flaps are used as lift devices at low speed. Leading edge flaps are provided on the outer wing for subsonic and transonic speeds, and ailerons on the trailing edge for low speed. At supersonic speeds, the inverted spoiler-slot deflector and spoiler-slot deflectors provide the primary roll control.

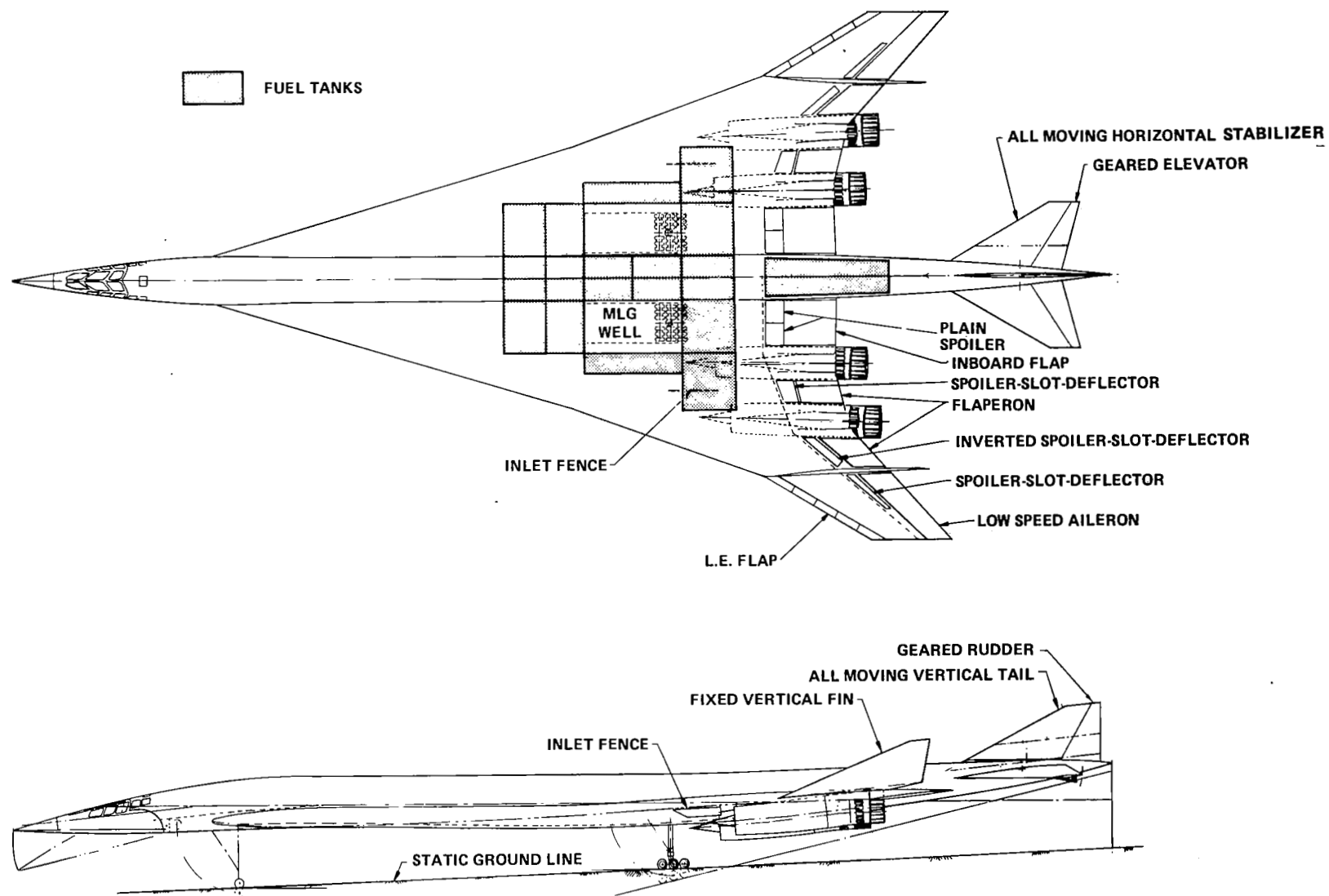


Figure 2. Final Airplane Arrangement

TABLE 1. FINAL AIRPLANE CONFIGURATION DATA

WING		
TOTAL AREA (S_W)	10923 ft ²	1014.69 m ²
REFERENCE AREA (S_{REF})	10500 ft ²	975.45 m ²
ASPECT RATIO (AR)	1.607	
TAPER RATIO (λ)	0.1135	
SPAN (b)	1590.0 in	40.386 m
ROOT CHORD (C_r)	2195.5 in	55.766 m
TIP CHORD (C_t)	249.2 in	6.330 m
MEAN AERODYNAMIC CHORD (C)	1351.1 in	34.317 m
L.E. SWEEP (Λ_{LE})		
(TO BL 391.2)	74 deg	1.292 rad
(TO BL 600)	70.84 deg	1.236 rad
(TO TIP)	60 deg	1.047 rad
FUSELAGE		
LENGTH	3444.0 in	87.5 m
WIDTH	135.0 in	3.4 m
DEPTH	166.0 in	4.2 m

TABLE 2. FINAL ENGINE DATA

ENGINE			BSTF 2.7-2 DUCT-BURNING TURBOFAN	
NUMBER OF ENGINES			4	
NOISE SUPPRESSION CRITERIA			FAR 36-5	
INLET/NOZZLE			AXISYMMETRIC/VARIABLE CONVERGENT - DIVERGENT	
LIFT-OFF SPEED			MACH 0.30	
THRUST/WEIGHT RATIO			0.36	
BYPASS RATIO			3.26	
FAN PRESSURE RATIO			3.0	
NET THRUST (a)	lbf (N)		89,500	(398,000)
ENGINE MASS (b)	lbm (kg)		12,781	(5,797)
CAPTURE AREA	ft ² (m ²)		38.0	(3.53)
MAX. DIAMETER	in (m)		96.4	(2.45)
COMPRESSOR DIAMETER	in (m)		85.0	(2.16)
NOZZLE DIAMETER	in (m)		96.4	(2.45)
ENGINE LENGTH	in (m)		267.5	(6.79)
INLET LENGTH	in (m)		203.9	(5.18)

- (a) SEA LEVEL STATIC, MAXIMUM POWER, UNINSTALLED
 (b) INCLUDES REVERSER AND SUPPRESSOR

Four duct-burning turbofan engines, each with 89,500-lbf (398,000-N) of uninstalled thrust, are mounted in under-wing pods having axisymmetric inlets and thrust reversers aft of the wing trailing edge. Engine configuration data are presented in Table 2. The engines are sized to provide a total thrust-to-airplane weight ratio of 0.36 at takeoff. The engine mounts are located aft of the wing rear beam and are attached to box beams which are cantilevered off the wing structural box.

The major portion of the lower fuselage is used for fuel and baggage stowage, with baggage and other requirements establishing the forward limit of fuel stowage. Forward of the fuel stowage area, the wing does not extend through the fuselage.

The tank arrangement shown in Figure 2 provides for a fuel storage capacity of 393,600-lbm (178,500-kg). Based on previous studies relating to fuel containment and management requirements for supersonic cruise aircraft, it was elected to stow a significant portion of the total fuel within the wing center section. The 16-tank system was designed to take advantage of the "protected-volume" of approximately 43-percent of the total storage capacity. In this location, the upper surface was exposed to the cooled and controlled environment of the fuselage cabin while the wing lower surface was shielded from the outside airstream by a fairing extending below and separated from the lower surface.

Fuel management scheduling for airplane center-of-gravity control was specifically planned to maximize the available heat sink capacity of the fuel by emptying the exposed outboard tanks as early as possible in the flight. Additional considerations included fuel usage to permit the aircraft to cruise with a minimum trim drag penalty. The landing and reserve fuel was located in the protected fuselage area.

DESIGN CRITERIA

Evaluation of structural concepts for the Mach 2.7 supersonic cruise aircraft was based on an aircraft with an economic life of 15 years and a service life of 50,000 flight hours, with the environment determined from a design flight profile for an international mission. The international mission (Figure 3) is approximately 3.4 hours in duration; three-quarters of that time, or 2.5 hours, is at Mach 2.62 (Hot Day) cruise.

For design purposes, a maximum taxi mass of 750,000-lbm (340,000-kg), a maximum landing mass of 420,000-lbm (190,000-kg), a payload of 49,000-lbm (22,000-kg), and a design range of 4200-nmi (7800-km) were specified for the airplane.

The design equivalent airspeeds shown in Figure 4 were selected to provide an operational envelope compatible with the design flight profile and satisfying the requirements of FAR 25. The structural design cruise speed (V_C) was selected as the planned operating speed in climb, cruise and descent. The design dive speed (V_D) was selected to provide a margin of safety for the inadvertent large excursions in excess of operating speed.

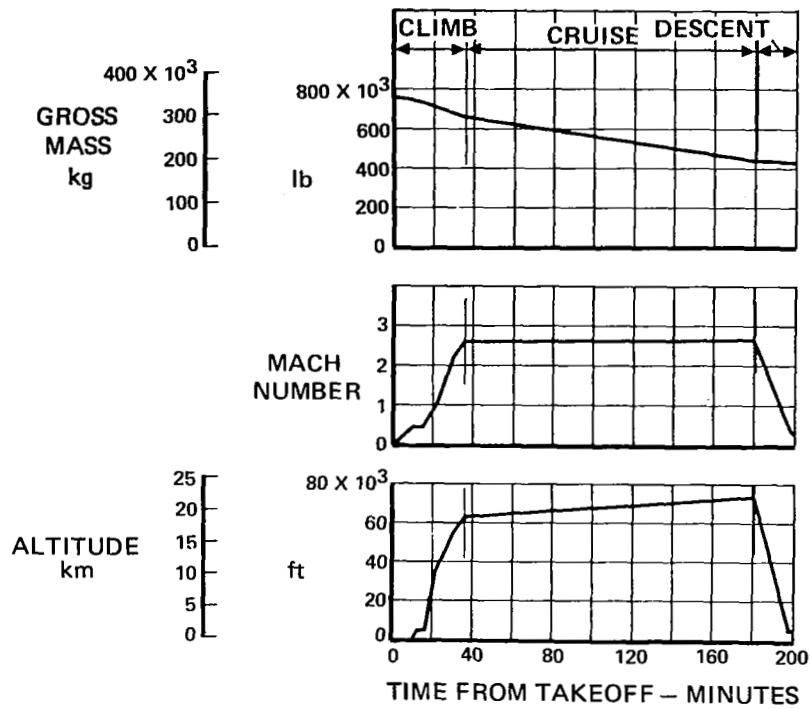


Figure 3. Design Flight Profile - International Mission
(Mach 2.62 - Hot Day)

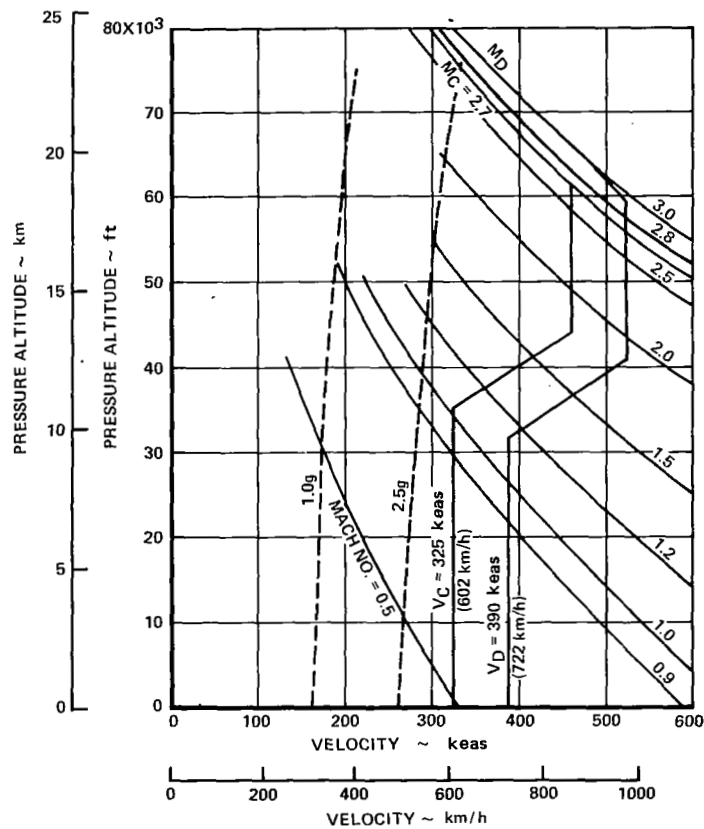


Figure 4. Structural Design Speeds

Maneuver loads analyses were based on solution of the airplane equations of motion for pilot-induced maneuvers. Except where limited by a maximum usable normal force coefficient or by available longitudinal controls deflections, the limit load factors (n_z) were as follows:

- (1) Positive maneuvers: $n_z = +2.5$ at all design speeds
- (2) Negative maneuvers: $n_z = -1.0$ up to V_C and varies linearly to zero at V_D
- (3) Rolling maneuver entry load factors:
 - Upper limit: $n_z = +1.67$ at all design speeds
 - Lower limit: $n_z = 0$ up to V_C and varies linearly up to $+1.0$ at V_D

Design cabin pressures were based on providing a 6000-ft (1.8-km) cabin altitude at a flight altitude of 70,000-ft (21.3-km). This resulted in a maximum design differential pressure of 11.7-psi (80.7-kPa) when accounting for anticipated variations and valve tolerances. A nominal differential pressure of 11.2-psi (77.2-kPa) was used for fatigue design considerations; and a maximum differential pressure of 11.6-psi (80-kPa) was used for fail-safe design.

Strength analyses were based on applied loads which included aerodynamic and inertia loadings, thermal loads and pressurization, and allowable material strengths at the predicted structural temperatures. Limit applied tension stresses were not allowed to exceed the lower of the material yield strength or two-thirds of the material ultimate strength at the appropriate temperature. Limit compressive and shear stresses were defined as the critical buckling stresses.

Fatigue analyses were based on a fatigue loading spectrum developed for the National SST Program (Reference 5) which provides a moderately conservative representation of a loading history for supersonic cruise aircraft. The reference load levels and oscillatory flight loads included representative tensile thermal stress increments and ground loadings. The basic fatigue criterion was to provide a structure with a service life of 50,000 flight hours. Appropriate multiplying factors were applied to the design life for use in establishing allowable design tension stresses. For structure designed by the spectrum loadings, the allowable stresses were defined using a factor of 2 times the design service life of 50,000 hours. For areas of the fuselage designed by constant amplitude cabin pressure loading, the allowable stresses were based on 200,000 flight hours of service (50,000 x 4).

A fail-safe design load of 100-percent limit load was used for the analysis of the assumed damage conditions. The residual strength of the damaged structure must be capable of withstanding these limit loads without failure.

The selection of minimum gages for regions not designed to specific strength or fatigue requirements was based on consideration of the structural concept employed, fabrication constraints, and foreign object damage (FOD) effects.

STRUCTURAL DESIGN CONCEPTS

A spectrum of structural approaches for primary structure design that have found application or had been proposed for supersonic aircraft, such as the Anglo-French Concorde supersonic transport, the Mach 3.0-plus Lockheed YF-12, and the proposed Lockheed L-2000 and Boeing B-2707 supersonic transports, were systematically evaluated for the given configuration and design criteria.

Design and manufacturing concepts studies established feasibility of the application of advanced manufacturing techniques to large-scale production. Basic design parameters and design guidelines were established for each structural arrangement and concept to provide consistency between manufacturing design studies and analyses. These studies examined the fabrication feasibility down to the smallest subcomponent level, and involved the design of structural concepts that represented both structural efficiency and applicability to advanced fabrication techniques.

Candidate materials included both metallic and composite material systems. Alpha-Beta (Ti-6Al-4V) and Beta (Beta C) titanium alloys, both annealed and solution treated and aged, were evaluated to identify the important characteristics for minimum mass designs as constrained by the specified structural approach and life requirements.

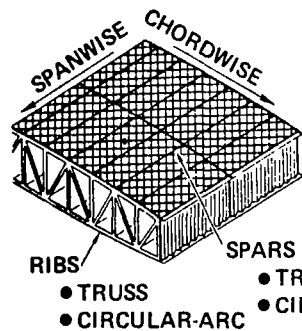
The composite materials considered included both organic (graphite-polyimide, boron-polyimide) and metallic (boron-aluminum) matrix systems. Selective reinforcement of the basic metallic structure was considered as the appropriate level of composite application for the near-term design. Furthermore, based on the principle of maximum return for minimum cost and risk, the application was primarily unidirectional reinforcing of members carrying primary axial loads, such as stringers, spar caps, rib caps and stiffeners of wing panel designs.

Wing Structure Concepts

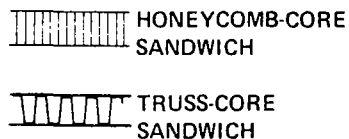
The structural design concepts for the wing primary load-carrying structure are shown in Figure 5.

Monocoque construction (Figure 5a) consists of biaxially-stiffened panels which support the principal loads in both the span and chord directions. The substructure arrangement consists of both multirib and multispar designs.

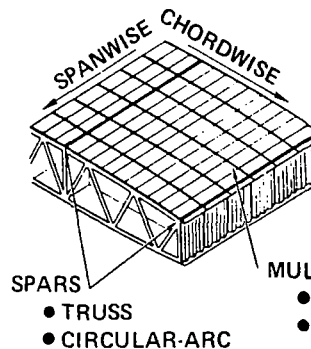
The monocoque construction has a smooth skin that results in minimum aerodynamic drag. However, thermal stresses are absorbed by the primary structural elements with minimal relief. Biaxial loading results in reduced fatigue allowables; yet criticality of other design parameters often controls minimum mass structural designs.



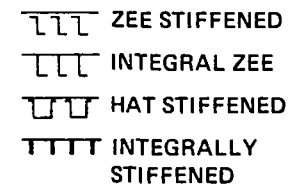
PANEL STRUCTURAL CONCEPTS



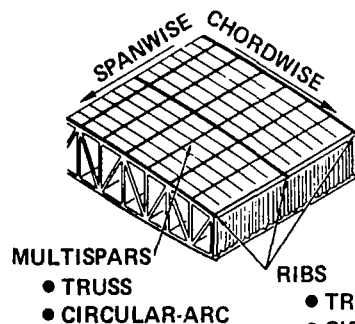
(A) MONOCOQUE (BIAXIALLY-STIFFENED)



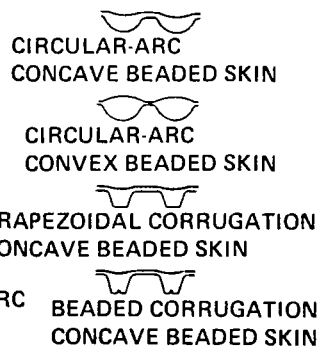
PANEL STRUCTURAL CONCEPTS



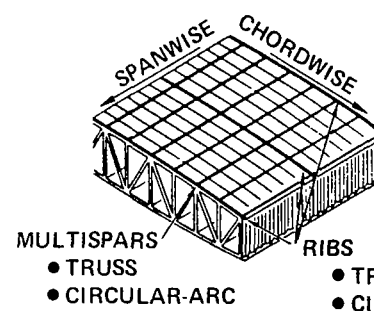
(B) SPANWISE-STIFFENED



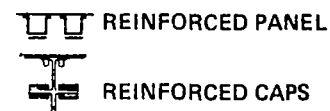
PANEL STRUCTURAL CONCEPTS



(C) CHORDWISE-STIFFENED



STRUCTURAL CONCEPTS



(D) CHORDWISE-STIFFENED COMPOSITE REINFORCED CONCEPTS

Figure 5. Wing Structure Concepts

The biaxially-stiffened panels considered were the honeycomb core and the truss-core sandwich concepts. The honeycomb core panels were assumed to be aluminum brazed (Aeronca process); both diffusion-bonded and welded (spot and EB) joining process were assumed for the truss-core sandwich panel configuration.

In the monocoque concepts, as well as in all the other primary structure concepts, circular-arc (sine-wave) corrugated webs were used at the tank closures. Truss-type webs were used for all other areas. The caps of the spars and ribs are inplane with the surface panels for the monocoque concepts to minimize the effect of eccentricities.

The two types of semimonocoque concepts are: (1) panels supporting loads in the spanwise direction (Figure 5b), and (2) panels supporting loads in the chordwise direction (Figure 5c). Both have the same type of rib and spar webs as the monocoque structure. Discrete spar and rib caps are provided for the semimonocoque concepts since the panels cannot support biaxial loads. Either the spar cap or rib cap must have sufficient area to support inplane loads acting normal to the panel stiffeners.

The spanwise-stiffened wing concept is essentially a multirib design with closely spaced ribs and widely spaced spars. The surface panel configurations shown in the figure have effective load-carrying capability in their stiffened direction. Smooth skins are required for aerodynamic performance.

The chordwise-stiffened arrangement is essentially a multispar structure with widely spaced ribs. Submerged spar caps are provided except at panel closeouts and at fuel tank bulkheads. The submerged caps afford reduced temperatures and increased allowable stresses (strength and fatigue). The surface panel concepts for this arrangement have stiffening elements oriented in the chordwise direction. Structurally efficient beaded-skin designs were explored. These efficient circular-arc sections of sheet metal construction provide effective designs when properly oriented in the airstream to provide acceptable performance, as demonstrated on the Lockheed YF-12 aircraft. The shallow depressions or protrusions provide smooth displacements under thermally induced strains and operational loads and offer significant improvement in fatigue life. Panel spanwise thermal stresses are minimized by allowing thermal deformation in the spanwise direction.

Selective reinforcement of the basic metallic structure (Figure 5d) was considered as the appropriate level of composite application for the near-term design. The chordwise-stiffened arrangement described above provides the basic approach offering the maximum mass saving potential and was used for the exploration of composite reinforcing. The many unique design features of the chordwise-stiffened arrangement are retained. In addition to the surface panels, structurally efficient, multielement (failsafe) composite reinforced spar cap designs are employed to transmit the spanwise bending moments as concentrated axial loads with minimum mass.

Fuselage Structure Concepts

The structural design concepts initially considered for fuselage design included both sandwich shell construction and skin-stringer and frame shell construction.

The sandwich shell design was thought to have a potential for mass savings over the more conventional skin-stringer and frame design, with specific advantages with regard to sonic-fatigue resistance and reduced sound and heat transmission. Preliminary structural design and analyses were conducted to assess the potential mass savings benefit and manufacturing/design feasibility of a sandwich shell. The manufacturing complexity and the parasitic mass which the sandwich must carry, in terms of core and bonding agents, proved to be a disadvantage, and thus this concept was not included as part of the study.

The basic structural arrangement for the design is a uniaxially stiffened structure of skin and stringers with closely spaced supporting frames (Figure 6). The stringer configurations with the potential of achieving minimum mass were the zee-stiffener and the open- and closed-hat stiffener sections. These stiffener concepts all contain flat elements which are amenable to composite reinforcing. Supporting frames that merited consideration were both the fixed and floating type. The joining methods evaluated for this arrangement include mechanical fastening, welding and bonding.

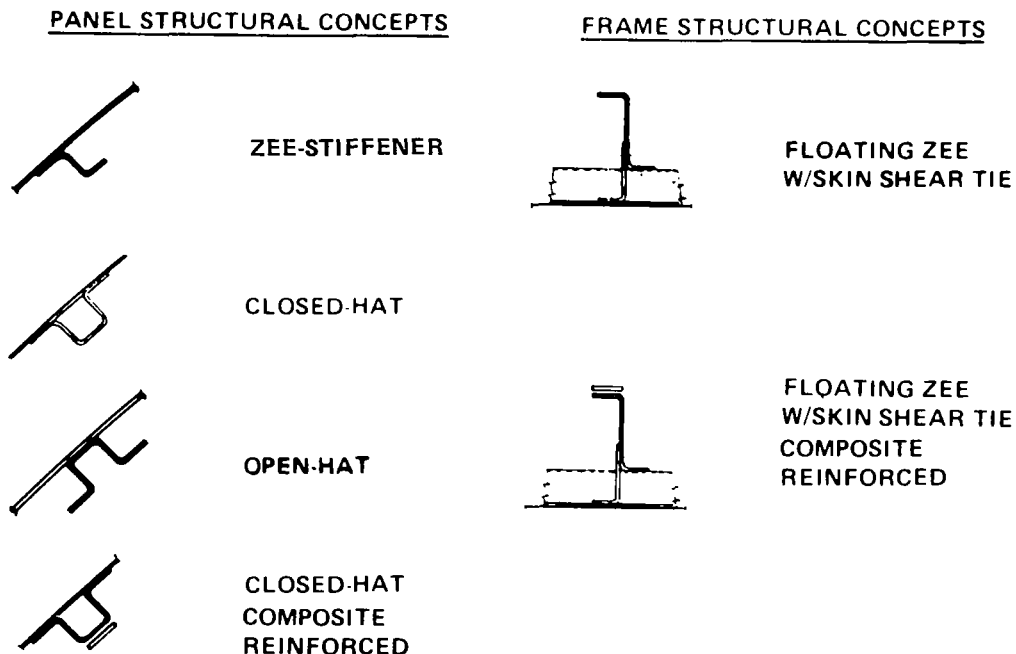


Figure 6. Fuselage Structural Arrangement -
Skin-Stringer and Frame

DESIGN METHODOLOGY

A systematic multidisciplinary design-analysis process was used for the structural evaluation. The corresponding analytical design cycle is illustrated in Figure 7. The evaluation encompassed in-depth studies involving the interactions between airframe strength and stiffness, static and dynamic loads, flutter, fatigue and fail-safe design, thermal loads, and the effects of variations in structural arrangement, concepts and materials on these interactions. Due to the complex nature of these studies, extensive use was made of computerized analysis programs, including the Lockheed-California Company's integrated NASTRAN-FAMAS structural analysis system. The system incorporates the Lockheed-California Company modified version of the NASTRAN finite element analysis program, and the Company's FAMAS program system for aeroelastic loads and flutter analysis.

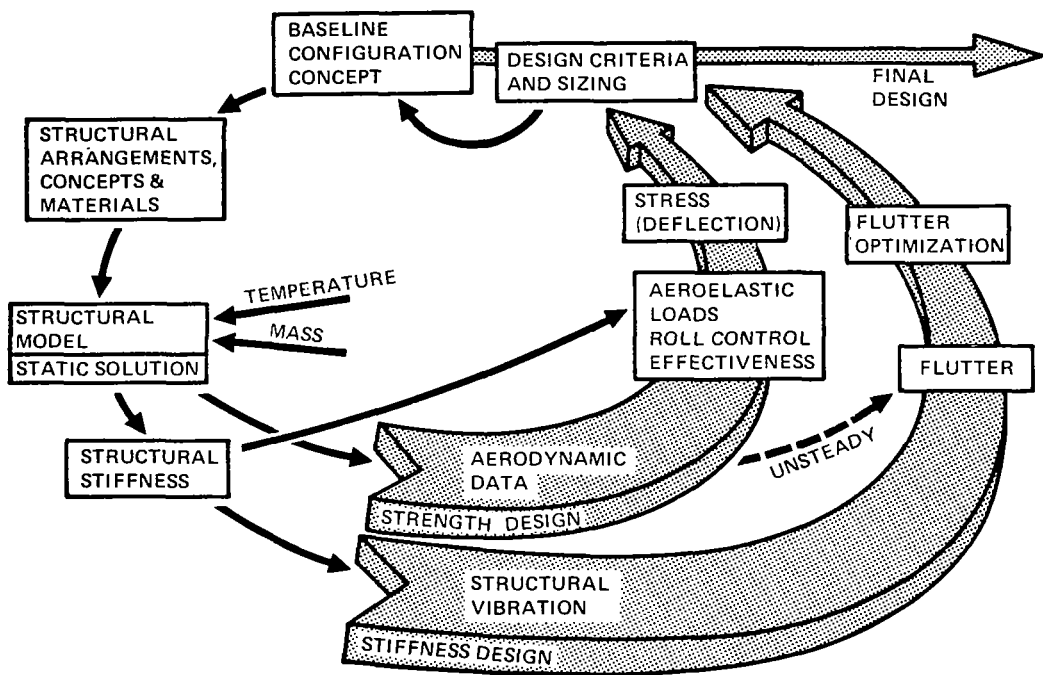


Figure 7. Analytical Design Cycle

Aerodynamic Heating Analysis

Local flow pressures, temperatures and velocities for all locations examined on the airplane external surface were calculated using the equations of compressible flow theory presented in Reference 6. Freestream air properties were based on the United States Standard (1962) Atmosphere tables (Reference 7). The "hot day" condition for these analyses was defined as an ambient temperature 8K above standard day temperature.

Heat transfer to the interior structure was determined using Lockheed's thermal analyzer program. Wing-structure temperatures were calculated using network models of the wing box, including representation of the upper and lower surface panels and the vertical webs. Heat transfer within the wing box included conduction, radiation, and convection to boundary layer air when leakage was a factor; and for fuel tank areas, convection to fuel and fuel vapor. The fuselage-structure temperatures were calculated using a network model of the fuselage shell, including the skin, frame, insulation and inner cabin wall. Heat transfer to the frame included conduction and radiation from the outer skin panels, and conduction from the surrounding insulation. Boundary conditions at the inner cabin wall included convection to the cabin air and radiation to the cabin interior.

Finite Element Model Analysis

A series of NASTRAN finite element structural analysis models were employed. These models were used to provide internal loads and displacements for stress analysis, to calculate structural influence coefficients (SIC's) for aeroelastic load and deflection analyses, and to determine reduced-order stiffness and mass matrices and compute vibration modes for flutter analyses.

Three simplified finite element models were developed for the initial design concepts evaluation. The three models represented the three general wing primary load-carrying structural arrangements: chordwise-stiffened, spanwise-stiffened, and biaxially-stiffened (monocoque). The modeling approach used for these models is illustrated in Figure 8. This modeling approach was used to provide a relatively rapid, cost-effective means for evaluating the effects of out-of-plane primary wing structure design loads on the various wing concepts and arrangements. In defining the models, the wing was represented as a structure symmetrical about the wing mid-plane, and the fuselage was represented as a simple beam with springs approximating the fuselage frame flexibility effects on the wing.

A more detailed, three-dimensional finite element model (Figure 9) was developed for the detail design of the final design airplane. In this model, the complete wing structure was represented directly, i.e., the upper and lower wing surfaces were modeled separately, and the actual camber and twist were included; in addition, flexible control surface actuators were incorporated. The fuselage was also represented directly as a symmetrical fuselage shell structure.

A total of 274 generalized coordinates were defined on the structural model for calculating the structural influence coefficient (SIC) matrices and the structural stiffness matrices. The SIC's were used directly to calculate the aeroelastic loads. The stiffness matrices, after being further reduced to 188 degrees-of-freedom (symmetric) or 178 degrees-of-freedom (anti-symmetric), were used for vibration and flutter analyses.

The 274 generalized coordinates were primarily associated with the vertical displacement; degrees-of-freedom for both the symmetric and anti-symmetric boundary conditions. However, lateral displacements of the wing

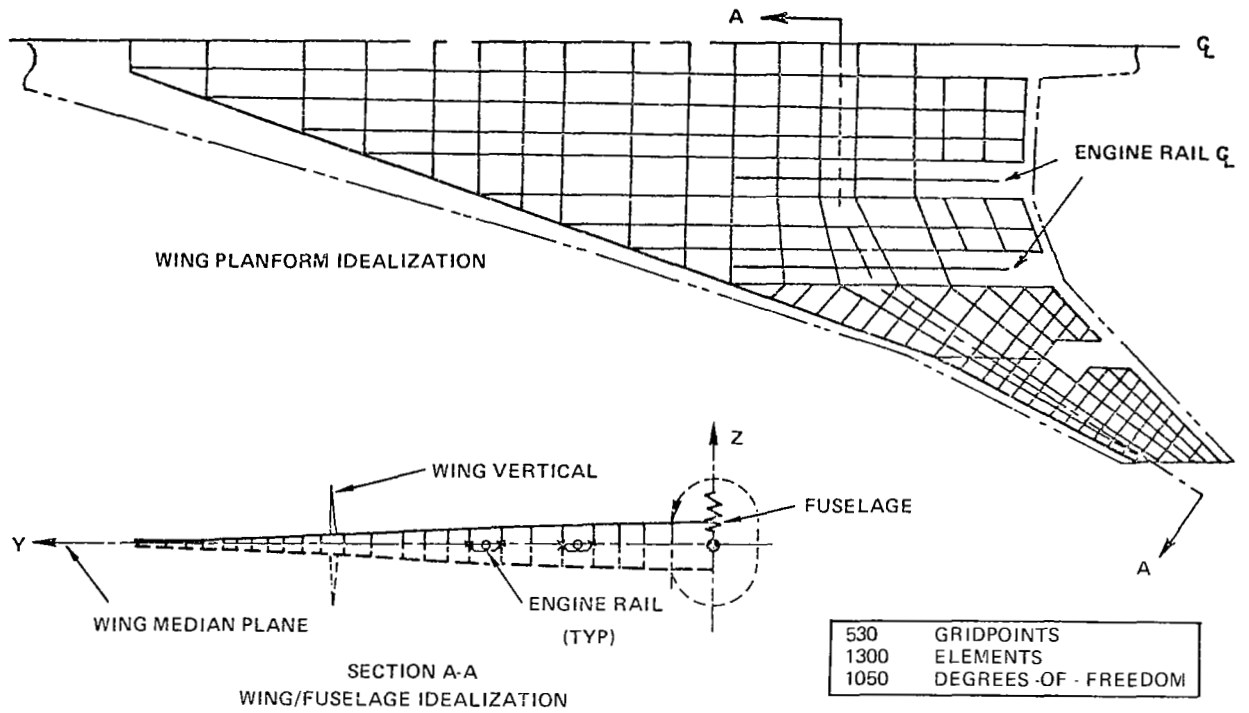


Figure 8. Finite Element Structural Model for Design Concept Evaluation

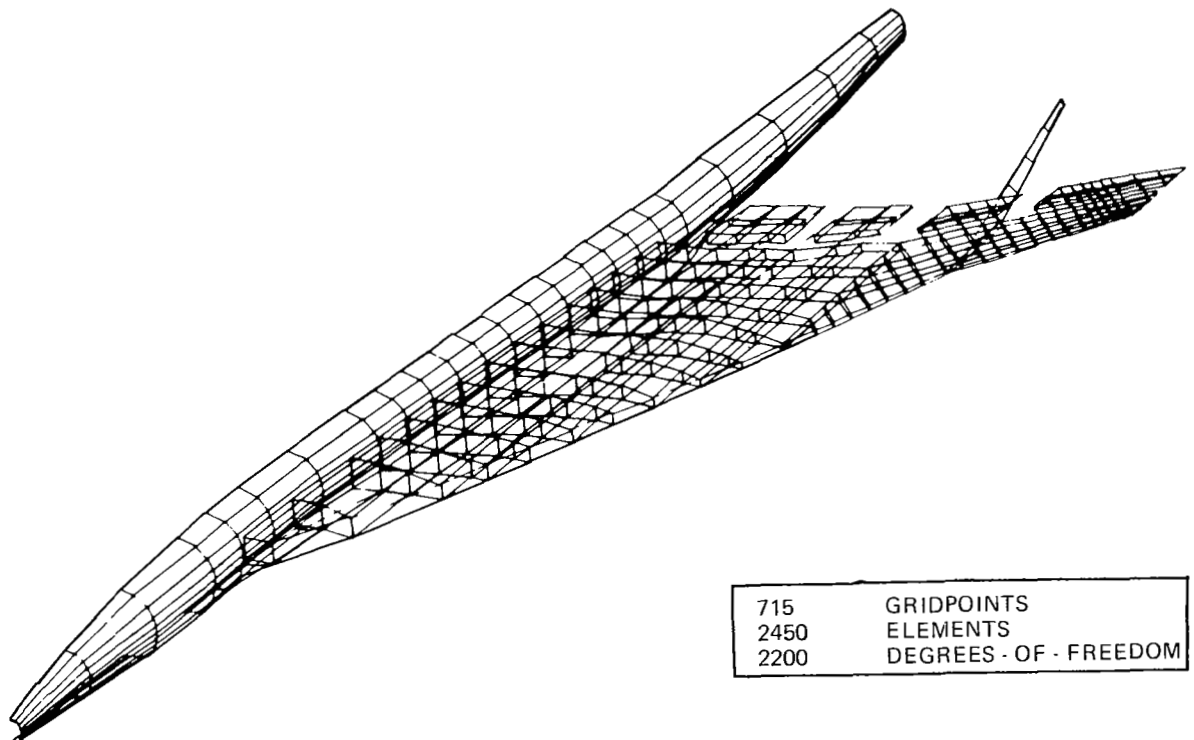


Figure 9. Finite Element Structural Model for Detail Design-Analysis

vertical fin were also included. In addition, lateral displacements of the fuselage were included for the antisymmetric boundary condition.

Aeroelastic Loads Analysis

Net aeroelastic loads were determined at preselected flight conditions by combining the detailed distributions of airloads and inertia loads, and accounting for the airframe flexibility effects. The subsonic and supersonic airload distributions were determined using the Direct Load Line Element (DDLE) and the Mach Box methods, respectively. The DDLE method is theoretically the same as the Doublet Lattice method of Reference 8; the Mach Box method is described in Reference 9. Typical aerodynamic-influence-coefficient (AIC) grids used for the determination of subsonic and supersonic aerodynamics are shown in Figure 10. The aerodynamic loads were transformed from the AIC grid to the load panel grid shown in Figure 11. The above load-panel-point grid coincides with the structural-influence-coefficient (SIC) grid used on the structural model.

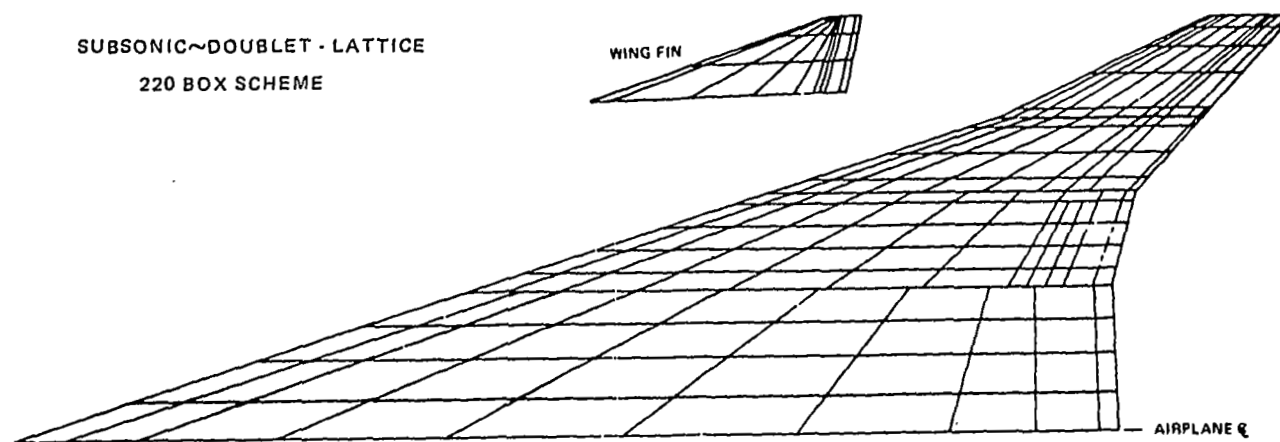
Inertia data for the airplane were determined for the operating mass empty, the payload and the fuel distributions. Inertia loads for the various design load conditions were derived from these data.

Vibration and Flutter Analysis

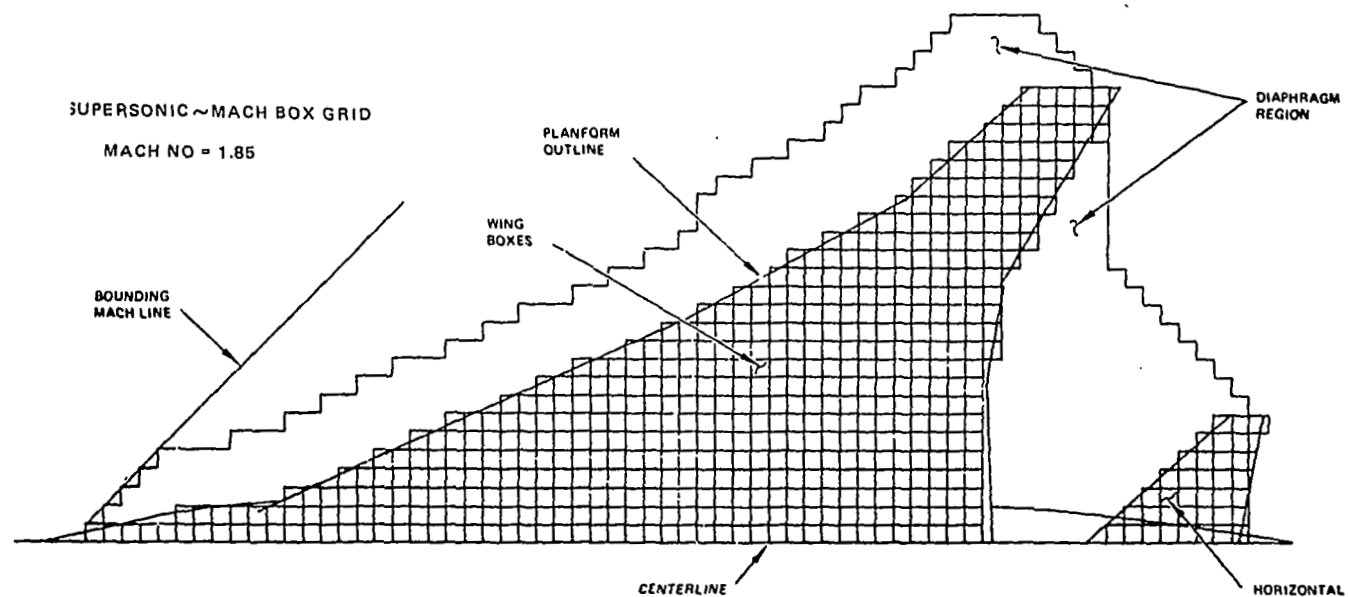
The vibration analyses employed a generalized coordinate system that was directly related to the structural influence coefficient (SIC) system, but reduced in the number of degrees-of-freedom. The network of coordinates for the symmetric condition (Figure 12) contained 188 degrees-of-freedom. One-hundred and seventy-eight degrees-of-freedom were used for the antisymmetric boundary condition. The stiffness matrices for the vibration analyses were obtained from the larger order stiffness matrices corresponding to the SIC network using Guyan reduction techniques. The modal analyses were performed using the Givens method contained in NASTRAN. The Givens method was selected after investigating the accuracy and computational time of this method, the Inverse Power method also available in NASTRAN, and the FAMAS QR method.

The stiffness matrices for each structural arrangement, as derived from the finite element models, were combined with the appropriate inertia matrices to compute the symmetric and antisymmetric eigenvectors and eigenvalues of the free-free airplane. The inertia matrices were formed for two airplane conditions only: the operating mass empty (OME), and the full-fuel and full-payload (FFFP). These conditions represent the extremes of minimum and maximum mass; no intermediate mass conditions were examined. In general, fifty vibration modes were extracted from each vibration solution for use in the flutter analyses and optimizations.

Steady and unsteady aerodynamic influence coefficients (AIC's) were calculated for Mach 0.60, 0.90, 1.25 and 1.85. The AIC's were computed for the wing, the wing vertical fin, and empennage surfaces. These AIC's were adjusted, when required, to reflect steady-state lift coefficients and aerodynamic centers obtained from wind tunnel force data. The Mach 0.60 and 0.90



(a) Subsonic Aerodynamic Grid



(b) Supersonic Aerodynamic Grid

Figure 10. Aerodynamic Influence Coefficient Grids

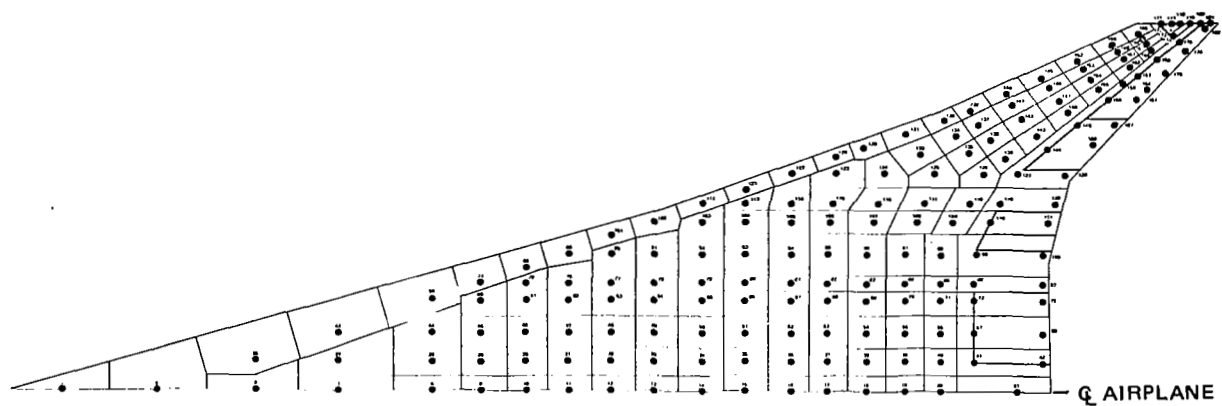


Figure 11. Load Panel Grid

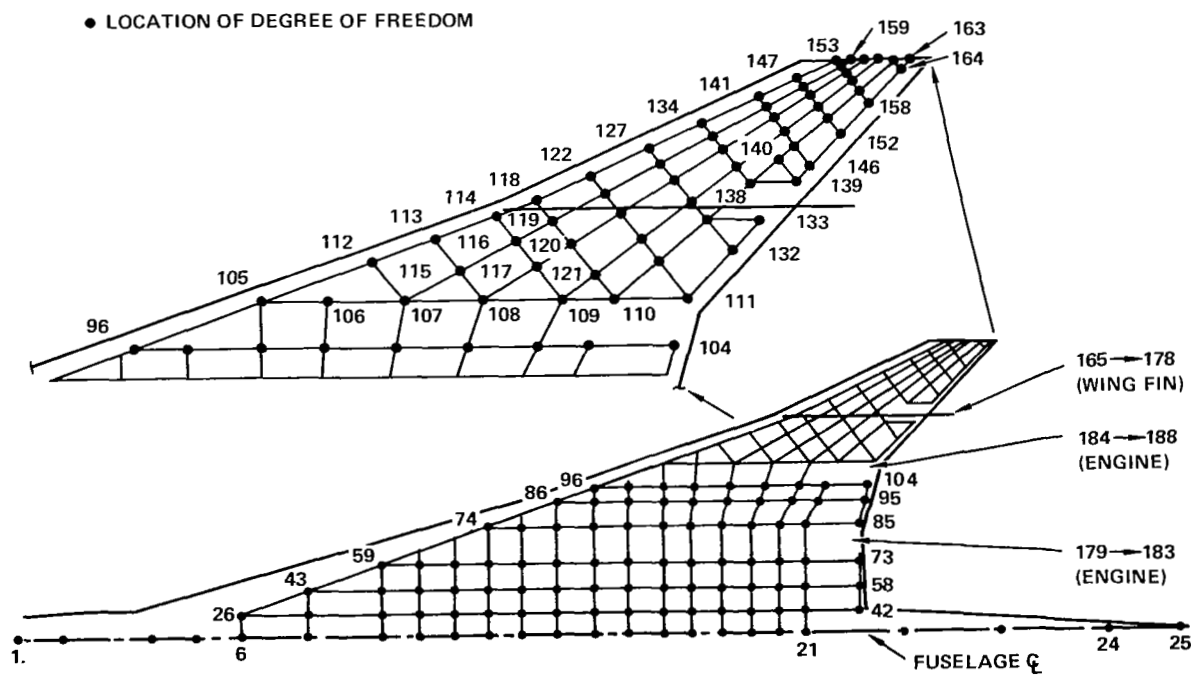


Figure 12. Symmetric Degrees-of-Freedom for Vibration Analyses

AIC calculations accounted for the interference between the wing and the wing vertical fin; the Mach 1.25 and 1.85 AIC's did not include this effect. Fuselage aerodynamics were not included in these analyses.

The flutter analyses were conducted using the method of solution described in Reference 10 as the p-k method. This method is contained in the FAMAS system and results in a solution which determines rate of decay and frequency for preselected values of speed and provides matched altitude, Mach number and reduced frequency for each mode at each preselected velocity. To ensure convergence in the flutter solutions, twenty or more vibration modes and nine or more reduced frequencies were used in all flutter analyses.

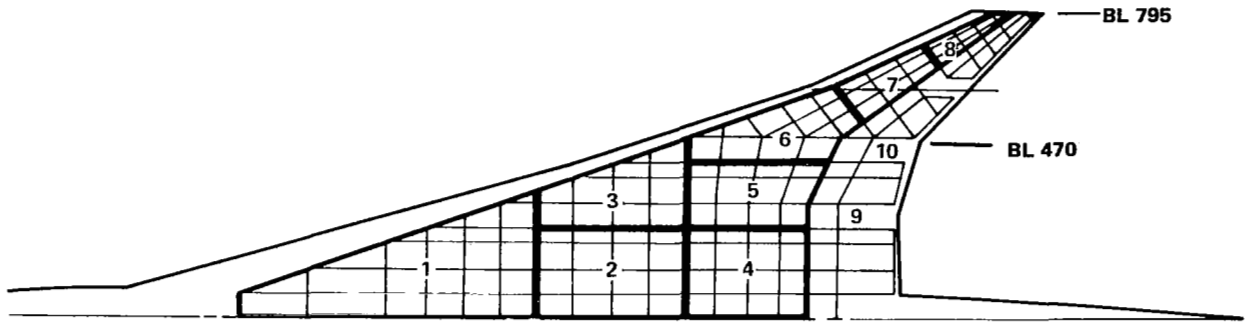
An interactive computer graphics program, GFAM, was used for flutter optimization. The GFAM program interactively determines the sensitivity of the flutter speed to changes in selected design variables, i.e., mass and stiffness changes within selected design regions; and thereby optimizes the placement of additional mass and/or stiffness to correct any flutter deficiencies while minimizing the total mass. An abbreviated description of the equations, method of solution, and optimization procedure is presented in Reference 11. In the initial optimization studies, the design regions were selected to provide a general assessment of the most effective distribution of material in the wing structure. For these studies, the wing planform was divided into ten regions (Figure 13a), which included the two engine support beam locations. Also shown (Figure 13b) is a more refined design region selection which was used for detailed optimizations of the wing tip structure (which was determined to be one of the most effective regions for additional structure to achieve the desired flutter speeds).

Point Design Analysis

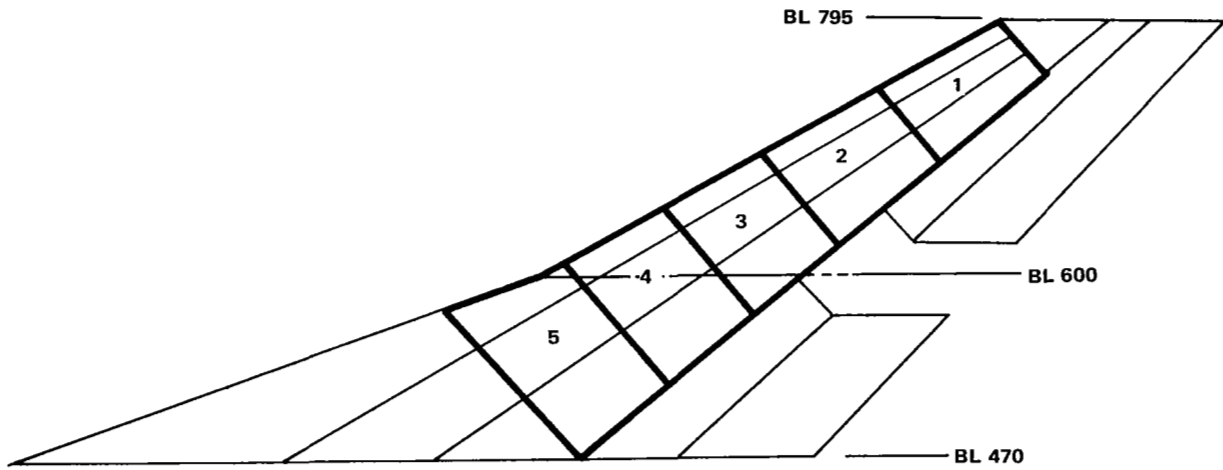
The candidate wing and fuselage structure design concepts were subjected to in-depth structural analyses using a point design approach. Representative structural regions in the wing and fuselage were selected as point design regions. For each region, unit structures were defined using the candidate concepts. The design load; temperature, and acoustic environments were then determined at these point design regions and used in detailed design analyses of the candidate concepts to establish minimum mass designs.

Six point design regions were defined for the wing structure (Figure 14a). The regions were identified by their corresponding NASTRAN panel element number. As indicated in the figure, only three of these were used in the initial screening of the design concepts; all six were used for the subsequent detail concept evaluation and the engineering design analyses. Four point design regions were used for evaluating the fuselage concepts (Figure 14b). These were located at fuselage stations (FS) 750, 2000, 2500 and 3000 for the design concepts evaluation; the equivalent locations for the engineering design-analyses were FS 900, 1910, 2525 and 2900.

The unit structures for the wing box included surface panel structure, spars and ribs, and associated non-optimum items. Similarly, the unit fuselage structures included both the fuselage shell structure, skin and stringers, and the supporting frame structure.

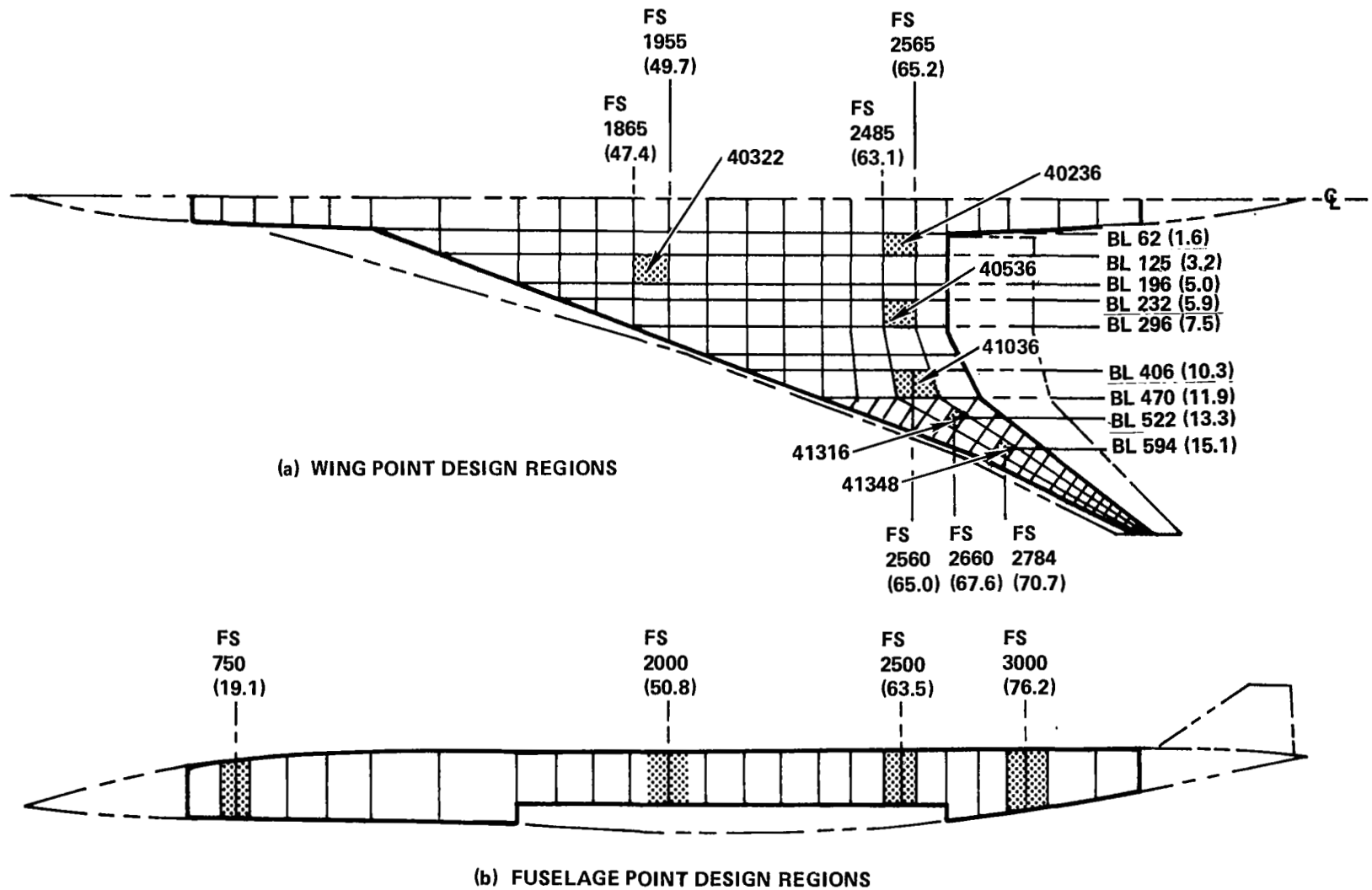


(a) Wing Design Regions



(b) Detailed Wing Tip Design Regions

Figure 13. Design Regions for Flutter Optimization



NOTE: 1. FS AND BL PRESENTED IN INCHES (METERS)

Figure 14. Point Design Regions

The unit structures at each point design region were analyzed for ultimate strength and fatigue requirements considering inplane loads from the finite element analyses, normal loads associated with aerodynamic pressure and/or fuel-head inertia, and temperatures and temperature gradients resulting from the aerodynamic heating analyses. Computerized stress analysis programs which incorporated optimization subroutines were used to define the minimum-mass proportions of the candidate panel concepts (Reference 1). The strength-sized components were also subjected to a fail-safe analysis to ensure that the structure, in the presence of an assumed damage condition, was capable of supporting the damage tolerance design load of 100-percent limit load.

For the sonic fatigue evaluation, design charts applicable to the two different types of panels being considered (orthotropic and isotropic panels) were used to calculate the allowable sound spectrum levels and panel natural frequencies. Sonic fatigue margins were established by subtracting the environmental sound spectrum level at the panel natural frequency from the allowable sound spectrum level. The detailed analysis and analytical methods are discussed in Reference 1.

DESIGN ENVIRONMENT

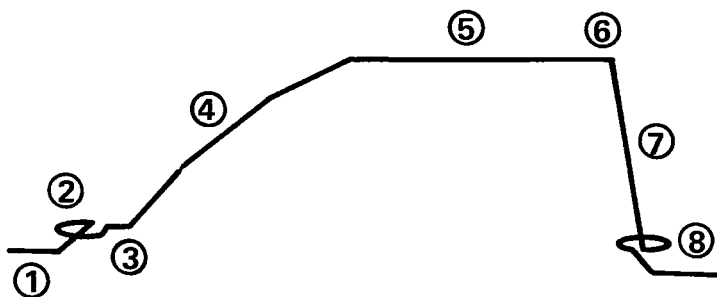
Mission Performance

The airplane performance over the design international mission of 4200-nmi (7780-km) is described in Figure 15. The segments are identified with the fuel used and the distance covered during each segment. Block fuel and range are totaled and the relevant takeoff and landing mass indicated. Time history of the wing reference plane angle-of-attack and Mach number time-history are shown in Figure 16 over the mission profile. These data were used for establishing design loads, and in the determination of the temperatures and temperature gradients.

Design Loads

Conditions for design were selected and aeroelastic analyses performed to define the design loads used for the structural analyses. The aeroelastic analyses incorporated airload, inertia load, and airframe flexibility effects so as to produce a set of balanced net loads for application to the finite element models.

Design Concepts Evaluation Loads.— Net aeroelastic loads were developed for the reference aircraft configuration using airframe stiffnesses representing the three wing structural arrangements: chordwise-stiffened, spanwise-stiffened and monocoque. Fifty design conditions were selected for analysis of the chordwise-stiffened wing arrangement. The flight loads encompassed level flight, steady maneuvers, and transient maneuvers. Two temperature conditions were included: mid-cruise and start-of-cruise. The net effect of thermal loads and air loads for these conditions were obtained by superposition of the appropriate temperature condition with the design loads conditions. In total, the design loads matrix included six ground handling,



SEGMENT	SEGMENT FUEL		SEGMENT DISTANCE	
	lbm	kg	n.mi.	km
① Ground Maneuver T.O. and Climb to 5000 ft (1526 m)	17,540	7,900	10	18.5
② Loiter @ 5000 ft (1526 m) for 4 min	3,910	1,772	0	0
③ Accelerate to 325 keas (602 km/hr)	17,741	790	1	1.85
④ Climb to Optimum Altitude	77,500	35,150	346	640
⑤ Cruise @ M = 2.62 (Hot Day)	219,668	99,500	3,714	6,870
⑥ Decelerate to 325 keas (602 km/hr) and	1,420	643	192	355.35
⑦ descend to 5000 ft. (1526 m) @ 325 keas (602) km/hr)				
⑧ Loiter @ 5000 ft (1526 in) for 5 min)	2,506	1,138	0	0
BLOCK FUEL	324,285	147,893		
RANGE			4,263	7,885.7

AIRCRAFT MASS		
DISPATCH	750,000 lbm	(340,000 kg)
LANDING	426,074 lbm	(192,107 kg)
RESERVE	64,074 lbm	(29,000 kg)
PAYLOAD	49,000 lbm	(22,200 kg)

Figure 15. Mission Segment Data

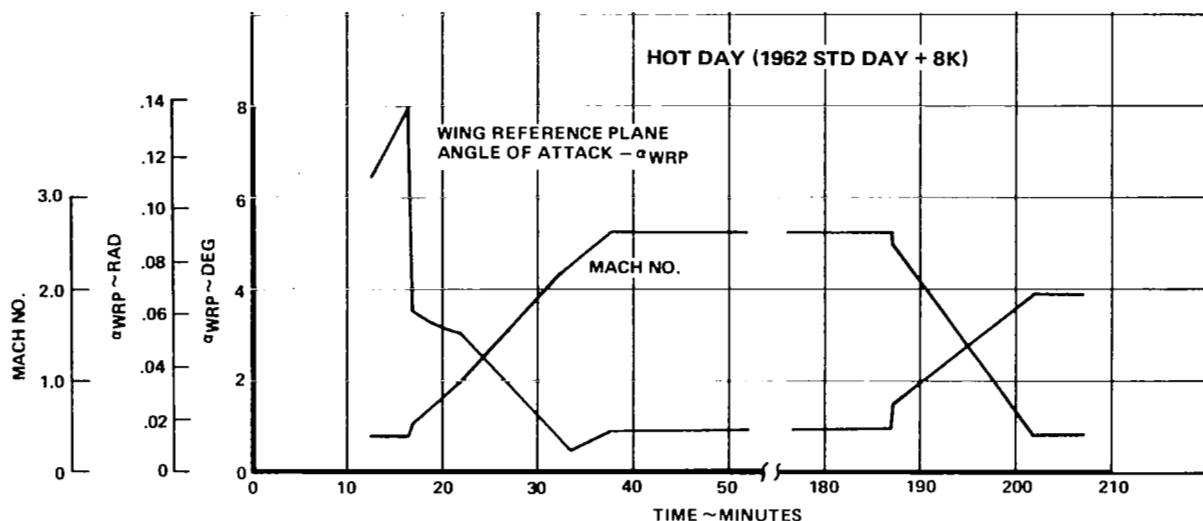


Figure 16. Mach Number/Trim Angle-of-Attack Profile

twenty-five positive symmetric flight, three negative symmetric flight, and sixteen asymmetric flight conditions. The design conditions are displayed on the design airspeed envelope on Figure 17.

The design loading conditions for analysis of the spanwise-stiffened and monocoque arrangements did not include the ground handling conditions, loading at negative load factors, or the asymmetric flight loads. These conditions were determined to be non-critical as the result of the internal loads evaluation of the chordwise-stiffened design.

Engineering Design-Analysis Loads.—Aeroelastic loads were calculated for the final design airplane using the airplane configuration shown in Figure 2. The design load conditions are identified in Table 3. These conditions were selected following the review of the design concepts evaluation results. Figure 18 displays these conditions superimposed on the design airspeed envelope.

The loading conditions included eight subsonic symmetric maneuvers (steady and transient); seven low supersonic conditions, including negative load factor, and steady and transient maneuvers at heavy and light masses; four Mach 2.7 conditions, including mid-cruise level flight and steady maneuver, and steady and transient maneuvers at start-of-cruise; two pseudo dynamic gust conditions at Mach 0.90 (positive and negative); and four dynamic landing conditions.

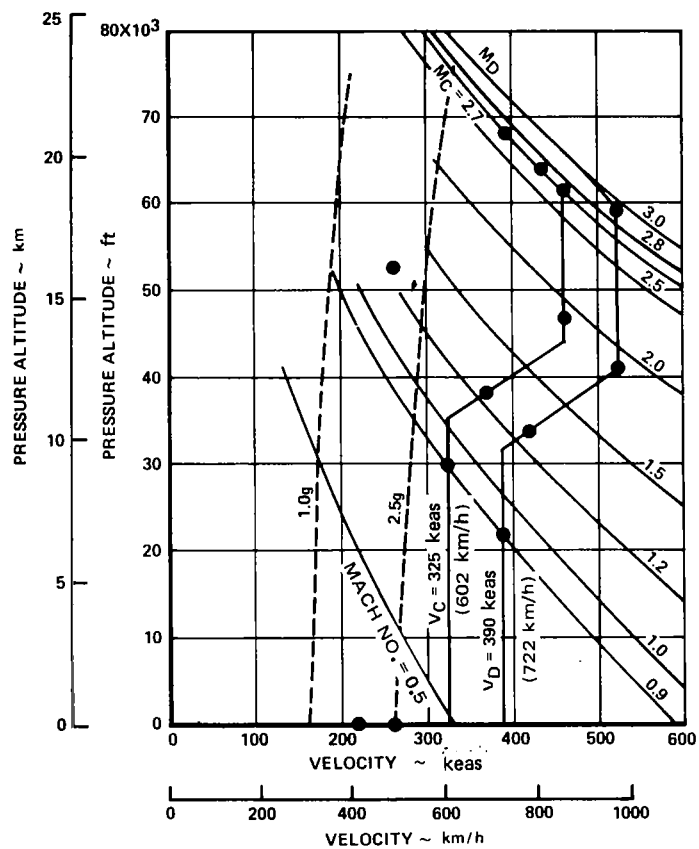


Figure 17. Design Loading Conditions - Design Concepts Evaluation

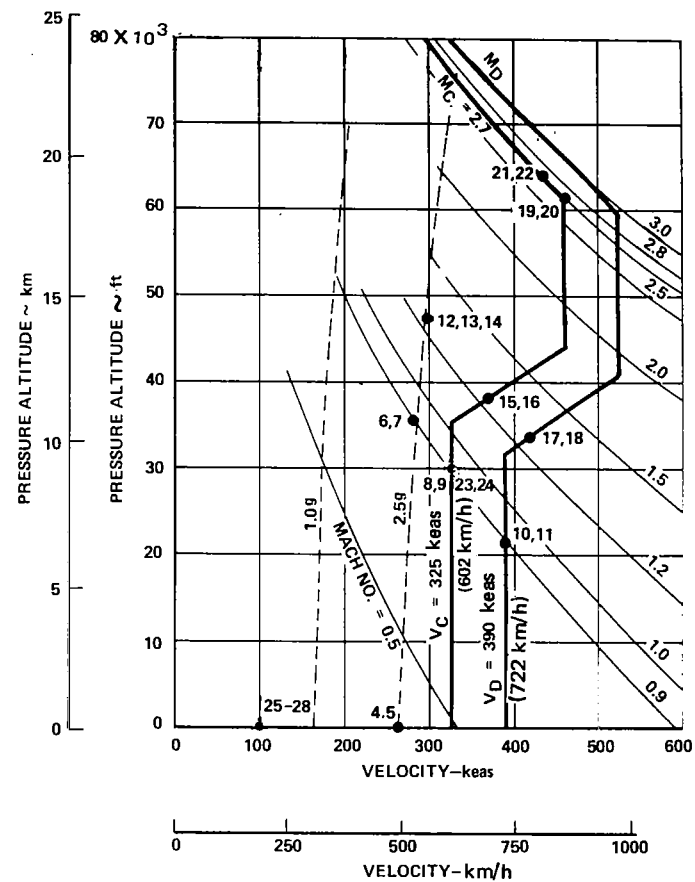


Figure 18. Design Loading Conditions - Engineering Design-Analysis

TABLE 3. DESIGN LOADING CONDITIONS DATA

NASTRAN COND. NO.	MASS		MACH NO.	ALTITUDE		LOAD FACTOR	AIRSPEED		REMARKS
	1000 lb	1000 kg		1000 ft	km		keas	km/h	
1	TEMPERATURE CONDITIONS								M2.7, START OF CRUISE
2									M2.7, MID-CRUISE
3									M1.25 DESCENT
4, 5	745	338	0.40	0.0	0.0	2.5	264.6	490	STRENGTH DESIGN
6, 7	700	318	0.90	36.0	10.97	2.5	282.4	523	STRENGTH DESIGN
8, 9	700	318	0.90	30.0	9.14	2.5	325.0	602	STRENGTH DESIGN
10, 11	700	318	0.90	22.0	6.71	2.5	390.0	722	STRENGTH DESIGN
12, 13	690	313	1.25	48.0	14.63	2.5	294.3	545	STRENGTH DESIGN
14	690	313	1.25	48.0	14.63	1.0	294.3	545	NEGATIVE FLIGHT
15, 16	690	313	1.25	38.2	11.64	2.5	372.0	689	STRENGTH DESIGN
17, 18	445	202	1.25	34.0	10.36	2.5	420.0	778	DESCENT – THERMAL
19, 20	660	299	2.70	61.5	18.74	2.5	460.0	852	START OF CRUISE
21, 22	550	249	2.70	64.0	19.51	1.0, 2.5	433.6	803	MID CRUISE
23, 24	700	318	0.90	30.0	9.14	—	325.0	602	PSUEDO – GUST (POSITIVE AND NEGATIVE)
25 - 28	430	195	—	0.0	0.0		100.0	185	DYNAMIC LANDING CONDITIONS

Design Temperatures

Time histories of structural temperatures for the Mach 2.7 cruise flight profile were calculated using the representative thermal analyzer network models. These models were used to define the temperatures and gradients at the selected wing and fuselage point design regions for the detailed stress analyses, and to define the average temperatures for input into the finite element analysis models. Figure 19 presents the resultant isotherm map for the Mach 2.62 Hot Day cruise condition.

Wing Panel Temperatures.— Representative temperature histories for upper and lower surface wing at point design panels region 40322 are presented for the chordwise-stiffened arrangements in Figures 20 and 21. The temperature gradients reach peak values near the start of cruise and during transonic descent. The panels are located in a fuel tank area and the temperature difference across the panel maintains a high value until the fuel is drained from the tank.

Fuselage Panel and Frame Temperatures.— Temperature histories developed for fuselage skin panels and circumferential frames are presented in Tables 4 and 5 for ten fuselage locations at four flight conditions: Mach 1.2 climb, start-of-cruise, mid-cruise, and Mach 1.2 descent. Table 4 shows mass-averaged temperatures for skin panels and temperature differentials between outer skin and stiffener crown. Table 5 shows mass-averaged frame temperatures and differentials between outer and inner flanges of the frame.

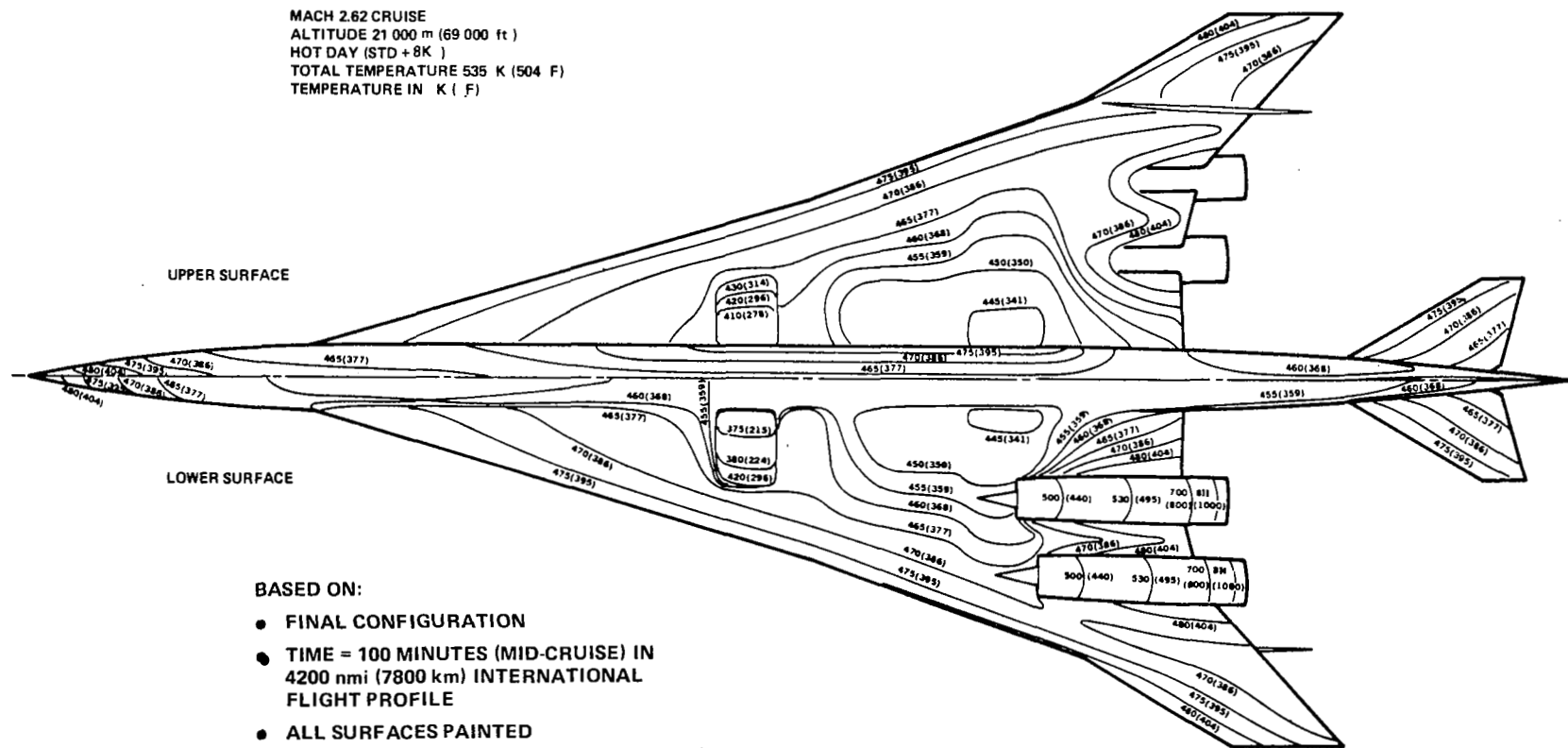


Figure 19. External Surface Isotherm - Mach 2.62 (Hot Day) Cruise

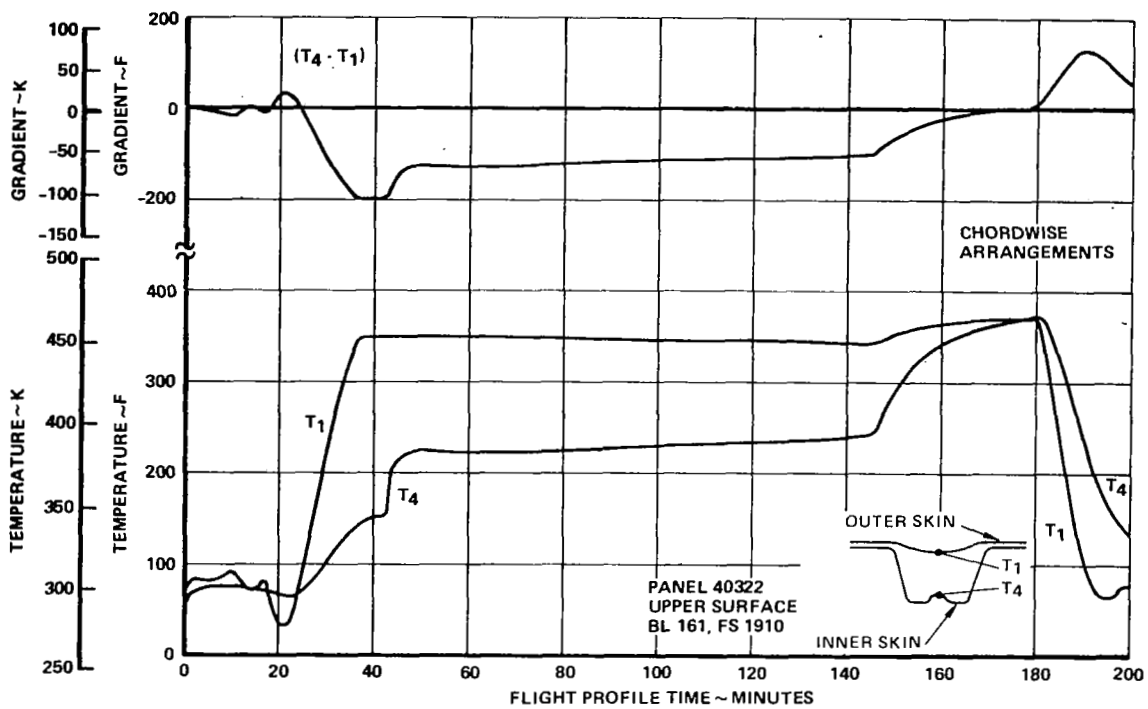


Figure 20. Chordwise-Stiffened Wing Panel Temperature Histories - 40322 Upper Surface

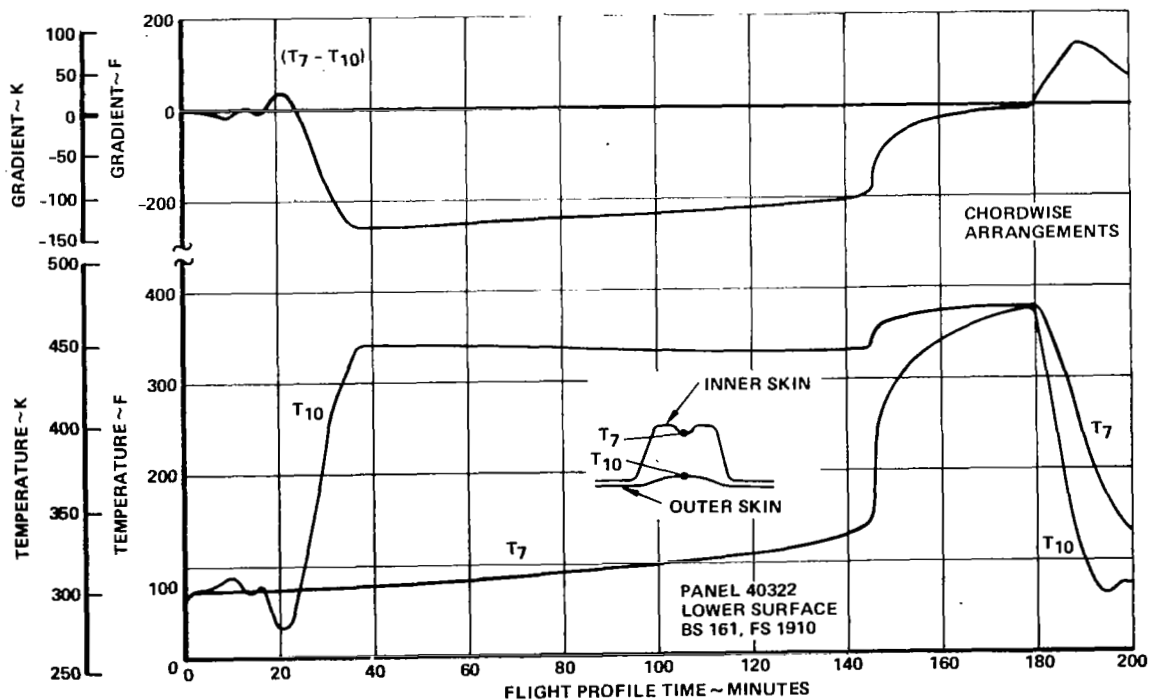


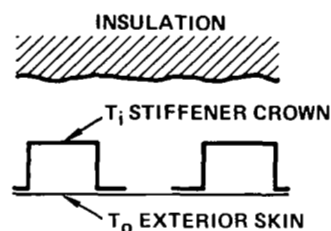
Figure 21. Chordwise-Stiffened Wing Panel Temperature Histories - 40322 Lower Surface

TABLE 4. TEMPERATURE AND GRADIENTS FOR FUSELAGE SKIN PANELS

NOTES:

1. BASED ON HOT DAY (STD+8K)
4200 nmi (7800 km) FLIGHT PROFILE.
2. HAT-STIFFENED PANELS,
EXCEPT ZEE-STIFFENED
AT FS 750.
3. 'TOP', 'BOTTOM' AT ϕ ;
'SIDE' AT 90° (1.57 rad)
OR ABOVE WING.

PANEL SCHEMATIC



TEMPERATURES IN F

LOCATION	FLIGHT CONDITION							
	MACH 1.2 CLIMB		START OF CRUISE		MID TO END OF CRUISE		MACH 1.2 DESCENT	
	$T_i - T_o$	T_{AVG}	$T_i - T_o$	T_{AVG}	$T_i - T_o$	T_{AVG}	$T_i - T_o$	T_{AVG}
<u>TOP</u>								
FS 750	+ 9	55	-105	342	-11	380	+111	114
2000	+23	53	-175	295	-11	374	+171	144
2500	+24	54	-186	281	-11	372	+181	156
3000	+23	53	-174	292	-11	371	+170	145
<u>SIDE</u>								
FS 750	+12	49	-106	332	-11	369	+109	108
2000	+21	50	-157	324	-11	394	+156	129
2500	+22	50	-171	311	-11	393	+170	139
3000	+23	47	-147	301	-11	358	+142	122
<u>BOTTOM</u>								
FS 750	+12	50	-106	333	-11	370	+109	109
3000	+28	47	-177	278	-10	360	+171	141

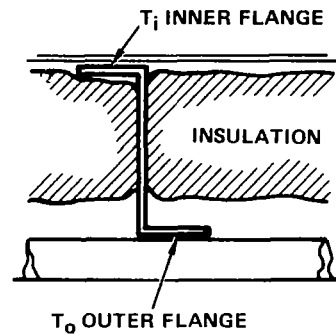
TEMPERATURES IN K

LOCATION	FLIGHT CONDITION							
	MACH 1.2 CLIMB		START OF CRUISE		MID TO END OF CRUISE		MACH 1.2 DESCENT	
	$T_i - T_o$	T_{AVG}	$T_i - T_o$	T_{AVG}	$T_i - T_o$	T_{AVG}	$T_i - T_o$	T_{AVG}
<u>TOP</u>								
FS 750	+ 5	286	- 58	445	-6	466	+ 62	319
2000	+13	285	- 97	419	-6	463	+ 95	335
2500	+13	285	-103	411	-6	462	+101	342
3000	+13	285	- 97	418	-6	461	+ 94	336
<u>SIDE</u>								
FS 750	+ 7	283	- 59	440	-6	460	+ 61	315
FS 2000	+12	283	- 87	435	-6	474	+ 87	327
2500	+12	283	- 95	428	-6	474	+ 94	333
3000	+13	281	- 82	423	-6	454	+ 79	323
<u>BOTTOM</u>								
FS 750	+ 7	283	- 59	440	-6	461	+ 61	316
3000	+16	281	- 98	410	-6	455	+ 95	334

TABLE 5. TEMPERATURE AND GRADIENTS FOR FUSELAGE FRAMES

NOTES:

1. BASED ON HOT DAY (STD + 8K)
4200 nmi (7800 km) FLIGHT PROFILE
2. 'TOP', 'BOTTOM' AT 0° ;
'SIDE' AT 90° (1.57 rad)
OR ABOVE WING.
3. INSULATION ASSUMED AT FS 3000
(AFT OF PRESSURE BULKHEAD)



TEMPERATURES IN F

LOCATION	FLIGHT CONDITION							
	MACH 1.2 CLIMB		START OF CRUISE		MID TO END OF CRUISE		MACH 1.2 DESCENT	
	$T_i - T_o$	T_{AVG}	$T_i - T_o$	T_{AVG}	$T_i - T_o$	T_{AVG}	$T_i - T_o$	T_{AVG}
<u>TOP</u>								
FS 750	+11	73	-133	145	-186	277	-56	202
2000	+ 6	74	- 74	115	-161	276	-76	233
2500	+ 5	74	- 63	109	-148	274	-72	242
3000	+ 6	74	- 73	114	-160	274	-76	232
<u>SIDE</u>								
FS 750	+14	71	-126	140	-179	269	-53	196
2000	+ 8	73	- 90	121	-171	291	-66	238
2500	+ 7	73	- 76	114	-158	291	-64	248
3000	+ 9	72	- 79	115	-152	266	-61	217
<u>BOTTOM</u>								
FS 750	+13	72	-126	140	-180	270	-53	196
3000	+ 8	73	- 63	108	-154	265	-76	226

TEMPERATURES IN K

LOCATION	FLIGHT CONDITION							
	MACH 1.2 CLIMB		START OF CRUISE		MID TO END OF CRUISE		MACH 1.2 DESCENT	
	$T_i - T_o$	T_{AVG}	$T_i - T_o$	T_{AVG}	$T_i - T_o$	T_{AVG}	$T_i - T_o$	T_{AVG}
<u>TOP</u>								
FS 750	+6	296	-74	336	-103	409	-31	368
2000	+3	296	-41	319	- 89	409	-42	385
2500	+3	296	-35	316	- 82	408	-40	390
3000	+3	296	-41	319	- 89	408	-42	384
<u>SIDE</u>								
FS 750	+8	295	-70	333	- 99	405	-29	364
2000	+4	296	-50	323	- 95	417	-37	388
2500	+4	296	-42	319	- 88	417	-36	393
3000	+5	295	-44	319	- 84	403	-34	376
<u>BOTTOM</u>								
FS 750	+7	295	-70	333	-100	405	-29	364
3000	+4	296	-35	315	- 86	403	-42	381

Fuel Tank Temperatures.- The design of the fuel storage and thermal protection systems reflected maintenance of heat sink capability, minimization of fuel vaporization (boiloff), retardation of residue formations, inhibition of thermochemical reaction of fuel vapor in hot tanks, and maintenance of tank sealant integrity. The design concepts accounted for the above by adopting as a reference fuel system the fuel system concepts developed and tested for: (1) the proposed L-2000 supersonic transport and (2) the YF-12 series supersonic aircraft.

Fuel heat sink capability was determined by the difference between the fuel temperature limit at the engine and bulk fuel temperature in the feed tanks. This capability was optimized by using fuel placement and scheduling similar to the reference system. For the reference fuel system, satisfactory cooling capacity was maintainable even under severe operating conditions and with a 100F (311K) fuel supply temperature. This was accomplished without insulating the tanks or providing active cooling.

Bulk fuel temperature histories for the wing tanks are shown in Figure 22. Temperatures are shown for each sectioned tank from start at 70F (294K) until the tank fuel level has dropped to two-percent of the original value (assumed usable limit). This fuel was pumped to the cool fuselage tanks before subsequent use. The wing tank temperatures were significantly below boiling temperature and inhibited fuel evaporation while fuel was being drawn from each tank.

The results of tests conducted on the reference fuel system, plus observation of YF-12 series aircraft fuel tanks (nitrogen-purged) subjected to higher temperatures, indicate that a nitrogen purge/pressurization system satisfying requirements for fuel tank inerting provided effective inhibition of vapor reaction and residue formation.

Experience with YF-12 series aircraft indicate that current fuel tank sealants retain effectiveness up to temperatures of at least 440F (500K). In eliminating the requirement for fuel tank insulation, the fuel system design assures easy access and maintenance when tank sealants must be repaired or replaced. The problem of fuel absorption in porous insulations in the event of slight seepage was also eliminated.

Acoustics

The acoustic environment which the aircraft would be subjected to during takeoff was estimated from empirical free-field acoustic levels generated by an existing turbojet engine. Adjustments were then made to account for the difference in the geometric characteristics of the turbofan engines, the operating parameters, the ambient environment, and the presence of structure within the acoustic field.

Isointensity Contours.- The overall sound pressure levels (OASPL) were determined using the reference contours of Figure 23 and the calculated incremental changes associated with the baseline design. Figure 24 displays the isointensity contours for the baseline engine location.

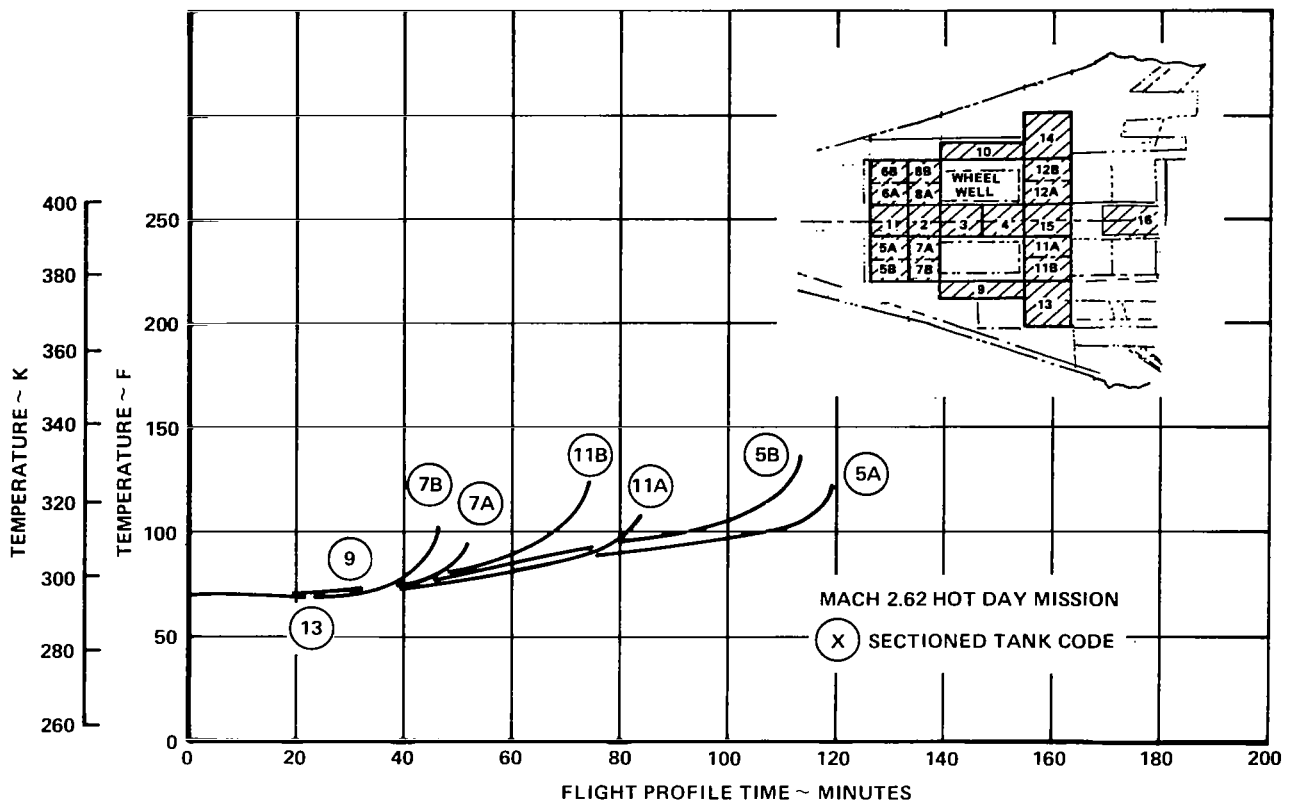


Figure 22. Bulk Fuel Temperatures in Wing Tanks

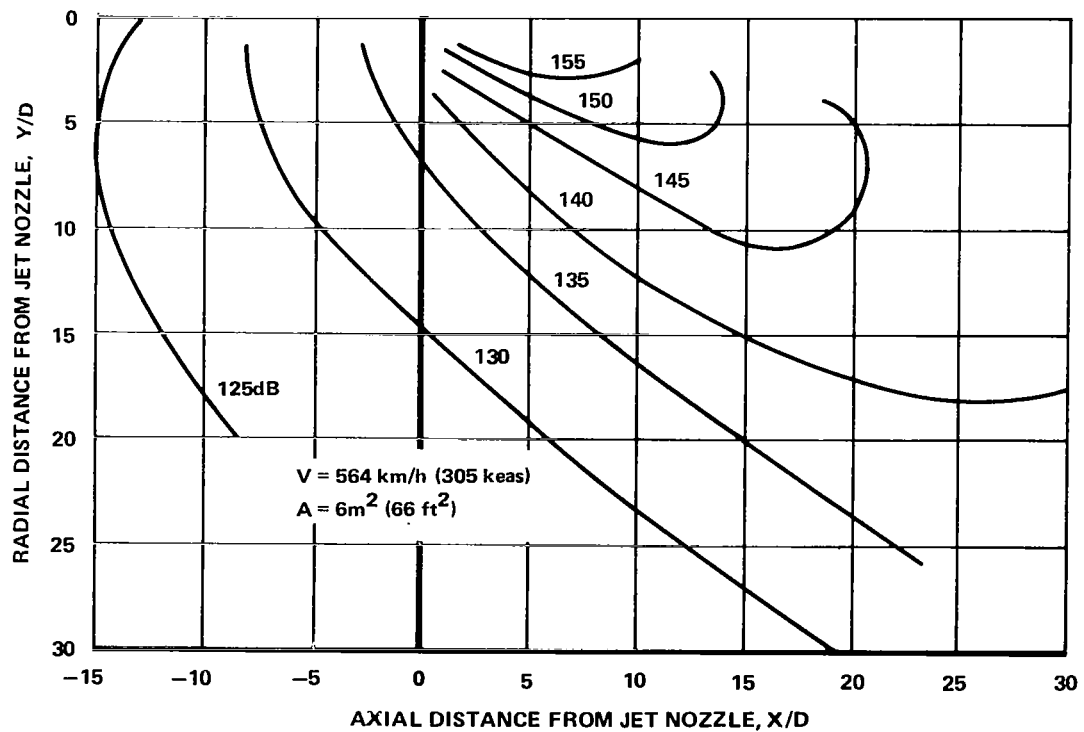


Figure 23. Near-Field Noise Contours - Reference Turbojet Engine

TABLE 6. WING PANEL LOAD/TEMPERATURE ENVIRONMENT - INITIAL SCREENING

MASS = 690 X 10³ LBM

ULTIMATE DESIGN LOADS	ITEM	UNITS	CHORDWISE STIFFENED ARRANGEMENT		SPANWISE STIFFENED ARRANGEMENT		MONOCOQUE ARRANGEMENT	
			UPPER SURFACE	LOWER SURFACE	UPPER SURFACE	LOWER SURFACE	UPPER SURFACE	LOWER SURFACE
AIR LOADS	N _x	lbf/in.	-1,305	1,305	306	-306	-3,171	3,171
	N _y	lbf/in.	-14,325	14,325	-16,986	16,986	-11,424	11,424
	N _{xy}	lbf/in.	2,354	2,354	2,541	2,541	4,847	4,847
THERMAL STRAIN	ε _x	in./in.	0	0	0	0	0	0
	ε _y	in./in.	0	0	0	0	0	0
	ε _{xy}	in./in.	0	0	0	0	0	0
PRESSURE	AERO	psi	-1.27	-.26	-3.03	-1.20	-1.27	-.26
	FUEL	psi	-5.67	-8.03	-5.93	-8.94	-5.67	-8.03
	NET	psi	-6.94	-8.29	-8.96	-10.14	-6.94	-8.29
TEMPERATURE	TAV	°F	147	136	139	139	147	148
	ΔT	°F	-115	-127	-130	-136	-131	-138

MASS = 313 X 10³ Kg

ULTIMATE DESIGN LOADS	ITEM	UNITS	CHORDWISE STIFFENED ARRANGEMENT		SPANWISE STIFFENED ARRANGEMENT		MONOCOQUE ARRANGEMENT	
			UPPER SURFACE	LOWER SURFACE	UPPER SURFACE	LOWER SURFACE	UPPER SURFACE	LOWER SURFACE
AIR LOADS	N _x	kN/m	-228	228	54	-54	-555	555
	N _y	kN/m	-2,508	2,508	-2,975	2,975	-2,000	2,000
	N _{xy}	kN/m	412	412	445	445	849	849
THERMAL STRAIN	ε _x	m/m	0	0	0	0	0	0
	ε _y	m/m	0	0	0	0	0	0
	ε _{xy}	m/m	0	0	0	0	0	0
PRESSURE	AERO	kPa	-8.76	-1.79	-20.88	-8.27	-8.76	-1.79
	FUEL	kPa	-39.09	-55.36	-40.88	-61.60	-39.09	-55.36
	NET	kPa	-47.85	-57.15	-61.76	-69.87	-47.85	-57.15
TEMPERATURE	TAV	°K	337	331	333	333	337	338
	ΔT	°K	-64	-71	-72	-75	-73	-77

- NOTES: (1) A 1.25 FACTOR HAS BEEN APPLIED TO THE THERMAL STRAIN WHEN THE SIGN IS SAME AS AIRLOAD SIGN OTHERWISE NO FACTOR APPLIED.
 (2) PRESSURE SIGN CONVENTION: NEGATIVE = SUCTION
 (3) CONDITION (3) ; MACH NO. = 1.25; n_z = 2.5
 (4) POINT DESIGN REGION 40536

TABLE 7. FUSELAGE PANEL LOAD INTENSITIES - INITIAL SCREENING

LOCATION	FUSELAGE PANEL LOAD INTENSITIES (ULT.)						
	DIRECTION	FS 2000, FS 3000			FS 2500		
UPPER PANEL	N _x	11600 (2031)	11700 (2049)	11600 (2031)	15700 (2749)	14600 (2557)	15690 (2748)
	N _{xy}	412 (72)	417 (73)	413 (72)	629 (110)	597 (104)	629 (110)
SIDE PANEL	N _x	377 (66)	406 (71)	300 (52)	422 (74)	545 (95)	416 (73)
	N _{xy}	1361 (238)	1357 (238)	1330 (233)	2025 (355)	2000 (350)	1998 (350)
LOWER PANEL	N _x	-11700 (-2049)	-11650 (-2040)	-12000 (-2100)	-16100 (-2819)	-16800 (-2942)	15900 (-2784)
	N _{xy}	415 (73)	412 (72)	426 (75)	645 (113)	670 (117)	633 (111)

XXXX = lbf/in; (XXXX) = kN/m

Chordwise-Stiffened Wing Concepts.--The panel structural mass data of Figure 25 compares the mass efficiency of the four candidate designs at the selected point design regions. The surface panel mass (upper and lower) is presented as a function of a variable spar spacing. The results show that the convex-beaded concept which employs structurally efficient circular-arc elements was minimum-mass at all design regions for the spar spacings investigated.

Spanwise-Stiffened Wing Concepts.--Comparative data of surface panel mass for the spanwise-stiffened concepts are presented in Figure 26. Graphical display of the sum of the upper and lower surface panel mass is shown as a function of rib spacing. The data show that the minimum-mass panel concept was the hat-stiffened design at all point design regions and rib spacings investigated, with one exception. At region 40536 for the 20-in (0.51-m) rib spacing, the most mass-efficient design was the zee-stiffened concept. The least efficient design was the integral-stiffened design.

Monocoque Wing Concepts.--The biaxially-stiffened panel concepts were subjected to the same depth of analysis as the uniaxially stiffened concepts. In addition, prior to screening the two biaxially-stiffened panel concepts, honeycomb sandwich and truss-core, an analysis was conducted to ascertain the panel proportions (aspect ratio) associated with minimum mass design.



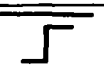
The aspect ratio parametric study was conducted using both multispar and multirib honeycomb-core sandwich panel structural box designs. The results of this analysis indicated that the multispar approach affords the most mass-efficient designs considering the panels alone, and considering the complete wing box structure. The inclusion of the substructure in the mass analysis resulted in a larger variation between the multirib and multispar designs and a clearer definition of the minimum mass arrangement.

The comparison of structural mass trends of the honeycomb sandwich design (brazed) and the truss-core design (diffusion bonded) is presented in Figure 27. The trends shown are for the multispar substructure considering both upper and lower surface panel mass. The data shows that the honeycomb panel concept was the more efficient design at the three design regions investigated.

Fuselage Shell Concepts.--A frame spacing study was conducted to define an appropriate spacing for panel screening analysis. This study was performed using two of the candidate shell concepts, zee- and hat-stiffened. Analyses were conducted at point design regions FS 2000, FS 2500, and FS 3000 using their respective environmental design data. Figure 28 presents the results of the study at FS 2500, indicating that the frame spacing between 20- and 25-in (0.51- and 0.64-m) offer minimum mass designs. Review of these data in conjunction with the wing study results, indicated that the lower bound value was the most realistic spacing.

The screening of the three candidate fuselage panel concepts were conducted using the results of aforementioned frame spacing study, i.e., 20.0-in (0.51-m) frame spacing. The average panel mass data for the panel concepts are shown in Table 8 and indicate the closed-hat panel concept is the minimum-mass design for each point design region with the exception of FS 750, where the zee-stiffened concept is lighter. Average panel mass ranged

TABLE 8. MASS TRENDS OF THE CANDIDATE FUSELAGE
PANEL CONCEPTS - INITIAL SCREENING

POINT DESIGN REGION	AVERAGE PANEL MASS					
						
FS 750	-	-	-	-	1.31	(6.40)
FS 2000	2.98	(14.55)	2.80	(13.67)	3.01	(14.70)
FS 2500	3.35	(16.36)	3.18	(15.53)	3.52	(17.19)
FS 3000	2.98	(14.55)	2.80	(13.67)	3.01	(14.70)
NOTES: 1. CONSTANT FRAME SPACING = 20.0 - in. (.51-m) 2. X.XX = lbm/ft ² ; (X.XX) = kg/m ²						

from a maximum value of 3.18-lbm/ft² (15.53-kg/m²) at FS 2500 to a minimum value of 1.31-lbm/ft² (6.40-kg/m²) at FS 750.

Detailed Concept Analyses

The most promising structural concepts (Figure 29) were subjected to further mass-strength analyses at an extended set of point design regions; a total of six wing and four fuselage regions. In addition, the application of composite material reinforcement to primary structure was investigated to evaluate potential mass saving benefits.

The panel concepts were combined with their associated substructures to form representative wing box and fuselage shell structures. In-depth structural analyses were conducted on each unit structural component, including ultimate and fatigue strength analyses, fail-safe analyses, and sonic fatigue analyses. Estimated total airplane mass data for each structural approach were obtained by extrapolation of the unit mass data of the point design regions over the remainder of the aircraft.

Vibration and flutter analyses, and flutter optimization studies were conducted using the finite element models representing each of the structural arrangements, i.e., chordwise-stiffened, spanwise-stiffened and monocoque, to determine the additional stiffness and mass needed to meet the flutter speed requirements.

Production costs were also developed for each of the wing concepts using the common skin-stringer-frame fuselage design. These costs were derived by evaluating the fabrication and assembly operation for each design on a point design basis and extrapolating these results to encompass the overall wing.





STRUCTURAL ARRANGEMENT	PANEL CONCEPT	GEOMETRY
CHORDWISE - STIFFENED WING	CIRCULAR-ARC/CONVEX BEADED SKIN	
SPANWISE - STIFFENED WING	HAT STIFFENED SKIN	
MONOCOQUE WING	HONEYCOMB SANDWICH - ALUMINUM BRAZED	
FUSELAGE - SKIN/STRINGER	CLOSED HAT STRINGERS	

Figure 29. Promising Structural Concepts

Strength-Design Analyses.—The results of the wing and fuselage detailed concept analyses, with the exception of the sonic fatigue analyses, are discussed in the following text. The sonic fatigue analyses indicated positive margins-of-safety for all designs; thus, the acoustic environment did not impact the selection process and the results of these analyses are not included.

The critical flight conditions and corresponding overall wing internal load and temperature distributions remained unchanged between these analyses and the prior initial screening analyses. The fuselage point design loads and temperatures are shown in Table 9 and reflect the internal loads, cabin pressure and temperature data for the start-of-cruise flight condition.

Chordwise-Stiffened Wing Arrangement: An example of the detailed mass-strength analysis results is presented in Figure 30 to indicate the magnitude of the strength-sizing effort conducted on, not only the chordwise-stiffened wing, but also the spanwise-stiffened and monocoque wing designs. The data present the component and total wing box mass at point design region 40536 as a function of a variable spar spacing. The components included in this investigation were the upper and lower surface panels (convex-beaded construction), spar-caps and webs, rib-caps and webs, and appropriate non-optimum structure.

Figure 31 displays the wing box mass resulting from the above mass-strength analyses for each of the six point design regions. The minimum mass designs at each of the regions occur at a spar spacing of 20-in (0.51-m), with the wing box mass varying from 3.79-lbm/ft² (18.50-kg/m²) at region 40322 (forward box) to 15.54-lbm/ft² (75.87-kg/m²) at region 41316 (wing tip).

To assess the damage tolerance of the strength-sized chordwise-stiffened designs, both surface panels and spars were subjected to a fail-safe evaluation. For the surface panels, a damage condition of a three-stringer pitch outer skin crack with two broken reinforcing stiffeners (inner bead) was selected. Depending upon the local geometry, this resulted in crack sizes between 5-in (0.13-m) to 13-in (0.33-m). A residual strength analysis was conducted and verified the fail-safe capability of the strength-design. Therefore, no mass penalty was assessed to the chordwise-stiffened panel concepts.

A broken spar cap damage condition was analyzed since in the chordwise-arrangement the spar caps carry the wing spanwise bending loads. To assess this damage condition, the spar cap was assumed to be completely broken and the adjacent structure analyzed for the redistributed loads. The strength-designed components for three spar spacings were evaluated at each point design region. The mass penalties associated with each structural component of the wing box are shown in Figure 32 for point design region 40536. The resultant mass penalties for the three point design regions for the damaged spar cap condition are presented in Table 10.

Spanwise-Stiffened Wing Arrangement: Ultimate and fatigue strength analyses were conducted on the spanwise-stiffened wing box structure using the minimum-mass hat-stiffened panel concept. The wing box unit mass at each of the six point designs is shown in Figure 33. Region 40536, which is located at approximately the mid span of the wing aft box, yields a minimum mass design of 13.58-lbm/ft² (66.3-kg/m²) for a 30-in (0.76-m) rib spacing. The unit mass at region 40322 was 4.71-lbm/ft² (23-kg/m²) for a 20-in (0.51-m) rib spacing.

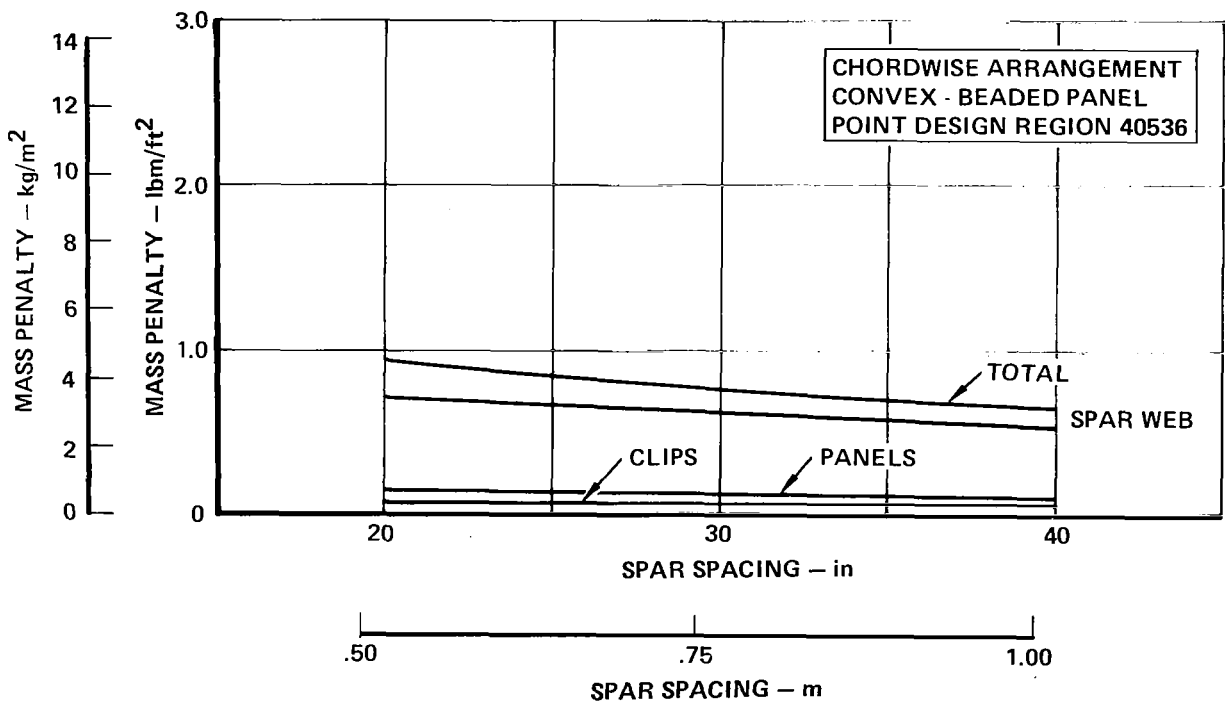


Figure 32. Component Mass Penalties for a Damaged Spar Cap - Chordwise-Stiffened Arrangement

TABLE 10. POINT DESIGN MASS PENALTIES FOR A DAMAGED
SPAR CAP - CHORDWISE-STIFFENED ARRANGEMENT

SPAR SPACING	20-in	(0.51-m)	30-in	(0.76-m)	40-in	(1.02-m)
POINT DESIGN REGION	lbm/ft ²	kg/m ²	lbm/ft ²	kg/m ²	lbm/ft ²	kg/m ²
40536	0.93	4.54	0.75	3.66	0.63	3.08
40322	0.10	0.49	0.20	0.98	0.27	1.32
40236	1.75	8.54	1.45	7.08	1.38	6.74

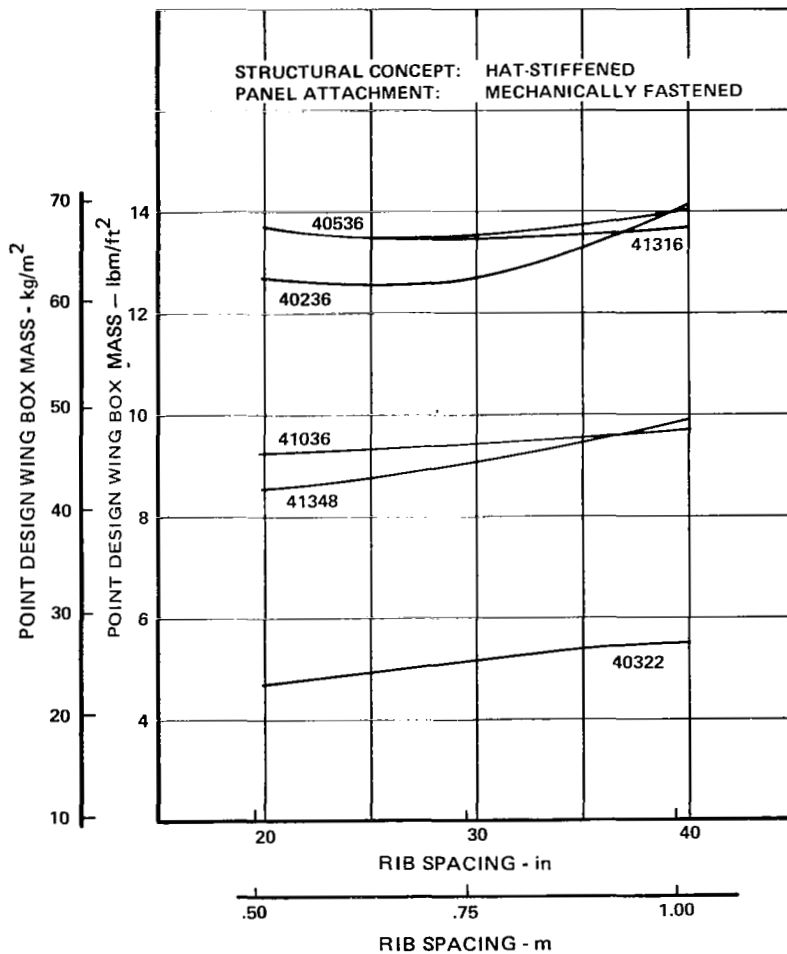


Figure 33. Optimum Rib Spacing for Spanwise-Stiffened
Wing Arrangement

TABLE 11. MASS TRENDS OF THE MONOCOQUE WING DESIGNS

POINT DESIGN REGIONS	SPAR SPACING		WING BOX MASS				
			MINIMUM - MASS ⁽¹⁾		NORMALIZED VALUES ⁽²⁾		
	(in)	(m)	(lbm/ft ²)	(kg/m ²)	MECH. FAST. - TUBULAR	WELDED - TUBULAR	MECH. FAST. - DENSIFIED CORE
40322	20	.51	4.00	19.5	1.13	1.09	1.00
40236	20	.51	8.26	40.3	N.A. ⁽³⁾	1.03	1.00
40536	20	.51	8.33	40.7	1.04	1.03	1.00
41036	20	.51	5.05	24.7	N.A. ⁽³⁾	1.04	1.00
41316	20	.51	7.02	34.3	N.A. ⁽³⁾	1.05	1.00
41348	20	.51	5.49	26.7	1.05	1.06	1.00

1. MINIMUM MASS ARRANGEMENT: MECHANICALLY FASTENED - DENSIFIED CORE
2. ALL VALUES NORMALIZED TO THE MINIMUM-MASS ARRANGEMENT
3. MASS DATA NOT AVAILABLE (N.A.)

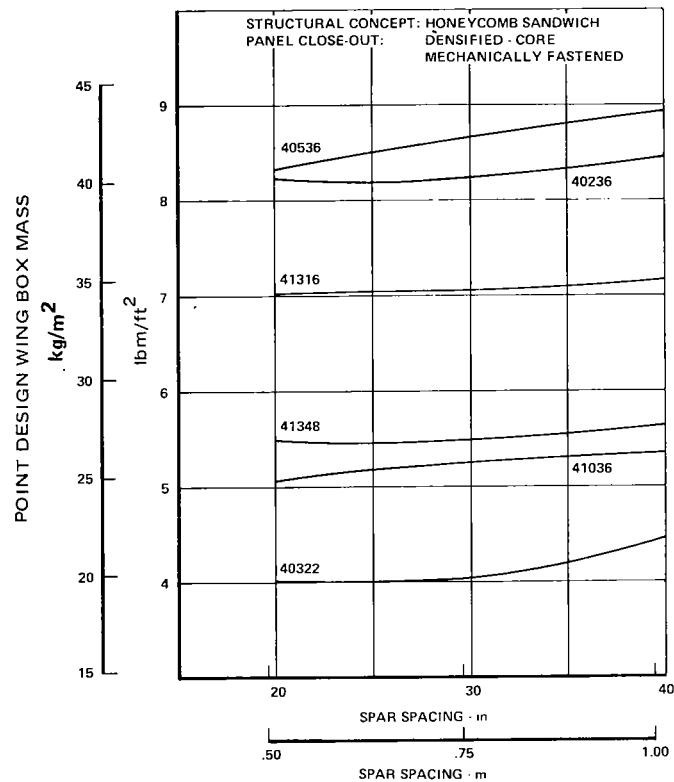


Figure 35. Optimum Spar Spacing for the Monocoque Wing Mechanically Fastened Densified-Core Design

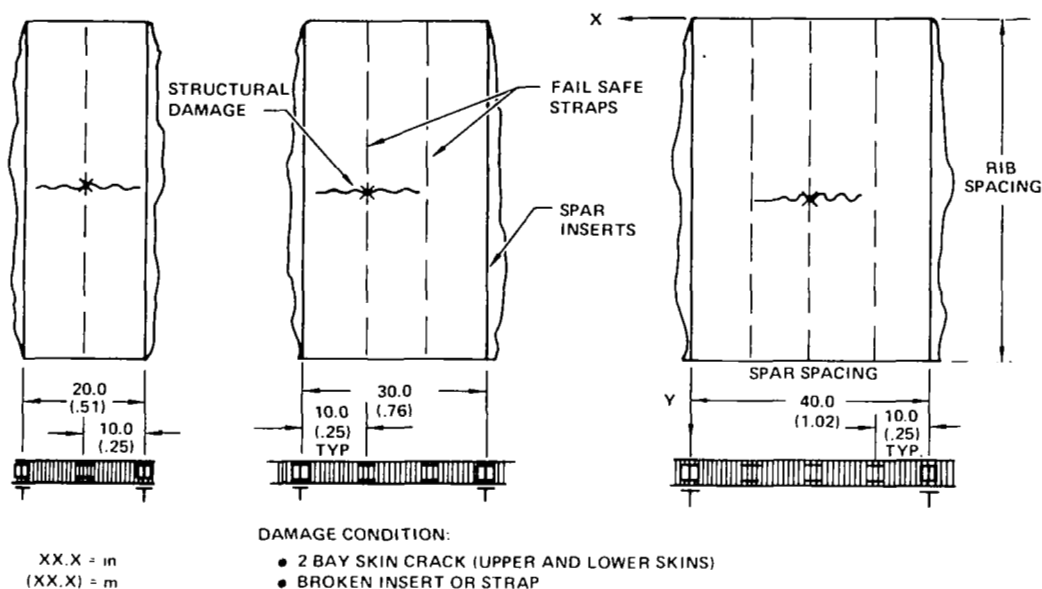


Figure 36. Monocoque Panel Damage Configurations

For the predominantly pressure-loaded surface panels the material systems considered for reinforcement were (1) MODMOR II/Skybond 703 graphite-polyimide, (2) Boron/Skybond 703 boron-polyimide, and (3) 5.6 boron/1100 aluminum with titanium interleaves. The surface-panel mass data for region 40536 are displayed in Figure 37 for the candidate material systems. The data indicate that the graphite-polyimide reinforced surface panel is the least-mass composite approach. It should be noted, however, that the metallic convex-beaded panel concept mass is approximately 8-percent lighter than the minimum mass graphite-polyimide composite reinforced design.

The component exhibiting the greatest potential mass saving was the submerged spar cap of the chordwise-stiffened arrangement which account for approximately 60-percent of the total box mass at region 40536. To evaluate the mass-saving potential, boron-polyimide was selected as the reinforcement material system to be applied unidirectionally to the titanium alloy 6Al-4V spar caps. The compressive stress efficiency, thermal strain compatibility with titanium, and tensile strain constraint dictated by the gross area tension stress cutoff of 90,000-psi (619-MPa) for the titanium alloy, were decisive factors in the selection of the boron-polyimide material system over the graphite-polyimide system selected for the surface panel design.

The results of the above investigations were applied to two different wing box designs. The first design used Gr/PI reinforced panels and B/PI spar caps. The second design employed an all metal design with only the spar caps employing composite reinforcement (B/PI). A comparison of wing box mass for these two arrangements with the least-mass metallic arrangement is shown in Figure 38. Both composite designs offer a mass reduction of approximately 35 percent over the all metallic designs for comparable spar spacings.

Table 12 summarizes the composite reinforced wing-box mass data for each of the wing design regions. Included in this table are the component mass of the chordwise-stiffened beaded panel design and the mass estimate for the composite reinforced spar caps. The mass savings for the composite reinforced design in the highly loaded wing region 40536 when compared with

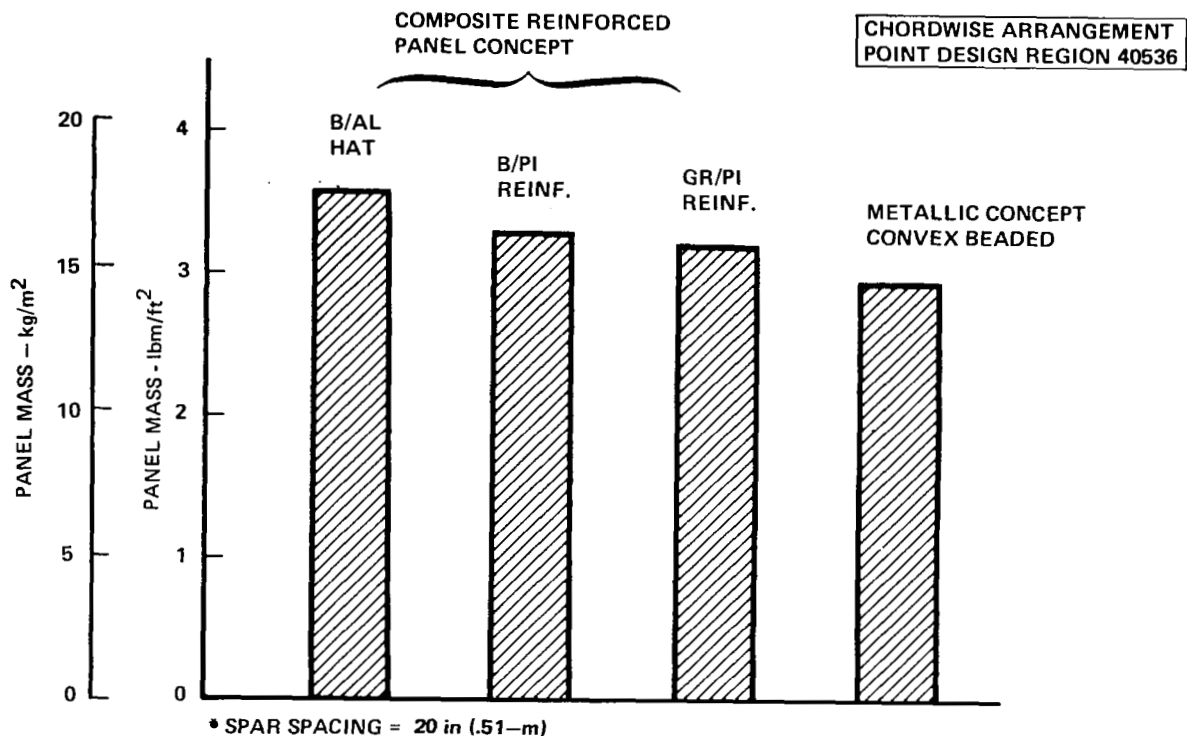


Figure 37. Mass Comparison of Candidate Composite Materials

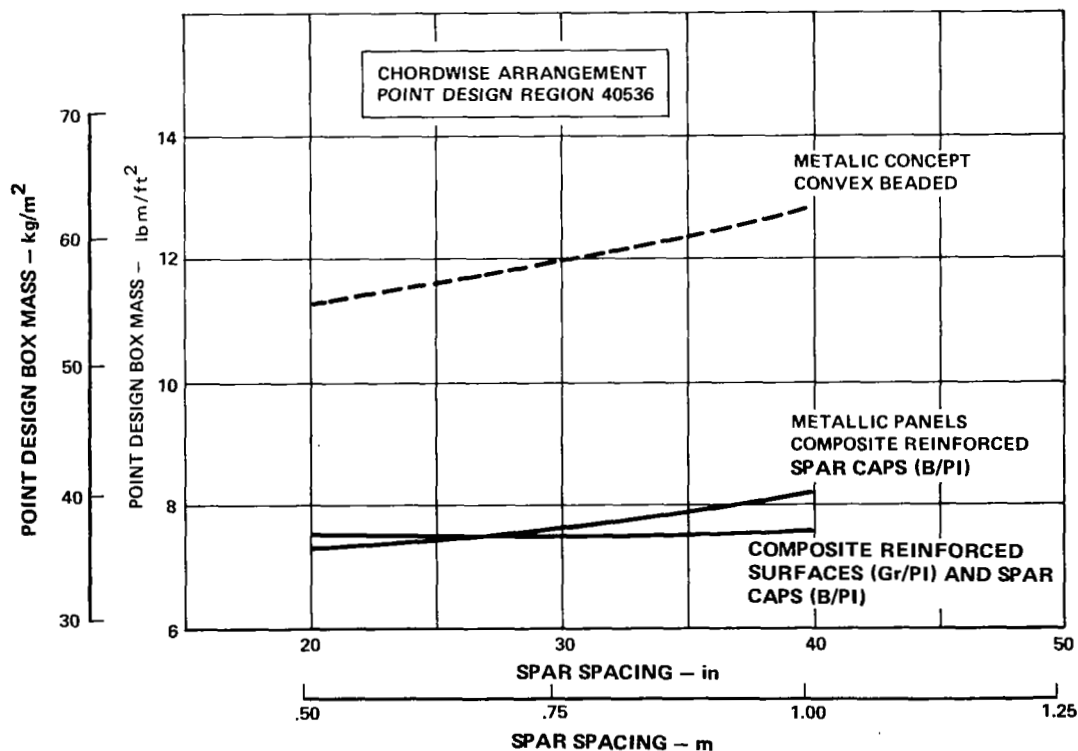


Figure 38. Optimum Spar Spacing for the Composite Reinforced Wing Arrangements (Region 40536)

TABLE 12. DETAILED WING BOX MASS FOR BEADED PANELS WITH COMPOSITE REINFORCED SPAR CAPS

POINT DESIGN REGION			40322	40236	40536	41036	41316	41348
SPAR SPAC (IN)			20	20	20	20	20	20
PANELS								
UPPER			0.825	1.032	1.609	1.452	2.571	1.632
LOWER			0.942	1.279	1.335	1.320	2.007	1.366
Σ			(1.767)	(2.311)	(2.944)	(2.772)	(4.578)	(2.998)
RIB WEBS								
BULKHEAD			0.298	0.279	0.238	0.111	0.270	0.106
TRUSS			0.074	0.237	0.228	0.060	—	—
Σ			(0.372)	(0.516)	(0.466)	(0.171)	(0.270)	(0.106)
SPAR WEBS								
BULKHEAD			0.336	0.361	0.270	0.109	0.439	0.291
TRUSS			0.301	0.544	0.490	0.359	—	—
Σ			(0.637)	(0.905)	(0.760)	(0.468)	(0.439)	(0.291)
RIB CAPS								
UPPER			0.058	0.070	0.116	0.093	0.160	0.103
LOWER			0.065	0.083	0.086	0.087	0.126	0.074
Σ			(0.123)	(0.153)	(0.202)	(0.180)	(0.286)	(0.177)
SPAR CAPS								
UPPER			0.241	1.240	1.140	0.900	1.440	1.060
LOWER			0.350	1.740	1.530	1.120	2.050	1.380
Σ			(0.591)	(2.980)	(2.670)	(2.020)	(3.490)	(2.440)
NON-OPTIMUM								
MECH. FAST.			0.180	0.200	0.200	0.200	0.200	0.200
WEB INTERS.			0.120	0.120	0.120	0.120	0.120	0.120
Σ			(0.300)	(0.320)	(0.320)	(0.320)	(0.320)	(0.320)
Σ	POINT DESIGN MASS	LBM FT ²	3.790	7.180	7.360	5.930	9.380	6.330

POINT DESIGN REGION			40322	40236	40536	41036	41316	41348
SPAR SPAC (m)			0.508	0.508	0.508	0.508	0.508	0.508
PANELS								
UPPER			4.028	5.039	7.856	7.090	12.553	7.968
LOWER			4.599	6.245	6.518	6.445	9.799	6.670
Σ			(8.627)	(11.284)	(14.374)	(13.535)	(22.352)	(14.638)
RIB WEBS								
BULKHEAD			1.455	1.362	1.162	0.542	1.318	0.518
TRUSS			0.361	1.157	1.113	0.293	—	—
Σ			(1.816)	(2.519)	(2.275)	(0.835)	(1.318)	(0.518)
SPAR WEBS								
BULKHEAD			1.640	1.763	1.318	0.532	2.143	(1.421)
TRUSS			1.470	2.656	2.392	1.753	—	—
Σ			(3.110)	(4.419)	(3.710)	(2.285)	(2.143)	(1.421)
RIB CAPS								
UPPER			0.283	0.342	0.566	0.454	0.781	(0.503)
LOWER			0.317	0.405	0.420	0.425	0.615	(0.361)
Σ			(0.600)	(0.747)	(0.986)	(0.879)	(1.396)	(0.864)
SPAR CAPS								
UPPER			1.177	6.054	5.566	4.394	7.031	5.176
LOWER			1.709	8.496	7.470	5.468	10.009	6.738
Σ			(2.886)	(14.550)	(13.036)	(9.862)	(17.040)	(11.914)
NON-OPTIMUM								
MECH. FAST.			0.879	0.976	0.976	0.976	0.976	0.976
WEB INTERS.			0.586	0.586	0.586	0.586	0.586	0.586
Σ			(1.465)	(1.562)	(1.562)	(1.562)	(1.562)	(1.562)
Σ	POINT DESIGN MASS	kg m ²	18.505	35.057	35.936	28.954	45.799	30.907

the chordwise-stiffened, the spanwise-stiffened, and the monocoque designs were 3.99-lbm/ft² (19.48-kg/m²), 6.38-lbm/ft² (31.15-kg/m²) and 0.97-lbm/ft² (4.74-kg/m²), respectively.

Composite reinforced spar caps were studied from the point of view of damage tolerance potential for the multiple element characteristics of the design. The load carried in the metallic substrate and each of the composite elements, as well as the total load, was calculated at the selected point design regions for the spar spacing boundary values, i.e., 20-in (0.51-m) and 40-in (1.02-m). An exception was the lower surface spar caps for 20-in (0.51-m) spacing at point design region 40322. Composite reinforcement was not used in this region due to the negligible mass saving indicated over the homogenous metal design. The results indicated that all composite reinforced spar caps were damage tolerant under the condition of a single broken element. The exception being the slightly negative margin (1-percent) indicated for the spar caps with 40-in (1.02-m) spacing at point design region 40322. No redesign of these caps was attempted since the strength analyses indicated the smaller spar spacings, between 20-in (0.51-m) and 30-in (0.76-m), were also close to the minimum-mass design.

Fuselage Shell: The most promising fuselage shell concepts surviving the initial screening analysis were subjected to an indepth structural evaluation at the four fuselage point design regions. These concepts consisted of the closed-hat and zee-stiffened designs, with the latter only applicable to the fuselage forebody, i.e., FS 750. In addition, only the minimum mass spacing, 20-in (0.51-m), defined in the initial screening analysis was used in the detail evaluation of these shell concepts. The point design environment used for this investigation is shown in Table 9.

In addition to the membrane analyses conducted on the shell, discontinuity analyses were conducted at the frame/shell interface to assess the total stress-state for both shell and frame. Typical results showing the circumferential material distribution for the hat-stiffened concept at FS 2500 are displayed in Table 13. Table 14 summarizes the total equivalent thickness for each point design region and the corresponding unit mass data. A maximum shell mass of 3.53-lbm/ft² (17.23-kg/m²) was indicated for the maximum fuselage bending region at FS 2500. A unit mass of 3.27-lbm/ft² (15.97-kg/m²) and 3.43-lbm/ft² (16.75-kg/m²) were indicated for FS 2000 and FS 3000, respectively.

The fuselage fail-safe evaluation considered both circumferential and longitudinal cracks for specified damage conditions. For circumferential cracks, a damage condition of a two-stringer pitch crack with one broken stringer was considered. The corresponding damage condition for the longitudinal cracks was a two-bay crack with the intermediate frame broken, i.e., a 40-in (1.02-m) crack for a fuselage frame spacing of 20-in (0.51-m).

In general, the results of the fail-safe analyses indicated positive margins-of-safety for the shell except for the side panels at FS 2000, 2500 and 3000. For these regions the circumferential crack damage condition was critical with a maximum negative margin of 55-percent noted on

TABLE 13. HAT-STIFFENED FUSELAGE PANEL GEOMETRY AT FS 2500

POINT DESIGN REGION	PANEL CONCEPT	CIRCUM. LOCATION	FUSELAGE PANEL DIMENSIONS						
			b_s	t_s	C	f	h	t_{st}	\bar{t}
			X.XX = in.; (X.XX) = mm						
FS 2500	HAT- STIFFENED	1 (TOP)	6.0 (152)	.100 (2.54)	1.50 (38.1)	.80 (20.3)	1.25 (31.8)	.090 (2.29)	0.184 (4.67)
		2	6.0 (152)	.070 (1.78)	1.50 (38.1)	.75 (19.1)	1.25 (31.8)	.070 (1.78)	0.134 (3.40)
		3	6.0 (152)	.063 (1.60)	1.50 (38.1)	.75 (19.1)	1.25 (31.8)	.063 (1.60)	0.121 (3.07)
		4 (SIDE)	6.0 (152)	.063 (1.60)	1.50 (38.1)	.75 (19.1)	1.25 (31.8)	.050 (1.27)	0.109 (2.77)
		5	6.0 (152)	.070 (1.78)	1.50 (38.1)	.75 (19.1)	1.25 (31.8)	.063 (1.60)	0.128 (3.25)

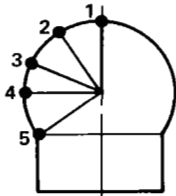
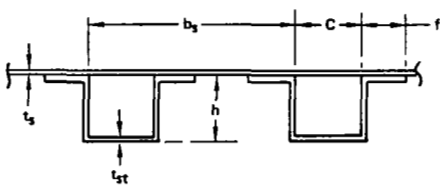
CIRCUMFERENTIAL LOCATIONS:	PANEL DIMENSIONS:
	

TABLE 14. FUSELAGE MASS SUMMARY FOR POINT DESIGN REGIONS

POINT DESIGN REGION	PANEL CONCEPT	EQUIV. PANEL THICKNESS ^(A)						UNIT MASS	
		FRAME		PANEL		TOTAL		lbm/ft ²	kg/m ²
		\bar{t}	\bar{t}	\bar{t}	\bar{t}	\bar{t}	\bar{t}		
FS 750	ZEE-STIFF.	0.011	(0.028)	0.056	(0.142)	0.067	(0.170)	1.54	7.52
FS 2000	HAT-STIFF.	0.023	(0.058)	0.119	(0.302)	0.142	(0.361)	3.27	15.97
FS 2500	HAT-STIFF.	0.022	(0.056)	0.131	(0.333)	0.153	(0.389)	3.53	17.23
FS 3000	HAT-STIFF.	0.023	(0.058)	0.126	(0.320)	0.149	(0.378)	3.43	16.75
(A) THICKNESS — in. ² /in. (cm ² /cm)									

the side panel at FS 2500. The mass penalty associated with this location was 1.43-lbm/ft² (6.98-kg/m²). Slight mass penalties were assessed to the remaining side panels at FS 2000 and FS 3000 which had less than 10-percent negative margins.

Stiffness-Design Analyses.-Vibration and flutter analyses were conducted for each of the structural arrangements (chordwise-stiffened, spanwise-stiffened and monocoque) using the stiffness and mass matrices from their respective strength-sized finite element models. The scope of this effort is presented in Table 15, and indicates the depth of the overall analysis and the rather extensive effort conducted on the chordwise-stiffened wing design. The chordwise-stiffened design evaluation was exploratory in nature and covered extensive combinations of mass, boundary conditions and Mach numbers to fully understand the flutter mechanisms and define the critical flutter condition. The spanwise-stiffened and monocoque arrangements were analyzed only for the critical flight conditions as defined in the chordwise-stiffened analyses.

Vibration analyses: A summary of the lower frequency symmetric vibration modes for the chordwise-stiffened arrangement are presented in Table 16. Mode frequency comparisons for the operating empty mass (OEM) and the full-fuel and full-payload (FFFP) mass conditions are shown for the strength-designed chordwise-stiffened arrangement. In addition, the lower frequency symmetric vibration modes for the spanwise-stiffened and the monocoque arrangements are presented in Table 17 for the FFFP condition. The chordwise-stiffened design results are included in this table for reference. A comparison of the mode frequency indicates that the monocoque design had the greatest stiffness and that the spanwise-stiffened design was the most flexible. The mode shapes for these three structural arrangements were virtually identical.

Flutter analyses: Symmetric flutter solutions were obtained for the chordwise-stiffened design at Mach 0.60, 0.90 and 1.25, for both OEM and FFFP conditions. In addition, the antisymmetric flutter condition at Mach 0.90 was investigated. As a result of these analyses, three distinct flutter modes were noted and are clearly illustrated in Figure 39 for the symmetric flutter solutions for the OEM condition at Mach 0.60. The mode identification numbers of 3 through 8 correspond to the mode number identification presented for the lower frequency symmetric vibrations modes of Table 16. Three distinct flutter modes are noted: the bending and torsion mode, the hump mode, and the stability mode. The flutter speeds for the bending and torsion mode, and the stability mode are 460-keas (852-km/h) and 500-keas (926-km/h), respectively.

A summary of the flutter speeds for each Mach number investigated for the chordwise-stiffened arrangement is presented in Figures 40 through 42 for the symmetric bending and torsion mode, the symmetric hump mode, and the symmetric stability mode. These figures show the V_D and $1.2 V_D$ envelopes as a function of pressure altitude versus knots equivalent airspeed overlayed with the analysis Mach number lines of 0.60, 0.90, and 1.25. Flutter boundaries for the various modes are indicated by the cross-hatched line. The lowest flutter speed of 379-keas (702-km/h) occurs for the symmetric bending and torsion mode at Mach 0.90. The flutter modes for this condition are shown in Figure 43.

TABLE 15. VIBRATION AND FLUTTER ANALYSES

BASELINE ARRANGE- MENT	VIBRATION ANALYSES				FLUTTER ANALYSES				
	SYMMETRIC		ANTISYMMETRIC		MACH NO	SYMMETRIC		ANTISYMMETRIC	
	AIRCRAFT MASS					AIRCRAFT MASS			
	OEM	FFFP	OEM	FFFP		OEM	FFFP	OEM	FFFP
CHORDWISE - STIFFENED	✓	✓	✓	✓	0.60	✓	✓		
					0.90	✓	✓	✓	✓
					1.25	✓	✓		
SPANWISE - STIFFENED		✓			0.60				
					0.90		✓		
					1.25				
MONOCOQUE		✓			0.60				
					0.90		✓		
					1.25				

OEM ~ AIRCRAFT MASS = 321,000 lbm (145,600 kg)

FFFP ~ AIRCRAFT MASS = 750,000 lbm (340,000 kg)

TABLE 16. LOWER FREQUENCY SYMMETRIC VIBRATION MODES FOR THE CHORDWISE-STIFFENED STRUCTURAL ARRANGEMENT

MODE NUMBER	MODE DESCRIPTION	MODE FREQUENCY Hertz	
		OEM	FFFP
1	RIGID BODY	0.000	0.000
2	RIGID BODY	0.001	0.001
3	WING 1ST BENDING	1.009	0.933
4	FUSELAGE 1ST BENDING	1.381	1.206
5	ENGINE PITCH IN PHASE	1.641	1.627
6	ENGINE PITCH OUT OF PHASE	1.817	1.815
7	FUSELAGE 2ND BENDING	2.784	2.261
8	WING 1ST TORSION	3.288	3.104

OEM ~ AIRCRAFT MASS = 321,000 lbm (145,600 kg)

FFFP ~ AIRCRAFT MASS = 750,000 lbm (340,000 kg)

TABLE 17. LOWER FREQUENCY FFFP SYMMETRIC VIBRATION MODES FOR STRUCTURAL ARRANGEMENTS

MODE NUMBER	MODE DESCRIPTION	MODE FREQUENCY Hertz		
		SPANWISE - STIFFENED ARRANGEMENT	CHORDWISE - STIFFENED ARRANGEMENT	MONOCOQUE ARRANGEMENT
1	RIGID BODY	0.000	0.000	0.000
2	RIGID BODY	0.000	0.001	0.000
3	WING 1ST BENDING	0.905	0.933	1.010
4	FUSELAGE 1ST BENDING	1.174	1.206	1.267
5	ENGINE PITCH IN PHASE	1.635	1.627	1.714
6	ENGINE PITCH OUT OF PHASE	1.825	1.815	1.955
7	FUSELAGE 2ND BENDING	2.129	2.261	2.236
8	WING 1ST TORSION	3.032	3.104	3.371

FFFP ~ AIRCRAFT MASS = 750,000 lbm (340,000 kg)

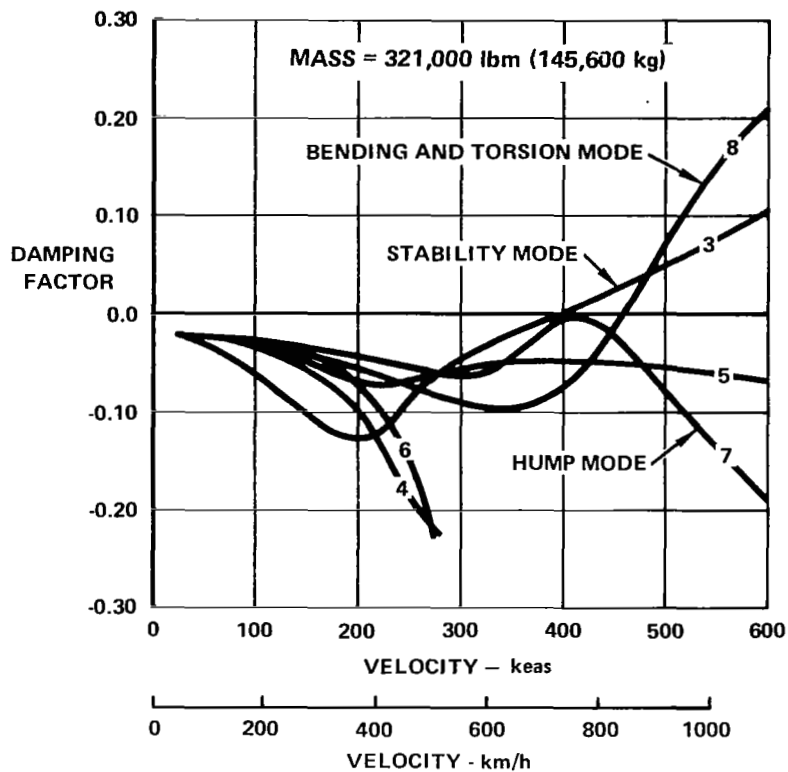


Figure 39. Symmetric Flutter Analysis for Chordwise-Stiffened Arrangement - Mach 0.6 - OEM

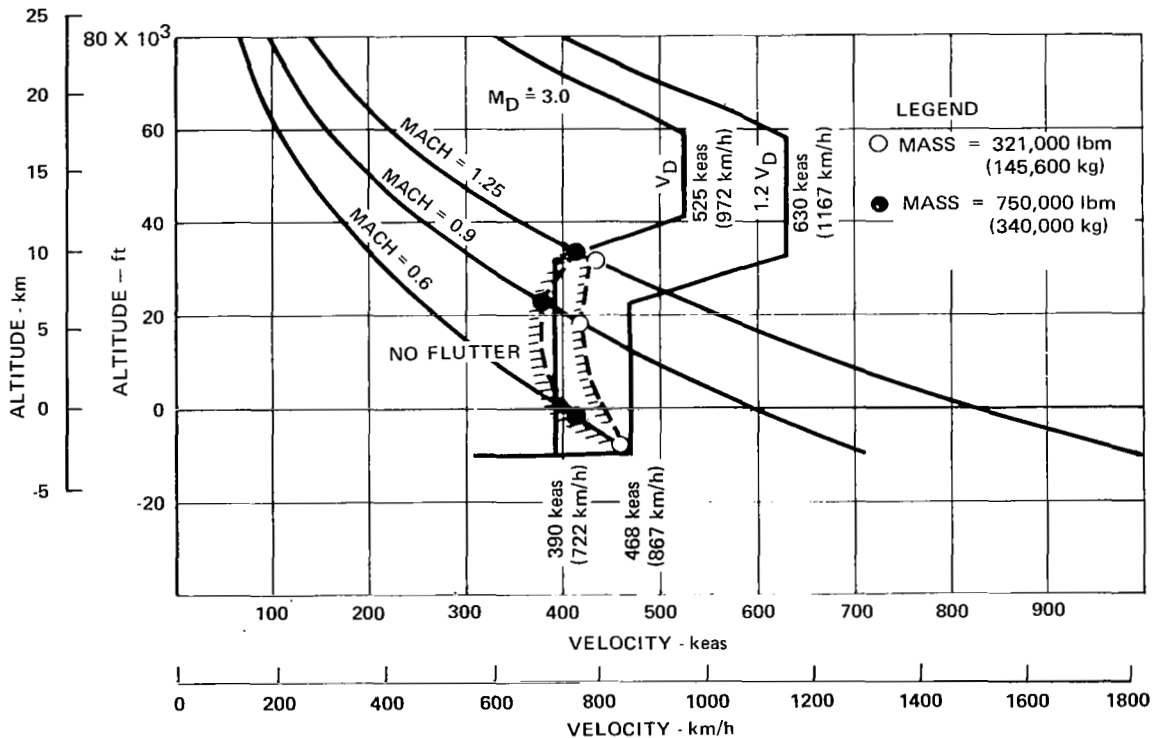


Figure 40. Flutter Speeds for Symmetric Bending and Torsion Mode - Chordwise-Stiffened Arrangement

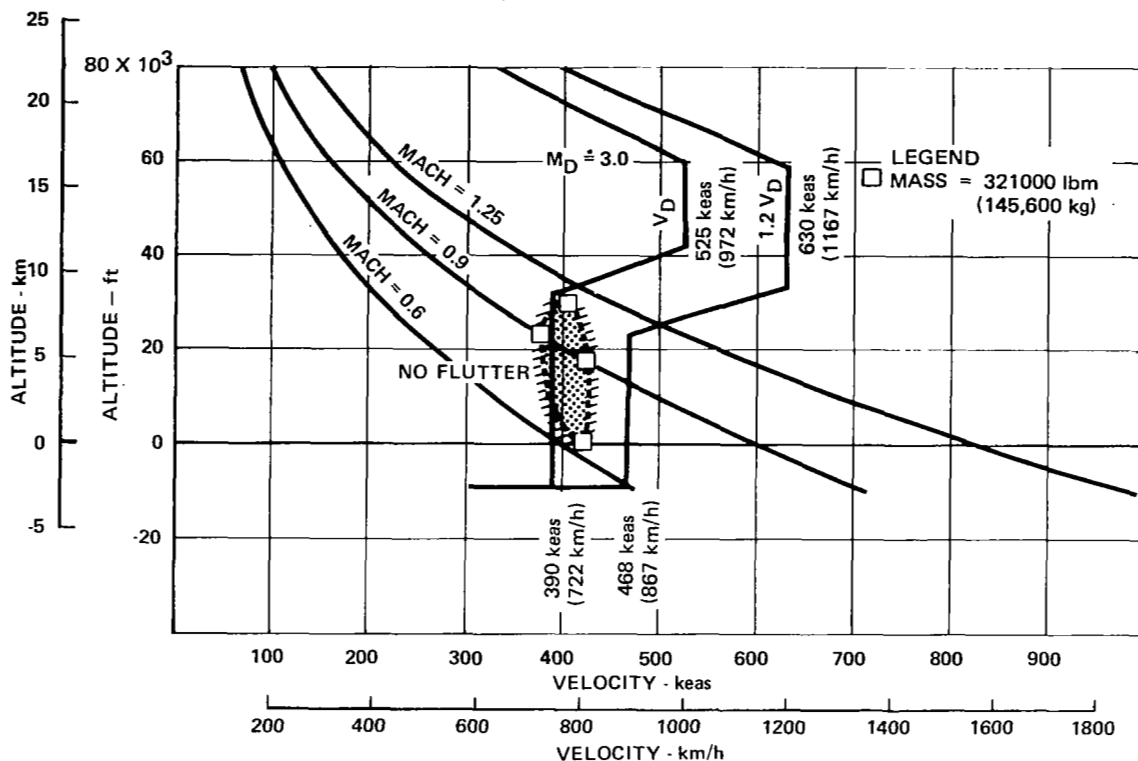


Figure 41. Flutter Speeds for Symmetric Hump Mode - Chordwise-Stiffened Arrangement

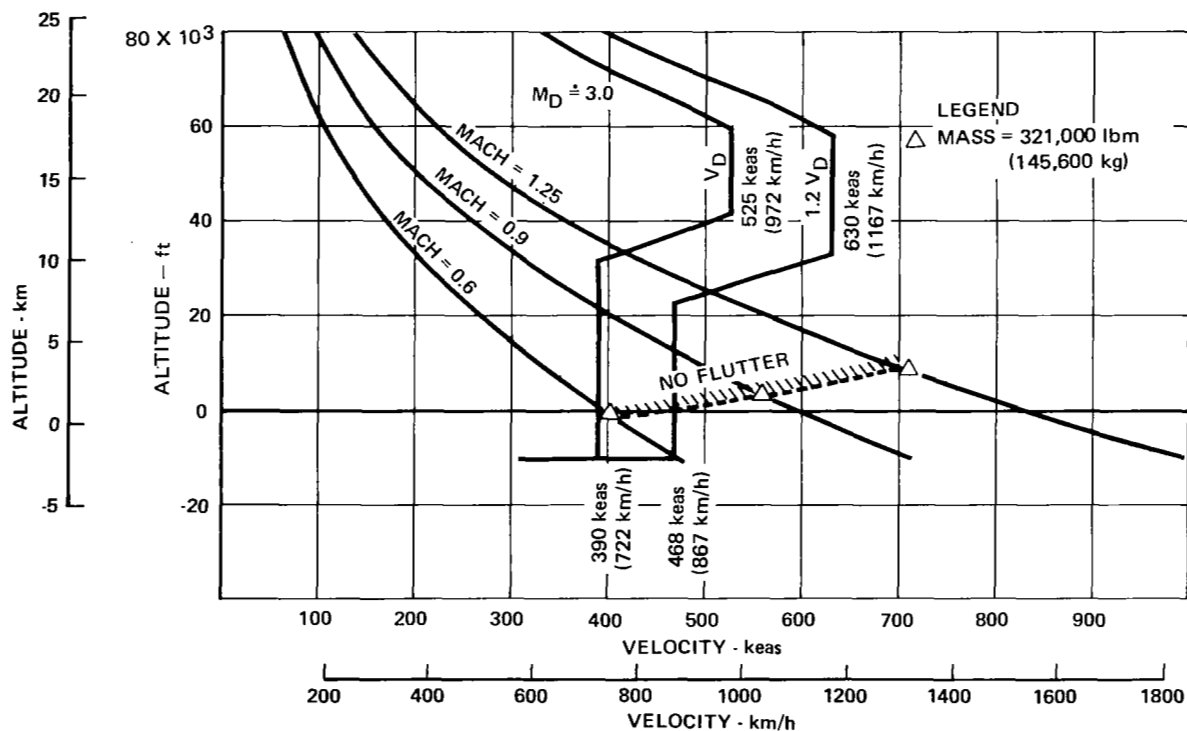


Figure 42. Flutter Speeds for Symmetric Stability Mode - Chordwise-Stiffened Arrangement

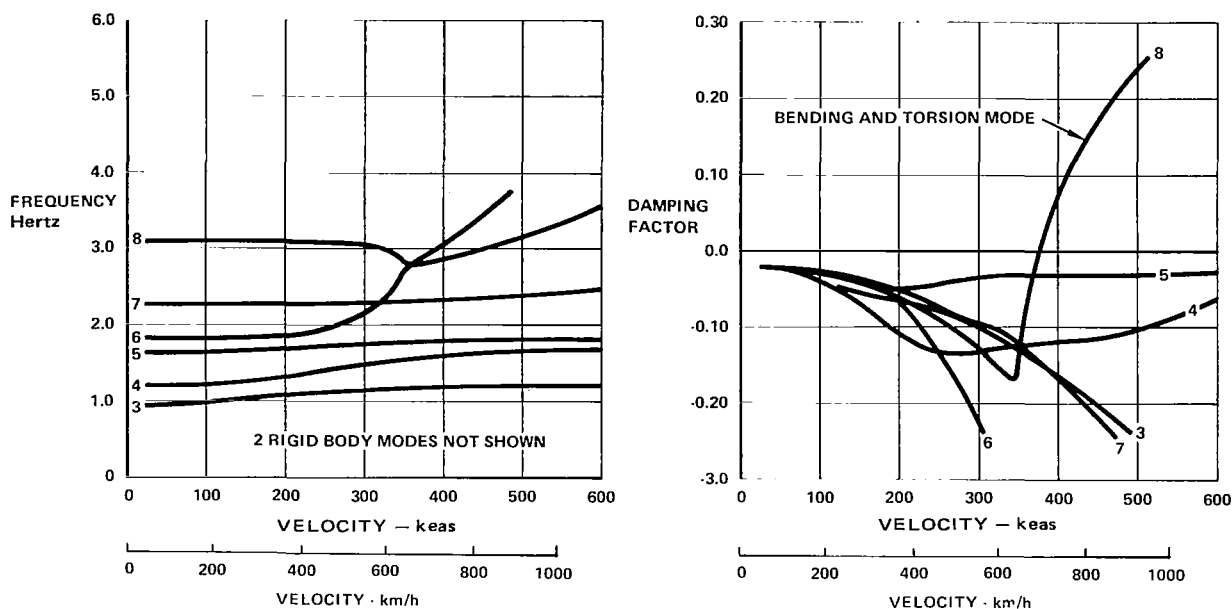


Figure 43. Symmetric Flutter Analysis - Mach 0.9 - FFFP
Chordwise-Stiffened Arrangement

A study was conducted to assess the effect the wing tip structure had on the control of the critical bending and torsion mode. For this investigation, the chordwise-stiffened arrangement was analyzed for the FFFP condition with the aircraft rigidized except for a flexible wing outboard of Buttline 470. The flutter analysis of this configuration indicated that for Mach 0.90, the wing 1st-bending mode rapidly increases in frequency with increasing velocity and coalesces with the wing 1st-torsion mode to flutter at 418-keas (774-km/h). This flutter mechanism was identical to the flutter mechanism for the flexible aircraft. For the flexible aircraft, Figure 43, the bending and torsion mode flutter velocity was 379-keas (702-km/h). Thus, infinite stiffness inboard of BL470 increased the flutter speed by only 10 percent. It is evident that the wing-tip structure (outer wing) controls the bending-and-torsion mode flutter mechanism.

Based on the results for the chordwise-stiffened design, the most significant flutter condition occurred at a Mach number of 0.90 for the FFFP condition for the symmetric boundary condition. This condition was, therefore, selected as the candidate for the flutter analysis of the spanwise-stiffened and monocoque wing designs. Symmetric flutter solutions for the FFFP conditions at Mach 0.90 are shown for the spanwise-stiffened and the monocoque arrangements on Figures 44 and 45, respectively. The analysis of the spanwise-stiffened design indicates only the bending and torsion mode and the stability mode were active whereas the bending and torsion mode was the only distinct mechanism noted for the monocoque design. The flutter speeds for

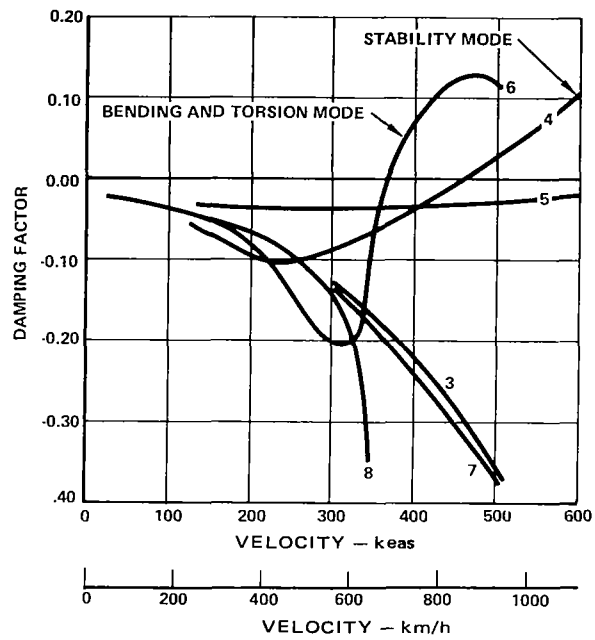


Figure 44. Symmetric Flutter Analysis - Mach 0.9 - FFFP - Spanwise-Stiffened Arrangement

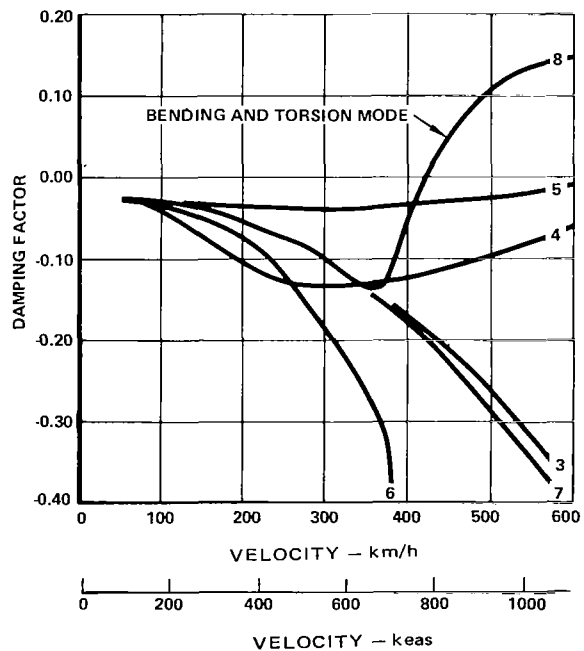


Figure 45. Symmetric Flutter Analysis - Mach 0.9 - FFFP - Monocoque Arrangement

the spanwise-stiffened and the monocoque arrangements were 364-keas (674-km/h) and 423-keas (783-km/h), respectively for the symmetric bending and torsion mode for the FFFP condition at Mach 0.90. For comparison purposes, the flutter speed for the chordwise-stiffened arrangement for the same condition was 379-keas (702-km/h).

Flutter optimization: The vibration and flutter analyses conducted on the chordwise-stiffened, the spanwise-stiffened, and the monocoque structural arrangements indicated that the symmetric bending and torsion mode for the FFFP condition at Mach 0.90 resulted in the lowest symmetric flutter speed. A review of the results of the foregoing analyses suggested that stiffening the wing tip structure would eliminate the hump mode flutter (symmetric and antisymmetric) and would permit the bending and torsion mode flutter speeds to be pushed beyond the $1.2 V_D$ envelope. Incremental stiffness requirements and resulting mass additions to push the flutter speed beyond the $1.2 V_D$ envelope of 468-keas (867-km/h) were determined for three structural arrangements.

To determine the effectiveness and the optimum distribution of material within a particular region of the airplane, the wing planform was divided into eight regions plus two additional regions for the two engine support beams. Figure 13a displays the location of these ten regions on the wing planform.

The GFAM flutter optimization program was employed in determining the most effective region for stiffness and mass additions to achieve the desired flutter speed for each of the structural arrangements.

The chordwise-stiffened arrangement was optimized by increasing spar cap areas and the skin and web thickness to provide an increase in spanwise bending and torsional stiffness, respectively. For the chordwise-stiffened arrangement, 2210-lbm (1002-kg) of additional structural material (per aircraft) was required in region 8 to increase the bending and torsion flutter speed from 379-keas (702-km/h) to 468-keas (867-km/h). The optimum stiffness/mass distribution was 425-lbm (193-kg) in the spar caps and 680-lbm (308-kg) in the webs and skin (per side), as shown in Figure 46.

The monocoque arrangement was also evaluated to determine the effectiveness of the design regions to achieve the required flutter speed. Region 8 was again the most effective region, requiring 1240-lbm (562-kg) of additional structural material (per side) to increase the bending and torsion flutter velocity from 423-keas (783-km/h) to 468-keas (867-km/h).

The flutter mass penalty for the spanwise-stiffened design was estimated using the data of the foregoing analyses. For both the chordwise-stiffened and monocoque arrangements, the incremental mass (per aircraft) required to raise the flutter speed by one-keas (1.852-km/h) was 27.6 lbm (12.5-kg). Thus, a flutter penalty of 2752-lbm (1248-kg) was added (per aircraft) to the spanwise-stiffened arrangement.

Production wing panel sizes were determined from the preliminary design drawings for each of the five wing designs. In general the structure was divided into six elements: the upper and lower skin assemblies plus two different spar and rib designs. This structural breakdown was typical in each wing area (forward, aft, tip) and for each wing design concept.

Production costs were estimated for: (1) the weld-bonded beaded panel design, (2) the weld-bonded hat-stiffened panel design, and (3) the aluminum brazed honeycomb core sandwich design, using appropriate advanced producibility techniques. The spar and rib configuration costs were determined for each wing design, considering such factors as metal removal and welding requirements. Production manhours were developed using the joint designs consistent with each design concept.

Fabrication data for the upper and lower skin assemblies were estimated by the manhours and material mass per square foot of each panel. The fabrication data for the linear structure, such as caps, webs, etc., were determined by the lineal foot. All assembly data were based on type of joint design, such as number of fasteners, length of weld, etc., and were also estimated by the lineal foot.

For each design concept, the total manhours, material costs and tool-make manhours to manufacture the first production aircraft were developed for the forward, aft, and wing tip areas. Table 18 summarizes these results in addition to presenting the wing mass for each wing design concept. A summary of the production costs in terms of "value per pound" are tabulated in Table 19. These "value per pound" increments are used as the cost input data for Lockheed-California's ASSET (Advanced System Synthesis and Evaluation Technique) computer program (Reference 1).

Concept Selection

The various wing design concepts, each with a conventional skin-stringer-frame fuselage design, were evaluated with respect to structural mass, performance and cost using the ASSET computer program. These factors were interrelated to yield comparison data for both a constant mass aircraft and a constant payload-range aircraft.

The structural mass data for the three main segments of the wing structure are shown in Table 20 for the five structural arrangements. These wing masses are divided into two major categories: a variable and a fixed mass increment for each wing design. The variable mass consists of that portion of the box structure which is calculated from the results of the ultimate and fatigue strength, fail-safe and sonic fatigue analyses conducted on a point design basis, as well as, the results of the overall aircraft flutter evaluations. The fixed mass consists of those items which are unaffected by box structural concept, such as main landing gear provisions, surface controls, engine support structure, and leading and trailing edge structure.

TABLE 18. TOTAL MANHOURS - MATERIALS AND TOOLING COSTS


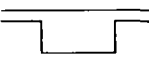

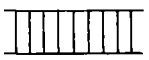

ITEM	UNITS	ARRANGEMENTS				
		CHORDWISE	SPANWISE	MONOCOQUE MECH. FAST.	MONOCOQUE WELDED	COMPOSITE REINFORCED
FABRICATION AND SUB ASSEMBLY MANHOURS	hr x 10 ³	456	394	701	717	439
JOINT ASSEMBLY AND TANK SEAL MANHOURS	hr x 10 ³	308	716	1623	90	354
TOTAL PRODUCTION MANHOURS	hr x 10 ³	764	1110	2324	807	793
MATERIAL COST	\$ x 10 ³	1566	1881	3982	4033	2432
TOOL-MAKE MANHOURS	hr x 10 ³	8024	5127	6249	6117	8058
MASS	lbm	71,000	69,000	57,000	60,000	54,000
	kg	32,200	31,300	25,800	27,200	24,500

TABLE 19. SUMMARY OF PRODUCTION COSTS

VALUE PER POUND	ARRANGEMENTS				
	CHORDWISE	SPANWISE	MONOCOQUE MECH. FAST.	MONOCOQUE WELDED	COMPOSITE REINFORCED
PRODUCTION MANHOURS/lbm	10.8	16.0	40.8	13.4	14.7
MATERIAL \$/lbm	22.2	27.1	70.0	67.1	45.0
TOOL MAKE MANHOURS/lbm	114.0	73.9	109.6	101.8	149.7

NOTE: (VALUE PER KILOGRAM) = 2.2 (VALUE PER POUND)

TABLE 20. WING MASS FOR STRUCTURAL ARRANGEMENTS

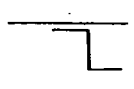


WING MASS AND SEGMENT		STRUCTURAL ARRANGEMENT				
		CHORDWISE	SPANWISE	MONOCOQUE	MONOCOQUE	CHORDWISE
		WELD BOND	WELD BOND	ALUM BRAZED	ALUM BRAZED	COMP. REINF.
		 MECH. FASTEN.	 MECH. FASTEN.	 MECH. FASTEN.	 WELDED	 SPARS ONLY
<u>VARIABLE MASS</u>	lbm	64,658	63,482	50,978	53,794	48,082
	(kg)	(29,328)	(28,795)	(23,123)	(24,400)	(21,810)
● FWD. BOX	lbm	22,090	25,364	21,982	24,057	20,580
	(kg)	(10,020)	(11,505)	(9,971)	(10,912)	(933)
● AFT BOX	lbm	29,016	25,242	19,692	20,153	17,384
	(kg)	(13,161)	(11,450)	(8,932)	(9,141)	(7,885)
● TIP	lbm	13,552	12,876	9,304	9,584	10,118
	(kg)	(6,147)	(5,840)	(4,220)	(4,347)	(4,589)
<u>FIXED MASS</u>	lbm	41,352	41,352	41,352	41,352	41,352
	(kg)	(18,757)	(18,757)	(18,757)	(18,757)	(18,757)
Σ TOTAL~	lbm	106,010	104,834	92,330	95,146	89,434
	(kg)	(48,085)	(47,552)	(41,880)	(43,157)	(40,566)

The component and total mass for the most promising fuselage approach is shown in Table 21. The results of the point design analyses are reflected in the shell mass which totals 23,148-lbm (10,500-kg). The total fuselage mass is 42,688-lbm (19,363-kg), which includes 19,540-lbm (8,863-kg) of fixed mass as delineated in the lower portion of this table.

In conjunction with the aforementioned wing and fuselage mass data, the production costs were input data for the ASSET program synthesis of the constant mass and constant payload-range aircraft.

Constant Mass Aircraft.—The structural mass of the aircraft was estimated for each of the candidate structural approaches based on the premise of a fixed vehicle size and taxi mass of 750,000-lbm (340,000-kg). This permitted the determination of the allowable fuel for the aircraft; hence the range capability, RDT&E, production and maintenance costs, for each of the candidate structural approaches were determined. A direct comparison of the structural mass, range and cost was made on the basis of constant airplane configuration and gross mass (Table 22a). A comparison of the various parameters (i.e., structural mass, range, cost) for the constant size/mass aircraft indicated a variation in these parameters and the minimum did not necessarily identify the best concept. The minimum-mass wing concept was the composite-reinforced chordwise-stiffened design; the spanwise-stiffened design was, however, the least initial cost concept as typified by the flyaway cost. It can be seen from the tabulated data that the mass savings realized by the application of composites to the spar caps permits approximately 16,600-lbm (7530-kg) of additional fuel to be carried. Hence, the range capability of the structurally efficient composite-reinforced design was approximately 340-nmi (630-km) greater than the basic chordwise-

TABLE 21. FUSELAGE MASS ESTIMATES

				
OPTIMUM UNIT MASS lbm/ft ² (kg/m ²) AT STATION:	750	1.56 (7.62)	1.56 (7.62)	1.54 (7.52)
	2000	3.54 (17.28)	3.51 (17.14)	3.27 (15.97)
	2500	4.03 (19.68)	3.86 (18.85)	3.53 (17.23)
	3000	3.54 (17.28)	3.51 (17.14)	3.43 (16.75)
	3723	2.15 (10.50)	2.15 (10.50)	2.15 (10.50)
AVERAGE SHELL MASS (INCL. NOF), $w_{SHELL}^{(1)}$	lbm/ft ²	3.44	3.39	3.23
	(kg/m ²)	(16.80)	(16.55)	(15.77)
SHELL MASS ⁽²⁾	(lbm)	24,654	24,296	23,148
	(kg)	(11,183)	(11,020)	(10,500)
FIXED MASS lbm (kg)				
NOSE AND FLIGHT STATION		2,500	(1134)	19,540 (8,863)
NLG WELL		900	(408)	
WINDSHIELD AND WINDOWS		1,680	(762)	
FLOORING AND SUPTS.		3,820	(1733)	
DOORS AND MECHANISM		4,170	(1891)	
UNDERWING FAIRING		1,870	(848)	
CARGO COMPARTMENT PROV.		1,060	(481)	
WING/BODY FITTINGS		1,500	(680)	
TAIL/BODY FITTINGS		600	(272)	
PROV. FOR SYSTEMS		740	(336)	
FINISH AND SEALING		700	(318)	
TOTAL FUSELAGE MASS	(lbm)	44,194	43,836	42,688
	(kg)	(20,046)	(19,884)	(19,363)

(1) AVERAGE SHELL MASS = $0.232 (w_{750} + w_{2000} + w_{2500} + w_{3000} + w_{3723})$

(2) SHELL AREA (FS 690 TO 3723) = 7167 ft² (666 m²)

TABLE 22. STRUCTURAL ARRANGEMENT EVALUATION DATA

(a) CONSTANT MASS AIRCRAFT

WING DESIGN CONCEPTS		CHORDWISE (MECHANICAL)	SPANWISE (MECHANICAL)	MONOCOQUE (MECHANICAL)	MONOCOQUE (WELDED)	CHORDWISE (COMP. REINF.)
CONSTANT TAKEOFF GROSS MASS (TOGM)						
TOGM	(lbm)	750,000	750,000	750,000	750,000	750,000
OEM	(lbm)	329,474	328,315	315,982	318,759	313,125
WING MASS	(lbm)	106,010	104,834	92,330	95,146	89,434
WING AREA	(ft ²)	10,822	10,822	10,822	10,822	10,822
WING UNIT MASS	(lbm/ft ²)	9.80	9.69	8.53	8.79	8.26
RANGE	(n-mi)	3830	3870	4123	4066	4166
FLYAWAY COST	(mil dol)	90.65	89.19	104.93	104.79	93.81
DOC	(c/sm)	1.94	1.92	2.03	2.04	1.92
IOC	(c/sm)	0.94	0.93	0.91	0.91	0.90
ROI	(%)	1.12	1.48	0.30	0.06	1.74
CONSTANT TAKEOFF GROSS MASS (TOGM)						
TOGM	(kg)	340,000	340,000	340,000	340,000	340,000
OWE	(kg)	149,100	148,600	130,000	144,300	141,700
WING MASS	(kg)	48,000	47,400	41,800	43,100	40,500
WING AREA	(m ²)	1005	1005	1005	1005	1005
WING UNIT MASS	(kg/m ²)	47.84	47.31	41.65	42.92	40.33
RANGE	(km)	7093	7167	7636	7530	7715
FLYAWAY COST	(mil dol)	90.65	89.19	104.93	104.79	93.81
DOC	(c/sm)	1.94	1.92	2.03	2.04	1.92
IOC	(c/sm)	0.94	0.93	0.91	0.91	0.90
ROI	(%)	1.12	1.48	0.30	0.06	1.74

(b) CONSTANT PAYLOAD-RANGE AIRCRAFT

WING DESIGN CONCEPTS		CHORDWISE (MECHANICAL)	SPANWISE (MECHANICAL)	MONOCOQUE (MECHANICAL)	MONOCOQUE (WELDED)	CHORDWISE (COMP. REINF.)
CONSTANT PAYLOAD-RANGE :						
TOGM	(lbm)	884,847	867,126	772,641	789,992	759,498
OEM	(lbm)	381,691	373,353	324,109	333,338	316,481
WING MASS	(lbm)	129,895	125,254	95,682	101,296	90,785
WING AREA	(ft ²)	12,768	12,512	11,149	11,399	10,959
WING UNIT MASS	(lbm/ft ²)	10.20	10.00	8.58	8.89	8.28
RANGE	(n-mi)	4200	4200	4200	4200	4200
FLYAWAY COST	(mil dol)	103.19	99.83	107.52	109.39	94.73
DOC	(c/sm)	2.14	2.09	2.06	2.11	1.93
IOC	(c/sm)	0.94	0.94	0.91	0.91	0.90
ROI	(%)	-1.37	-0.74	-0.11	-0.64	1.55
CONSTANT PAYLOAD-RANGE :						
TOGM	(kg)	400,500	392,400	349,700	357,500	343,700
OEM	(kg)	712,800	169,000	146,700	150,900	143,200
WING MASS	(kg)	58,800	56,700	43,300	45,800	41,100
WING AREA	(m ²)	1186	1162	1036	1059	1018
WING UNIT MASS	(kg/m ²)	49.80	48.82	41.89	43.41	40.43
RANGE	(km)	7778	7778	7778	7778	7778
FLYAWAY COST	(mil dol)	103.19	99.83	107.52	109.39	94.73
DOC	(c/sm)	2.14	2.09	2.06	2.11	1.93
IOC	(c/sm)	0.94	0.94	0.91	0.91	0.90
ROI	(%)	-1.37	-0.74	-0.11	-0.64	1.55

stiffened wing design. None of the concepts, however, met the range criterion of 4200-nmi (7778-km). A reduction in structural mass of 1700-lbm (771-kg) was required for the composite-reinforced design to satisfy the payload-range requirement.

Constant Payload-Range Aircraft.-The airplane configuration and gross mass were resized to meet the payload 49,000-lbm (22,000-kg), and range 4200-nmi (7,800-km), requirements. The purpose of the resizing was not to suggest that the airplane configuration (size) be changed, but rather to provide a tool for assessing the impact of the candidate structural concepts and materials evaluated on a common basis, i.e., constant payload-range performance.

The constant payload-range data of Table 22b indicate that the take-off gross mass of the resized aircraft varies from a maximum of 885,000-lbm (401,400-kg) to a minimum of 760,000-lbm (344,700-kg). The data also indicated that the minimum structural mass, size and cost are achieved with the composite-reinforced design.

Hybrid Design Concept.-Based on a constant-mass airplane the ranking of the design concepts shown in Table 23 was obtained. The wing mass data reflect the division of the total wing mass by the planform area. When these design concepts were applied to a constant payload-range airplane and ranked in terms of total system cost, the ranking of the concepts was unchanged (Table 24). The relative costs presented in the table show the other concepts to be 7-to 11-percent more expensive than the composite-reinforced design.

The best homogenous (single concept applied to total wing) structural approach for design of the Mach 2.7 supersonic cruise aircraft was the least-cost and -mass chordwise-stiffened design with metallic surface panels and composite-reinforced spars. Approximately 6000-lbm (2722-kg) of composite materials was used and resulted in 16,600-lbm (7530-kg) saving of wing structural mass.

The importance of minimum mass structural concepts was emphasized by the increasing cost trends with an increase in wing structural mass as shown in Table 24. Mass inefficiencies evaluated under the constant payload-range constraints can and do raise costs. Consequently, this class of aircraft exhibits a high growth factor, i.e., a 1-lbm (0.45-kg) increase in structural mass results in a 6-lbm (2.72-kg) increase in the aircraft takeoff gross mass. As a result, considerable effort is warranted to remove unnecessary mass to minimize the cascading effects on aircraft size and take-off gross mass.

From a review of the structural mass data for the various regions of the wing structure shown in Table 20, it appeared that combining the minimum mass design concept regions into a hybrid wing design would result in the best approach for a Mach 2.7 design. Thus, the recommended structural approach for the detailed engineering design-analyses was a hybrid design using a combination of a primarily chordwise-stiffened wing structure arrangement, with a biaxially-stiffened monocoque arrangement for the wing tip (to satisfy flutter requirements), and a conventional frame-supported fuselage shell. The airplane mass and cost parameters are

TABLE 23. CONCEPT EVALUATION SUMMARY - CONSTANT MASS AIRCRAFT

CONCEPT	WING MASS		RELATIVE MASS
	lbm/ft ²	kg/m ²	
(1) CHORDWISE STIFFENED - CONVEX-BEADED PANELS	9.80	47.85	1.19
(2) SPANWISE STIFFENED - HAT-STIFFENED PANELS	9.69	47.31	1.17
(3) MONOCOQUE - ALUMINUM BRAZED HONEYCOMB CORE PANELS	8.53	41.65	1.03
(4) MONOCOQUE - ALUMINUM BRAZED HONEYCOMB CORE PANELS (WELDED)	8.79	42.92	1.06
(5) CHORDWISE STIFFENED - CONVEX-BEADED PANELS; B/PI REINFORCED SPARS	8.26	40.33	1.00

TABLE 24. CONCEPT EVALUATION SUMMARY - CONSTANT PAYLOAD-RANGE AIRCRAFT

STRUCTURAL ARRANGEMENT AND CONCEPT	WING MASS			COST	
	lbm/ft ²	kg/m ²	RELATIVE MASS	DOC (C/SM)	RELATIVE COST
(1) CHORDWISE STIFFENED - CONVEX-BEADED PANELS	10.20	49.80	1.23	2.14	1.11
(2) SPANWISE STIFFENED - HAT-STIFFENED PANELS	10.00	48.82	1.21	2.09	1.08
(3) MONOCOQUE - ALUMINUM BRAZED HONEYCOMB CORE PANELS	8.58	41.89	1.04	2.06	1.07
(4) MONOCOQUE - ALUMINUM BRAZED HONEYCOMB CORE PANELS (WELDED)	8.89	43.40	1.07	2.11	1.09
(5) CHORDWISE STIFFENED - CONVEX-BEADED PANELS; B/PI REINFORCED SPARS	8.28	40.43	1.00	1.93	1.00

shown in Table 25 for this hybrid design, for both the constant-mass and the constant payload-range criteria. As indicated, this preliminary design very nearly satisfies the payload-range requirements specified for the 750,000-lbm (340,000-kg) baseline configuration.

TABLE 25. EVALUATION DATA FOR HYBRID STRUCTURAL ARRANGEMENT

STRUCTURAL ARRANGEMENT		HYBRID ARRANGEMENT (MECHANICALLY FASTENED)	
CONSTANT MASS AIRCRAFT			
TOGM	lbm (kg)	750,000	(340,000)
OEM	lbm (kg)	312,322	(141,700)
WING MASS	lbm (kg)	88,620	(40,200)
WING AREA	ft ² (m ²)	10,822	(1,005)
WING UNIT MASS	lbm/ft ² (kg/m ²)	8.19	(40)
RANGE	n mi (km)	4183	(7,747)
FLYAWAY COST	(mil dol)	93.57	
DOC	(c/sm)	1.91	
IOC	(c/sm)	0.90	
ROI A.T.	(%)	1.82	
CONSTANT PAYLOAD-RANGE AIRCRAFT			
TOGM	lbm (kg)	754,665	(342,300)
OEM	lbm (kg)	313,963	(142,400)
WING MASS	lbm (kg)	89,216	(40,500)
WING AREA	ft ² (m ²)	10,889	(1,012)
WING UNIT MASS	lbm/ft ² (kg/m ²)	8.20	(40)
RANGE	n mi (km)	4200	(7778)
FLYAWAY COST	(mil dol)	94.02	
DOC	(c/sm)	1.92	
IOC	(c/sm)	0.90	
ROI A.T.	(%)	1.73	

ENGINEERING DESIGN-ANALYSES

Detailed engineering design-analyses of the hybrid design concept (Figure 47) were made to define the critical design parameters and the estimated structural mass of the final design airplane. These analyses were conducted using an iterative design procedure in which the detail structure was sized to meet the design strength requirements, and then the total airframe was evaluated to determine the additional structure required to eliminate any flutter deficiencies. The results of these design-analyses were then used to update the airframe stiffness and to repeat the design procedure until all of the design criteria were satisfied and a minimum-mass structure satisfying the design objectives achieved.

A detailed three-dimensional finite element model was developed for these analyses, incorporating the results of the configuration refinement investigations as well as those of the design concepts evaluation. This model was used to define the internal load environment for the point design analyses, and the airframe stiffness for the aeroelastic loads and flutter analyses.

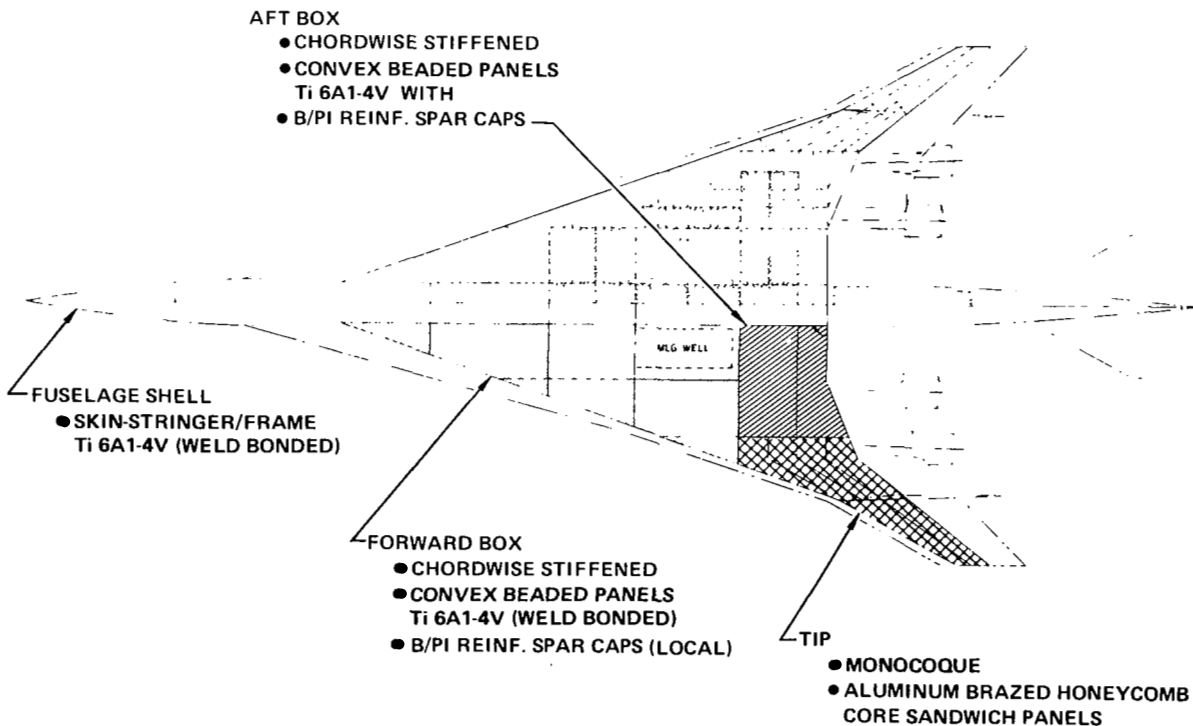


Figure 47. Hybrid Structural Approach

Wing Strength Analyses

The convex-beaded wing panel design was analyzed at point design region 40322 on the forward wing box and point design regions 40236 and 40536 on the aft wing box. The honeycomb sandwich design was analyzed at point design regions 41036, 41316 and 41348 on the wing tip and transition structure. Table 26 presents the load-temperature design environments at these regions for one of the most critical flight conditions, Mach 1.25 symmetrical maneuver.

Wing Ultimate and Fatigue Strength Analysis.-Panel cross sectional geometry, unit mass data and design conditions are shown in Tables 27 and 28 for the chordwise-stiffened and the monocoque surface panel designs, respectively. The convex-beaded panel designs were predominately sized by normal pressure with the minimum gage constraint, foreign object damage (FOD), active for the majority of the design region. The honeycomb sandwich designs were sized by the stiffness requirements for flutter suppression.

Table 29 summarizes the spar cap analysis results at the six point design regions. The spar spacing, cap areas and unit mass data are shown for each point design region. In the heavily loaded aft wing-box, composite-reinforced (B/PI) spar caps were employed.

The component and wing box unit mass data, resulting from the above strength analyses, are presented in Table 30. For the chordwise-stiffened design regions, a minimum mass of 3.80-lbm/ft² (18.55-kg/m²) occurs in the forward box (region 40322), and a maximum mass of 6.99-lbm/ft² (34.13-kg/m²) was noted in the aft box (region 40536). With respect to the honeycomb sandwich wing box designs, a unit mass of 7.44-lbm/ft² (36.33-kg/m²) is noted on the wing tip with a unit mass of 4.60-lbm/ft² (22.46-kg/m²) indicated for the transition region.

Wing Sonic Fatigue Analyses.-Table 31 presents a summary of the analyses to assess the sonic fatigue capability of the convex-beaded and honeycomb-sandwich surface designs. Appropriate panel locations, natural frequencies, applied and allowable spectrum sound levels are noted. A minimum sonic fatigue margin of +12 dB/Hz was indicated for the convex-beaded lower surface panels in the aft box region. As can be seen from these tables, positive margins-of-safety exist on each of the point design regions; thus, no mass penalty was assessed.

Wing Fail-Safe Analyses.-Fail-safe analyses of the convex-bead and honeycomb-sandwich designs indicated several panels were deficient and required additional structural material to meet the fail-safe criterion. A summary of the wing panel fail-safe analysis results is presented in Table 32. This table summarizes the pertinent fail-safe data, margins-of-safety and the corresponding mass penalties. The largest penalty associated with the convex-beaded concept was 1.47-lbm/ft² (7.18-kg/m²) for the lower panel at region 40536. Similarly, the maximum penalty for the honeycomb sandwich panel concept was 0.84-lbm/ft² (4.10-kg/m²) for the lower panel at region 41036. No added structural reinforcement was required on the convex-beaded concept at region 40322 and 40236 or the lower surface honeycomb sandwich panel at region 41348.

TABLE 26. WING POINT DESIGN ENVIRONMENT - MACH 1.25 SYMMETRIC MANEUVER-FINAL DESIGN

CONDITION 12 SYMMETRICAL FLIGHT, STEADY MANEUVER AT MACH 1.25 (V_p , $n_z = 2.5$)

ULTIMATE DESIGN LOADS	ITEM	UNITS	POINT DESIGN REGION											
			40322		41316		41348		40236		40536		41036	
			UPPER SURFACE	LOWER SURFACE	UPPER SURFACE	LOWER SURFACE	UPPER SURFACE	LOWER SURFACE	UPPER SURFACE	LOWER SURFACE	UPPER SURFACE	LOWER SURFACE	UPPER SURFACE	LOWER SURFACE
AIR LOADS	N_x	lbf/in	- 242	- 434	- 1,331	- 1,451	- 1,201	- 1,431	- 113	- 62	- 331	- 699	- 2,464	+ 1,898
	N_y	lbf/in	- 1,034	- 1,455	- 1,024	- 1,333	- 9,094	- 1,090	- 1,456	- 1,622	- 1,372	- 15,508	- 5,645	+ 4,697
	N_{xy}	lbf/in	102	111	- 1,070	- 1,739	2,116	2,551	491	791	1,615	1,646	2,334	1,812
THERMAL STRAIN	ϵ_x	in/in	0	0	0	0	0	0	0	0	0	0	0	0
	ϵ_y	in/in	0	0	0	0	0	0	0	0	0	0	0	0
	ϵ_{xy}	in/in	0	0	0	0	0	0	0	0	0	0	0	0
PRESSURE	AERO	psi	- 1.17	+ 1.17	- 4.21	- 1.24	- 5.07	- 1.91	- 3.03	- 1.20	- 1.27	- 0.26	- 1.27	- 0.11
	FUEL	psi	- 4.97	- 1.10					- 5.02	- 9.31	- 4.50	- 1.50	0	0
	NET	psi	- 4.44	- 1.33	- 4.91	- 1.24	- 5.07	- 1.91	- 5.11	- 10.51	- 5.77	- 4.76	- 1.27	- 0.11
TEMPERATURE	T_{AV}	F	RT	RT	RT	RT	RT	RT	RT	RT	RT	RT	RT	RT
	ΔT	F	0	0	0	0	0	0	0	0	0	0	0	0

ULTIMATE DESIGN LOADS	ITEM	UNITS	POINT DESIGN REGION											
			40322		41316		41348		40236		40536		41036	
			UPPER SURFACE	LOWER SURFACE	UPPER SURFACE	LOWER SURFACE	UPPER SURFACE	LOWER SURFACE	UPPER SURFACE	LOWER SURFACE	UPPER SURFACE	LOWER SURFACE	UPPER SURFACE	LOWER SURFACE
AIR LOADS	N_x	kN/m	-42	+76	-338	+290	-210	+250	-32	+11	-146	+122	-431	+332
	N_y	kN/m	-181	+250	-2318	+1985	-1517	+1418	-2882	+2911	-2867	+2716	-988	+822
	N_{xy}	kN/m	18	29	113	480	467	488	86	137	283	288	409	317
THERMAL STRAIN	ϵ_x	cm/cm	0	0	0	0	0	0	0	0	0	0	0	0
	ϵ_y	cm/cm	0	0	0	0	0	0	0	0	0	0	0	0
	ϵ_{xy}	cm/cm	0	0	0	0	0	0	0	0	0	0	0	0
PRESSURE	AERO	kPa	-10.14	+0.44	-34.34	-1.79	-34.96	+6.62	-20.89	-8.27	-8.76	-1.79	-8.76	+0.76
	FUEL	kPa	-34.27	-61.19			0	0	-35.02	-64.19	-31.03	-31.03	0	0
	NET	kPa	-44.41	-60.68	-34.34	-1.79	-34.96	+6.62	-55.91	-72.46	-39.79	-32.82	-8.76	+0.76
TEMPERATURE	T_{AV}	K	RT	RT	RT	RT	RT	RT	RT	RT	RT	RT	RT	RT
	ΔT	K	0	0	0	0	0	0	0	0	0	0	0	0

NOTES: (1) A 1.25 FACTOR HAS BEEN APPLIED TO THE THERMAL STRAIN WHEN THE SIGN IS SAME AS THE AIRLOAD SIGN, OTHERWISE NO FACTOR APPLIED.

(2) PRESSURE SIGN CONVENTION: NEGATIVE = SUCTION

TABLE 27. CONVEX-BEADED PANEL DATA

DESIGN DATA	POINT DESIGN REGIONS											
	40322				40236				40536			
	UPPER		LOWER		UPPER		LOWER		UPPER		LOWER	
SPACING, in. (m)	60.0	(1.52)	60.0	(1.52)	60.0	(1.52)	60.0	(1.52)	60.0	(1.52)	60.0	(1.52)
RIB	22.7	(0.58)	22.7	(0.58)	21.2	(0.54)	21.2	(0.54)	21.2	(0.54)	21.2	(0.54)
SPAR												
DIMENSIONS												
t_L , in. (cm)	.013	(.033)	.015	(.038)	.015	(.038)	.020	(.051)	.023	(.058)	.019	(.048)
t_U , in. (cm)	.015	(.038)	.020	(.051)	.015	(.038)	.020	(.051)	.026	(.066)	.020	(.051)
R_L , in. (cm)	.80	(2.03)	1.00	(2.54)	.80	(2.03)	1.00	(2.54)	.90	(2.29)	.70	(1.78)
θ , degrees (rad)	87	(1.52)	87	(1.52)	87	(1.52)	87	(1.52)	87	(1.52)	87	(1.52)
b , in. (cm)	.75	(1.90)	.75	(1.90)	.75	(1.90)	.75	(1.90)	.75	(1.90)	.75	(1.90)
pitch, in. (cm)	2.35	(5.97)	2.75	(6.98)	2.35	(5.97)	2.75	(6.98)	2.55	(6.48)	2.15	(5.46)
MASS DATA												
\bar{t} , in. (cm)	.033	(.084)	.041	(.104)	.036	(.091)	.048	(.122)	.058	(.147)	.048	(.117)
W , lbm/ft ² (kg/m ²)	.760	(3.71)	.945	(4.6)	.829	(4.05)	1.11	(5.42)	1.34	(6.54)	1.05	(5.13)
CRITICAL DESIGN COND.	12	12	20	20	16	16	16	16	12	12	12	12

DIMENSIONS:

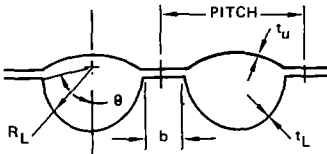
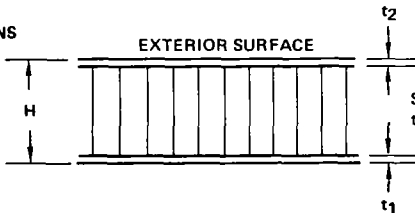


TABLE 28. HONEYCOMB SANDWICH PANEL DATA

DESIGN DATA	POINT DESIGN REGIONS					
	41036		41316		41348	
	UPPER	LOWER	UPPER	LOWER	UPPER	LOWER
SPACING, in. (m)	60.0 (1.52)	60.0 (1.52)	40.0 (1.02)	40.0 (1.02)	40.0 (1.02)	40.0 (1.02)
RIB	21.2 (0.54)	21.2 (0.54)	40.0 (1.02)	40.0 (1.02)	30.0 (0.76)	30.0 (0.76)
SPAR						
DIMENSIONS						
H, in. (cm)	.642 (1.63)	.202 (.513)	1.00 (2.54)	.500 (1.27)	1.00 (2.54)	.500 (1.27)
t_1 , in. (cm)	.026 (.067)	.023 (.058)	.062 (.157)	.075 (.190)	.068 (.172)	.068 (.172)
t_2 , in. (cm)	.018 (.046)	.028 (.071)	.062 (.157)	.075 (.190)	.068 (.172)	.068 (.172)
t_c , in. (cm)	.002 (.005)	.002 (.005)	.002 (.005)	.002 (.005)	.002 (.005)	.002 (.005)
S, in. (cm)	.275 (.698)	.500 (1.27)	.500 (1.27)	.500 (1.27)	.500 (1.27)	.500 (1.27)
MASS DATA						
\bar{t} , in. (cm)	.052 (.132)	.052 (.132)	.131 (.332)	.153 (.388)	.143 (.363)	.139 (.353)
W , lb./ft ² (kg/m ²)	1.20 (5.86)	1.20 (5.86)	3.02 (14.74)	3.52 (17.19)	3.29 (16.06)	3.20 (15.62)
CRITICAL DESIGN COND.	12	12	FLUTTER	FLUTTER	FLUTTER	FLUTTER

DIMENSIONS



S = CELL SIZE
 t_c = CORE FOIL THICKNESS

TABLE 29. SUMMARY OF WING SPAR CAP DATA

POINT DESIGN REGION	CAP LOCATION	CAP DESIGN	SPAR SPACING b		CAP AREA						CAP MASS W	
			in.	m	A _C		A _M		A _{TOTAL}		lbm/ft ²	kg/m ²
					in. ²	cm ²	in. ²	cm ²	in. ²	cm ²		
40322	UPPER	ALL METAL	22.7	0.577	—	—	0.24	1.55	0.24	1.55	0.24	1.17
	LOWER	6Al-4V Ti CAP	22.7	0.577	—	—	0.40	2.58	0.40	2.58	0.41	2.00
40236	UPPER	6Al-4V Ti CAP	21.2	0.538	1.51	9.74	0.45	2.90	1.96	12.64	1.23	6.00
	LOWER	WITH B/PI REINF	21.2	0.538	2.50	16.13	0.45	2.90	2.95	19.03	1.71	8.35
40536	UPPER	6Al-4V Ti CAP	21.2	0.538	1.50	9.68	0.45	2.90	1.95	12.58	1.22	5.96
	LOWER	WITH B/PI REINF.	21.2	0.538	2.30	14.84	0.45	2.90	2.75	17.74	1.61	7.86
41036	UPPER	6Al-4V Ti CAP	21.2	0.538	0.41	2.64	0.45	2.90	0.86	5.55	0.69	3.37
	LOWER	WITH B&PI REINFORCEMENT	21.2	0.538	0.50	3.22	0.45	2.90	0.95	6.12	0.73	3.56
41316	UPPER	ALL METAL	40.0	1.016	—	—	0.21	1.35	0.21	1.35	0.12	0.59
	LOWER	6Al-4V Ti CAP	40.0	1.016	—	—	0.18	1.16	0.18	1.16	0.12	0.59
41348	UPPER	ALL METAL	30.0	0.762	—	—	0.21	1.35	0.21	1.35	0.16	0.78
	LOWER	6Al-4V Ti CAP	30.0	0.762	—	—	0.18	1.16	0.18	1.16	0.14	0.68
NOTES: A _C = COMPOSITE AREA A _M = METAL AREA A _{TOTAL} = A _C + A _M W = EQUIVALENT SURFACE PANEL MASS $144(A_C \rho_C + A_M \rho_M)/b$												
					ρ_C = COMPOSITE (B/PI) DENSITY; 0.072 lbm/in. ³ (1993 – kg/m ²) ρ_M = METAL (6Al-4V) DENSITY; 0.160 lbm/in. ³ (4429 – kg/m ²) b = SPAR SPACING							

TABLE 30. DETAIL WING MASS FOR THE HYBRID STRUCTURAL ARRANGEMENT

POINT DESIGN REGION			40322	40236	40536	41036	41316	41348
<u>SPACING (in.)</u>								
SPAR			22.70	21.20	21.20	21.20	40.00	30.00
RIB			60.00	60.00	60.00	60.00	40.00	40.00
<u>PANELS</u>								
UPPER			0.76	0.83	1.34	1.20	3.02	3.29
LOWER			0.95	1.11	1.05	1.20	3.52	3.20
Σ			(1.71)	(1.94)	(2.39)	(2.40)	(6.54)	(6.49)
<u>RIB WEBS</u>								
BULKHEAD			0.30	0.28	0.24	0.13	0.19	0.10
TRUSS			0.07	0.24	0.23	0.11	—	—
Σ			(0.37)	(0.52)	(0.47)	(0.24)	(0.19)	(0.10)
<u>SPAR WEBS</u>								
BULKHEAD			0.34	0.36	0.28	0.10	0.19	0.30
TRUSS			0.30	0.54	0.49	0.19	—	—
Σ			(0.64)	(0.90)	(0.77)	(0.29)	(0.19)	(0.30)
<u>RIB CAPS</u>								
UPPER			0.06	0.08	0.12	0.08	0.08	0.08
LOWER			0.07	0.09	0.09	0.07	0.07	0.09
Σ			(0.13)	(0.17)	(0.21)	(0.15)	(0.15)	(0.17)
<u>SPAR CAPS</u>								
UPPER			0.24	1.23	1.22	0.69	0.12	0.16
LOWER			0.41	1.71	1.61	0.73	0.12	0.14
Σ			(0.65)	(2.94)	(2.83)	(1.42)	(0.24)	(0.30)
<u>NON-OPTIMUM</u>								
MECH. FAST.			0.18	0.20	0.20	0.05	0.03	0.04
WEB INTERS.			0.12	0.12	0.12	0.05	0.03	0.04
Σ			(0.30)	(0.32)	(0.32)	(0.10)	(0.06)	(0.08)
Σ	POINT DESIGN MASS	$\frac{\text{lbm}}{\text{ft}^2}$	3.80	6.79	6.99	4.60	7.37	7.44

TABLE 30. DETAIL WING MASS FOR THE HYBRID STRUCTURAL ARRANGEMENT
(Continued)

POINT DESIGN REGION			40322	40236	40536	41036	41316	41348
<u>SPACING (m)</u>								
SPAR			0.577	0.577	0.577	0.577	1.016	0.762
RIB			1.524	1.524	1.524	1.524	1.016	1.016
<u>PANELS</u>								
UPPER			3.71	4.05	6.54	5.86	14.74	16.06
LOWER			4.64	5.42	5.13	5.86	17.19	15.62
Σ			(8.35)	(9.47)	(11.67)	(11.72)	(31.93)	(31.68)
<u>RIB WEBS</u>								
BULKHEAD			1.46	1.37	1.17	0.63	0.93	0.49
TRUSS			0.34	1.17	1.12	0.54	—	—
Σ			(1.80)	(2.54)	(2.29)	(1.17)	(0.93)	(0.49)
<u>SPAR WEBS</u>								
BULKHEAD			1.66	1.75	1.37	0.49	0.93	1.46
TRUSS			1.46	2.64	2.39	0.93	—	—
Σ			(3.12)	(4.39)	(3.76)	(1.42)	(0.93)	(1.46)
<u>RIB CAPS</u>								
UPPER			0.29	0.39	0.59	0.39	0.39	0.39
LOWER			0.34	0.44	0.44	0.34	0.34	0.44
Σ			(0.63)	(0.83)	(1.03)	(0.73)	(0.73)	(0.83)
<u>SPAR CAPS</u>								
UPPER			1.17	6.00	5.96	3.37	0.59	0.78
LOWER			2.00	8.35	7.86	3.56	0.59	0.68
Σ			(3.17)	(14.35)	(13.82)	(6.93)	(1.18)	(1.46)
<u>NON-OPTIMUM</u>								
MECH. FAST.			0.88	0.98	0.98	0.24	0.15	0.20
WEB INTERS.			0.59	0.59	0.59	0.24	0.15	0.20
Σ			(1.47)	(1.57)	(1.57)	(0.48)	(0.30)	(0.40)
Σ	POINT DESIGN MASS	$\frac{\text{kg}}{\text{m}^2}$	18.55	33.15	34.13	22.46	35.98	36.33

TABLE 31. SUMMARY OF WING PANEL SONIC FATIGUE ANALYSES

POINT DESIGN REGION	WING SURFACE	NATURAL FREQUENCY f, (Hz)	SPECTRUM LEVEL(1)(2) (dB/Hz)		MINIMUM(3) SONIC FATIGUE MARGIN (dB/Hz)
			ALLOW.	ENVIR.	
40322	UPPER	120.4	110.0	91.0	+19.0
	LOWER	140.8	115.0	90.8	+24.2
40236	UPPER	138.9	114.0	101.6	+12.4
	LOWER	164.5	118.0	101.2	+16.8
40536	UPPER	151.3	120.0	101.8	+18.2
	LOWER	125.4	114.0	102.0	+12.0
41036	UPPER	234	137.9	101.6	+36.2
	LOWER	66	136.2	106.0	+30.2
41316	UPPER	175	146.0	105.0	+41.6
	LOWER	79	146.0	106.8	+39.2
41348	UPPER	264	146.3	105.4	+41.3
	LOWER	122	145.0	106.6	+38.4
NOTES: (1) ALLOWABLE SOUND LEVEL (2) APPLIED SOUND LEVEL (ENVIRONMENT) (3) SONIC-FATIGUE MARGIN: (ALLOWABLE dB/Hz – ENVIRONMENT dB/Hz)					

TABLE 32. SUMMARY OF WING PANEL FAIL-SAFE ANALYSES

DESIGN CONCEPT	POINT DESIGN REGION	WING SURFACE	MARGIN OF SAFETY	MASS PENALTY	
				lbm/ft ²	(kg/m ²)
CONVEX-BEADED PANELS	40322	UPPER LOWER	LARGE +1.28	NONE NONE	NONE NONE
	40236	UPPER LOWER	+1.52 +0.08	NONE NONE	NONE NONE
	40536	UPPER LOWER	+0.03 +0.06	0.16 1.47	0.78 7.18
HONEYCOMB- SANDWICH PANELS	41036	UPPER LOWER	+0.05 +0.01	0.55 0.84	2.68 4.10
	41316	UPPER LOWER	+0.05 +0.01	0.10 0.71	0.49 3.47
	41348	UPPER LOWER	+0.50 +0.11	NONE 0.09	NONE 0.44

The assumed damage condition for the wing spar analysis was that of a single broken member (composite reinforcement or metal substrate) with the applied limit loads redistributed to the remaining undamaged members. The results showed that all composite-reinforced caps were fail-safe with a minimum positive margin of 2-percent existing on the lower spar cap at point design region 41036.

Wing Box Mass.—The wing box mass resulting from the ultimate and fatigue strength, fail-safe and sonic fatigue analyses are presented in Table 33. The total wing box mass varies from 3.80-lbm/ft² (18.55-kg/m²) at the forward wing point design region to a maximum of 8.62-lbm/ft² (42.09-kg/m²) at the aft wing region.

Fuselage Strength Analyses

The zee-stiffened and closed hat-stiffened panel designs were subjected to point design analyses using the load-temperature environments at FS 900, FS 1910, FS 2525, and FS 2900. For each region, the analyses were conducted for six panel locations around the circumference, from the top centerline to the floor line or lower centerline (Figure 48). Table 34 presents the load-temperature environment at FS 2525 for the most critical flight condition for fuselage design, Mach 2.7 start-of-cruise symmetric maneuver. Dynamic landing, vertical gust and the other conditions which designed specific regions of the fuselage were also investigated.

TABLE 33. WING BOX MASS FOR POINT DESIGN REGIONS

POINT DESIGN REGION	STRENGTH	SONIC FATIGUE	FAIL-SAFE	TOTAL
	lbm/ft ² (kg/m ²)			
40322	3.80 (18.55)	0.00 (0.00)	0.00 (0.00)	3.80 (18.55)
40236	6.79 (33.15)	0.00 (0.00)	0.00 (0.00)	6.79 (33.15)
40536	6.99 (34.13)	0.00 (0.00)	1.63 (7.96)	8.62 (42.09)
41036	4.60 (22.46)	0.00 (0.00)	1.39 (6.78)	5.99 (29.24)
41316	7.37 (35.98)	0.00 (0.00)	0.81 (3.96)	8.18 (39.94)
41348	7.44 (36.33)	0.00 (0.00)	0.09 (0.44)	7.53 (36.77)

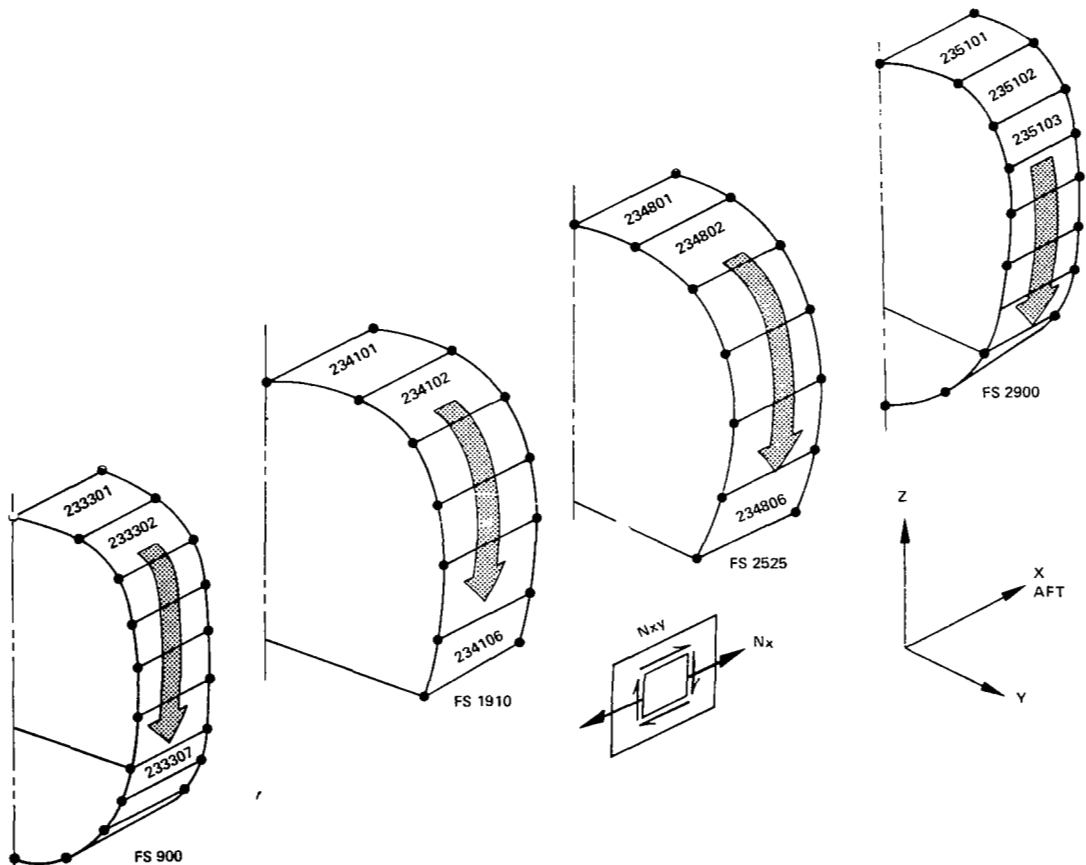


Figure 48. Fuselage Panel Identification

TABLE 34. FUSELAGE POINT DESIGN ENVIRONMENT - MACH 2.7 START-OF-CRUISE

CONDITION 20 SYMMETRIC MANEUVER AT MACH 2.70 (START-OF-CRUISE, $n_z = 2.5$)
WEIGHT = 660,000-lb

ITEM	UNITS	FS 2525 (23XXXX)					
		4801	4802	4803	4804	4805	4806
N_X	lbf/in	-12413	-7932	-4066	-1222	+664	+2319
N_{XY}	lbf/in	+67	+67	+6	-59	-120	-187
$N_{X, TH}$	lbf/in	+329	+57	-301	-646	-785	-272
$N_{XT, TH}$	lbf/in	+5	+14	+26	+24	+14	-10
AERO PRESS.	psi	-	-	-	-	-	-
INTERNAL PRESS.	psi	17.55	17.55	17.55	17.55	17.55	17.55
NET PRESS.	psi	17.55	17.55	17.55	17.55	17.55	17.55
T_{AVG}	F	281	287	293	300	307	311
ΔT	F	-186	-183	-180	-177	-173	-171

MASS = 299,400 kg

ITEM	UNITS	FS 2525 (23XXXX)					
		4801	4802	4803	4804	4805	4806
N_X	kN/m	-2174	-1389	-712	-214	116	406
N_{XY}	kN/m	12	12	1	-10	-21	-33
$N_{X, TH}$	kN/m	58	10	-53	-113	-137	-48
$N_{XT, TH}$	kN/m	1	2	5	4	2	-2
AERO PRESS.	kPa	-	-	-	-	-	-
INTERNAL PRESS.	kPa	121	121	121	121	121	121
NET PRESS.	kPa	121	121	121	121	121	121
T_{AVG}	K	411	415	418	422	426	428
ΔT	K	-103	-102	-100	-98	-96	-95

Fuselage Ultimate and Fatigue Strength Analyses.—The results of the stiffened panel design analyses are presented in Table 35 for each design region. The FS 900 region was designed by the normal operating condition at Mach 2.7. The fuselage skin thickness of 0.036-in (0.091-cm) was determined from circumferential loading on the shell which was limited to a gross area allowable tension stress of 25,000-psi (172-MPa). Use of this fatigue allowable stress was dictated by the predominant pressurization loading which occurred every flight.

The remaining three regions were designed for the ultimate loads at the start-of-cruise condition. The closed hat-stiffened design was constrained to a constant 6.0-in (0.152-m) pitch, a crown-width of 1.5-in (3.8-cm), and a height of 1.25-in (3.18-cm). These dimensions were established from results of initial studies which included practical consideration for splices and standard shear-ties.

The individual panel results were averaged to obtain the equivalent panel thickness and unit mass data shown in Table 36 for each design region. The centerbody and aftbody shells have a unit mass of approximately 2.5-lbm/ft² (12.2-kg/m²); whereas, the forebody mass is 1.3-lbm/ft² (6.3-kg/m²).

The fuselage frame point design analyses determined the equivalent panel thickness and unit mass circumferentially at each point design region. These data are summarized in Table 37 as an average-equivalent thickness and unit mass. The forebody and aftbody frame unit mass was approximately

TABLE 35. FUSELAGE PANEL GEOMETRY

POINT DESIGN REGION	PANEL CONCEPT	CIRCUMF. LOCATION	FUSELAGE PANEL DIMENSIONS						
			b_s	t_s	C	f	h	t_{st}	\bar{t}
FS 900	ZEE-STIFFENED	233301- 233307	4.0 (10.2)	.036 (.091)	.55 (1.40)	0.75 (1.90)	1.00 (2.54)	.036 (.091)	.056 (.142)
FS 1910	HAT-STIFFENED	234101	6.0 (15.2)	.070 (.178)	1.5 (3.81)	0.80 (2.03)	1.25 (3.18)	.060 (.152)	.129 (.328)
		234106	6.0 (15.2)	.060 (.152)	1.5 (3.81)	0.80 (2.03)	1.25 (3.18)	.060 (.152)	.119 (.302)
FS 2525	HAT-STIFFENED	234801	6.0 (15.2)	.070 (.178)	1.5 (3.81)	0.80 (2.03)	1.25 (3.18)	.080 (.203)	.149 (.378)
		234806	6.0 (15.2)	.040 (.102)	1.5 (3.81)	0.80 (2.03)	1.25 (3.18)	.040 (.102)	.079 (.200)
FS 2900	HAT-STIFFENED	235101	6.0 (15.2)	.070 (.178)	1.5 (3.81)	0.80 (2.03)	1.25 (3.18)	.070 (.178)	.139 (.353)
		235107	6.0 (15.2)	.050 (.127)	1.5 (3.81)	0.80 (2.03)	1.25 (3.18)	.040 (.102)	.089 (.226)
		234109	6.0 (15.2)	.070 (.178)	1.5 (3.81)	0.80 (2.03)	1.25 (3.18)	.080 (.203)	.149 (.378)

X.XX = in.; (X.XX) = cm

PANEL DIMENSIONS:

ZEE-STIFFENED CONCEPT HAT-STIFFENED CONCEPT

TABLE 36. FUSELAGE PANEL MASS DATA

POINT DESIGN REGION	PANEL CONCEPT	\bar{t}		w	
		(in. ² /in.)	cm ² /cm	lbm/ft ²	kg/m ²
FS 900	ZEE-STIFFENED	0.056	.142	1.29	6.30
FS 1910	HAT-STIFFENED	0.104	.264	2.40	11.72
FS 2565	HAT-STIFFENED	0.110	.279	2.53	12.35
FS 2900	HAT-STIFFENED	0.111	.282	2.56	12.50
\bar{t} = AVERAGE EQUIVALENT PANEL THICKNESS w = AVERAGE PANEL UNIT MASS					

TABLE 37. SUMMARY OF FRAME GEOMETRY AND MASS

POINT DESIGN REGION	FUSELAGE FRAME PROPERTIES							
	FRAME SPACING, b		AREA, A		\bar{t}		w	
	(in.)	(cm)	(in ²)	(cm ²)	(in ² /in)	(cm ² /cm)	(lbm/ft ²)	(kg/m ²)
FS 900	21.21	53.87	0.197	1.27	0.0093	0.0236	0.21	1.02
FS 1910	23.23	59.00	0.465	3.00	0.0200	0.0508	0.46	2.25
FS 2525	21.25	53.98	0.474	3.06	0.0223	0.0566	0.51	2.49
FS 2900	21.00	53.34	0.178	1.15	0.0085	0.0216	0.20	0.98
<p>A = AVERAGE FRAME AREA, in² OR cm²</p> <p>$= \frac{\sum_{i=1}^n C_i A_i}{\sum_{i=1}^n C_i} \quad \begin{array}{l} C_i = \text{CIRCUMFERENTIAL LENGTH OF } i^{\text{th}} \text{ ELEMENT, in OR cm} \\ A_i = \text{FRAME AREA OF } i^{\text{th}} \text{ ELEMENT, in}^2 \text{ OR cm}^2 \end{array}$</p> <p>$\bar{t}$ = EQUIVALENT SURFACE PANEL THICKNESS, in²/in. OR cm²/cm</p> <p>= A/b</p> <p>w = EQUIVALENT SURFACE PANEL WEIGHT, lbm/ft² OR kg/m²</p>								

0.20-lbm/ft² (0.98-kg/m²); the centerbody frame unit mass was approximately 0.50-lbm/ft² (2.44-kg/m²).

Fuselage Sonic Fatigue Analyses.-Table 38 summarizes the results of the fuselage sonic fatigue analyses. Panel information, natural frequencies, spectrum levels, and sonic fatigue margins are displayed. The minimum margin of +9.8dB/Hz resulted on the side panel at FS 2900.

Fuselage Fail-Safe Analyses.-Table 39 summarizes the results of the fuselage fail-safe analyses. This table presents a summary of the data derived from the detail calculations, indicates the margin-of-safety and mass penalty associated with the specific panels, and the average mass penalty for the entire point design region. All regions required additional structure to meet the fail-safe requirements. The highest penalty, 0.46-lbm/ft² (2.24-kg/m²) was associated with the midbody region at FS 2525; the aftbody region at FS 2900 exhibited the highest fail-safe capability, i.e., lowest penalty, at 0.10-lbm/ft² (0.49-kg/m²).

Selective panel stiffening was required to meet the circumferential crack criteria; whereas, all regions required circumferential fail-safe straps to attain the longitudinal crack criteria.

Fuselage Shell Mass.-The results of the ultimate and fatigue strength, fail-safe and sonic fatigue analyses were combined to establish the fuselage unit mass at each point design region. Table 40 summarizes these results. The fuselage unit mass varies from 1.75-lbm/ft² (8.54-kg/m²) in

TABLE 38. SUMMARY OF FUSELAGE SONIC FATIGUE ANALYSES

POINT DESIGN REGION	PANEL CONCEPT	LOCATION	NATURAL FREQUENCY f, (Hz)	SPECTRUM LEVEL (1)(2) (dB/Hz)		SONIC(3) FATIGUE MARGIN (dB/Hz)
				ALLOW.	ENVIR.	
FS 900	ZEE- STIFFENED	TOP	245.0	121.0	84.0	+37.0
		SIDE	245.0	121.0	84.0	+37.0
		BOTTOM	245.0	121.0	84.0	+37.0
FS 1910	HAT- STIFFENED	TOP	255.0	131.0	92.0	+39.0
		SIDE	255.0	130.5	92.0	+38.5
FS 2525	HAT- STIFFENED	TOP	350.0	134.0	99.4	+34.6
		SIDE	330.0	128.0	99.6	+28.4
FS 2900	HAT- STIFFENED	TOP	340.0	132.0	116.2	+15.8
		SIDE	300.0	126.0	116.2	+9.8
		BOTTOM	350.0	134.0	116.1	+17.9
NOTES: (1) ALLOWABLE SOUND LEVEL						
(2) APPLIED SOUND LEVEL (ENVIRONMENT)						
(3) SONIC-FATIGUE MARGIN = (ALLOWABLE dB/Hz – ENVIRONMENT dB/Hz)						

TABLE 39. SUMMARY OF FUSELAGE FAIL-SAFE ANALYSES

DESIGN CONCEPT	POINT DESIGN REGION	PANEL LOCATION	TYPE OF CRACK	MARGIN OF SAFETY	MASS PENALTY (ΔW)		
					PANEL		POINT DESIGN REGION
					lbm/ft ²	kg/m ²	
ZEE-STIFF.	FS 900	TOP SIDE	CIRCUM CIRCUM	+1.25 +HIGH	NONE NONE	NONE NONE	0.25 lbm/ft ² (1.22 kg/m ²)
		TOP SIDE	LONG LONG	+0.01 +0.01	0.25 0.25	1.22 1.22	
HAT-STIFF. CONCEPT	FS 1910	TOP SIDE	CIRCUM CIRCUM	+0.51 +2.11	NONE NONE	NONE NONE	0.22 lbm/ft ² (1.07 kg/m ²)
		TOP SIDE	LONG LONG	+0.46 +0.02	0.06 0.15	0.29 0.73	
HAT-STIFF. CONCEPT	FS 2525	TOP SIDE	CIRCUM CIRCUM	+0.74 +0.01	NONE 2.34	NONE 11.42	0.46 lbm/ft ² (2.24 kg/m ²)
		TOP SIDE	LONG LONG	+0.52 +1.18	0.06 0.06	0.29 0.29	
HAT-STIFF.	FS 2900	TOP SIDE	CIRCUM CIRCUM	+1.27 +1.11	NONE NONE	NONE NONE	0.10 lbm/ft ² (0.49 kg/m ²)
		BOTTOM	CIRCUM	+0.25	NONE	NONE	
		TOP SIDE	LONG LONG	+0.50 +0.04 +0.44	0.07 0.22 0.07	0.34 1.07 0.34	

NOTES:

PANEL MASS PENALTY

$$\Delta \bar{t}_i = \Delta \bar{t}_{\text{PANEL}} + A_{\text{STRAP}}/b$$

$$\Delta W_i = 144\rho\Delta \bar{t}_i$$

WHERE:

$$\Delta \bar{t}_i = \text{EQUIVALENT SURFACE PANEL THICKNESS OF } i^{\text{th}} \text{ PANEL}$$

$$\Delta \bar{t}_{\text{AVG}} = \text{AVERAGE SURFACE PANEL THICKNESS OF FUSELAGE CROSS-SECTION}$$

$$C_i = \text{CIRCUMFERENCE OF } i^{\text{th}} \text{ SURFACE PANEL}$$

$$\Delta \bar{t}_{\text{PANEL}} = \text{ADDITIONAL THICKNESS OF } i^{\text{th}} \text{ PANEL FOR FAIL-SAFE}$$

$$A_{\text{STRAP}} = \text{STRAP AREA OF } i^{\text{th}} \text{ PANEL FOR FAIL-SAFE}$$

$$b = \text{FRAME SPACING}$$

POINT DESIGN REGION MASS PENALTY

$$\Delta \bar{t}_{\text{AVG}} = \Sigma C_i \Delta \bar{t}_i / \Sigma C_i$$

$$\Delta W = 144\rho\Delta \bar{t}_{\text{AVG}}$$

TABLE 40. FUSELAGE SHELL MASS AT POINT DESIGN REGIONS

POINT DESIGN REGION	STRENGTH DESIGN			SONIC FATIGUE ANALYSES	FAIL-SAFE ANALYSIS	FINAL
	PANEL	FRAME	TOTAL			
FS 900	1.29 (6.30)	0.21 (1.02)	1.50 (7.32)	0.0	0.25 (1.22)	1.75 (8.54)
FS 1910	2.40 (11.72)	0.46 (2.25)	2.86 (13.97)	0.0	0.22 (1.07)	3.08 (15.04)
FS 2525	2.53 (12.35)	0.51 (2.49)	3.04 (14.84)	0.0	0.46 (2.24)	3.50 (17.08)
FS 2900	2.56 (12.50)	0.20 (0.98)	2.76 (13.48)	0.0	0.10 (0.49)	2.86 (13.97)

X.XX = lbm/ft² (X,XX) = kg/m²

the forebody region, to a maximum of 3.50-lbm/ft² (17.08-kg/m²) in the centerbody, and decreases to 2.86-lbm/ft² (13.96-kg/m²) in the afterbody. All regions were assessed with a mass penalty to meet the damage tolerance criteria; conversely, the acoustic environment did not impact the designs and no mass penalty was required.

Flutter Analyses

The vibration and flutter analyses performed during the design concepts evaluation of the chordwise-stiffened, the spanwise-stiffened, and the monocoque structural arrangements, indicated that the symmetric bending and torsion mode for the full-fuel and full-payload (FFFP) condition at Mach 0.90 resulted in the lowest flutter speed. The evidence of a stability mode flutter mechanism for the operating mass empty (OME) condition at Mach 0.60 was also noted. The results of the analyses suggested that stiffening the wing tip structure would eliminate the hump mode flutter and would permit the bending and torsion mode flutter speeds to be pushed beyond the 1.2 V_D envelope. Elimination of the stability mode flutter would most probably be accomplished by stiffening the fuselage or the engine support structure.

During the engineering design-analyses of the hybrid structural arrangement, a series of vibration and flutter analyses were conducted using the applicable structural model to determine the additional stiffness and mass required to correct flutter deficiencies.

Symmetric vibration analyses of the hybrid design were conducted for the operating empty mass (OEM) and the full-fuel and full-payload (FFFP) conditions. A summary of the lower frequency symmetric vibration modes and frequencies for the final design airplane is presented in Table 41.

Symmetric flutter analyses were first performed at Mach 0.90 for both the OEM and FFFP conditions using the strength-designed model. The flutter solutions indicated that the flutter speed was insensitive to fuel and payload, and that a flutter deficiency still existed for the strength-designed hybrid concept for the symmetric bending and torsion mode (Figure 49). A flutter optimization, focused on the wing tip region, was conducted to eliminate the deficiency. This resulted in the addition of 1201-lbm (545-kg) of structural mass to each wing tip. The element properties of the structural model were altered to reflect this change.

Symmetric and antisymmetric flutter analyses were then conducted for both the OEM and FFFP conditions at Mach 0.90, and for the OEM condition at Mach 0.60 and 1.85. The results of these analyses are shown on Figure 50 for the bending and torsion mode and the stability mode. The more than necessary increase in the flutter speed at Mach 0.9 was primarily due to imposing design and manufacturing considerations on the stiffening requirements indicated by the flutter optimization. An additional small portion, 5-keas, was attributed to the assumption in the optimization of linear stiffness variation for the design variables.

Flutter deficiencies were indicated (Figure 50) at Mach numbers of 0.60 and 1.85. At Mach 0.60, the stability mode was critical. The GFAM (interactive computer graphics) flutter optimization program was used to investigate the effectiveness of adding bending stiffness to the fuselage, and to the inner and outer engine support beams (Figure 51). Contrary to the preliminary indications, fuselage stiffening did not increase the flutter speed. The optimization solution resulted in increasing the bending stiffness of the aft portion of the inboard engine support beam. This increase in bending stiffness was obtained with no mass penalty through use of boron-aluminum reinforcement for the support beam.

The critical flutter mode at Mach 1.85 was the bending and torsion mode. To correct this deficiency, flutter optimization was conducted on the wing tip structure at Mach 1.85 to determine the required increases in stiffness and mass. This resulted in a further addition of 599-lbm (272-kg) of structural mass to each wing tip. The final thicknesses for the wing tip surface panels and spar webs are shown in Figure 52. Figure 53 displays the effects of the wing tip stiffening at the Mach 0.90 and 0.60 conditions resulting from the aforementioned analysis. A summary of the critical mass and boundary conditions, flutter mechanisms and speeds, and the associated mass penalties to attain $1.2 V_D$ are shown in Table 42.

Roll Control Effectiveness

Reversal speeds and FAR requirements were compared for both the normal scheduled surface combinations, and for selected fail-safe conditions which involved the loss of a surface which has the most adverse effect on roll-control reversal speed. The primary surfaces used for roll control

TABLE 41. LOWER FREQUENCY SYMMETRIC VIBRATION MODES - FINAL DESIGN

MODE DESCRIPTION	MODE FREQUENCY Hertz	
	OEM	FFFP
RIGID BODY	0.000	0.000
RIGID BODY	0.000	0.000
WING 1ST BENDING	0.996	0.915
FUSELAGE 1ST BENDING	1.645	1.345
ENGINE PITCH IN PHASE	1.499	1.494
ENGINE PITCH OUT OF PHASE	1.752	1.735
FUSELAGE 2ND BENDING	3.025	2.478
WING 1ST TORSION	3.694	3.174

OEM ~ AIRPLANE MASS = 314,000 lbm (142,400 kg)

FFFP ~ AIRPLANE MASS = 750,000 lbm (340,000 kg)

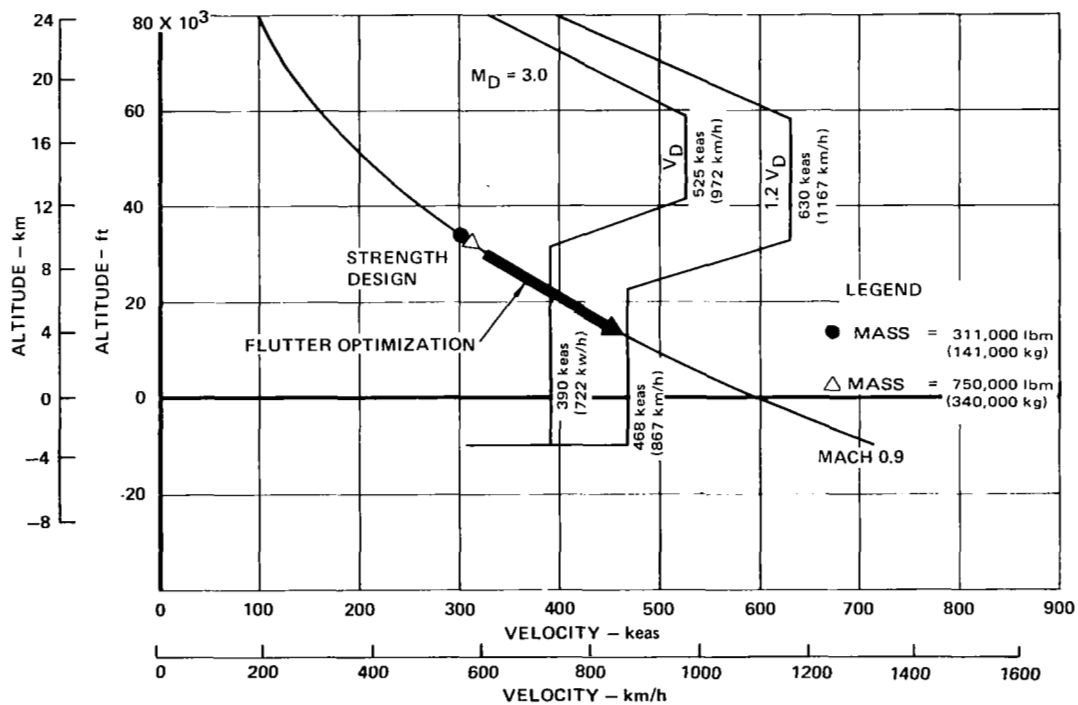


Figure 49. Flutter Speeds for Symmetric Bending and Torsion Mode - Strength Design

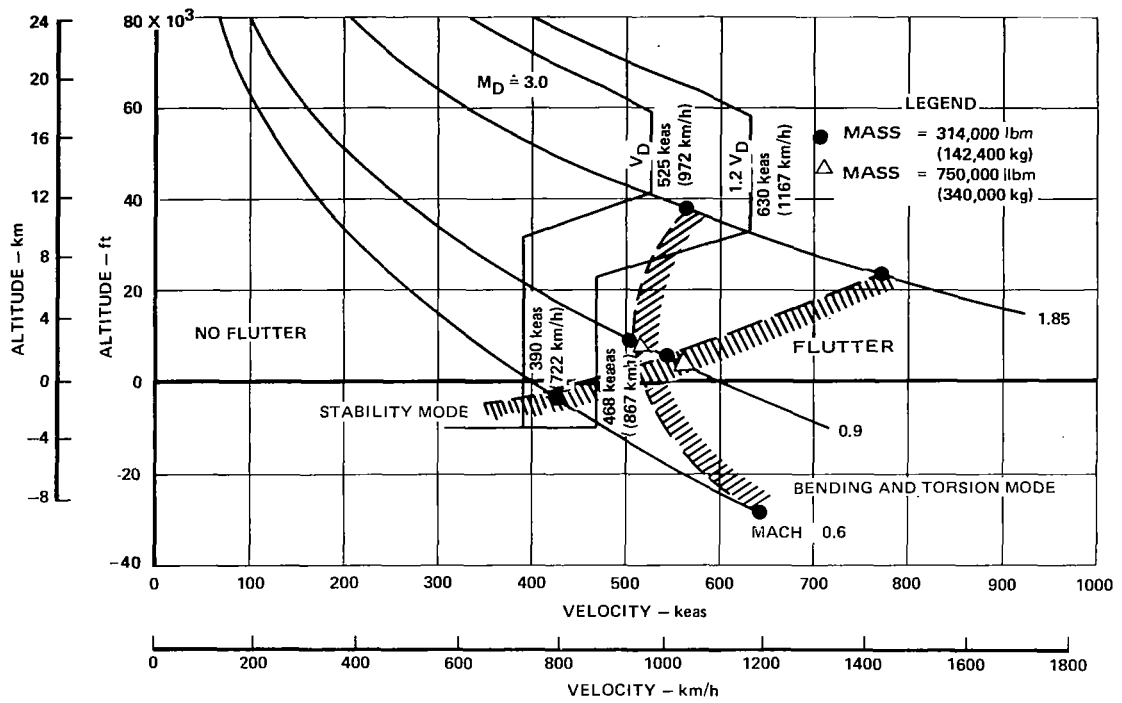


Figure 50. Flutter Speeds for Strength + Stiffness Design

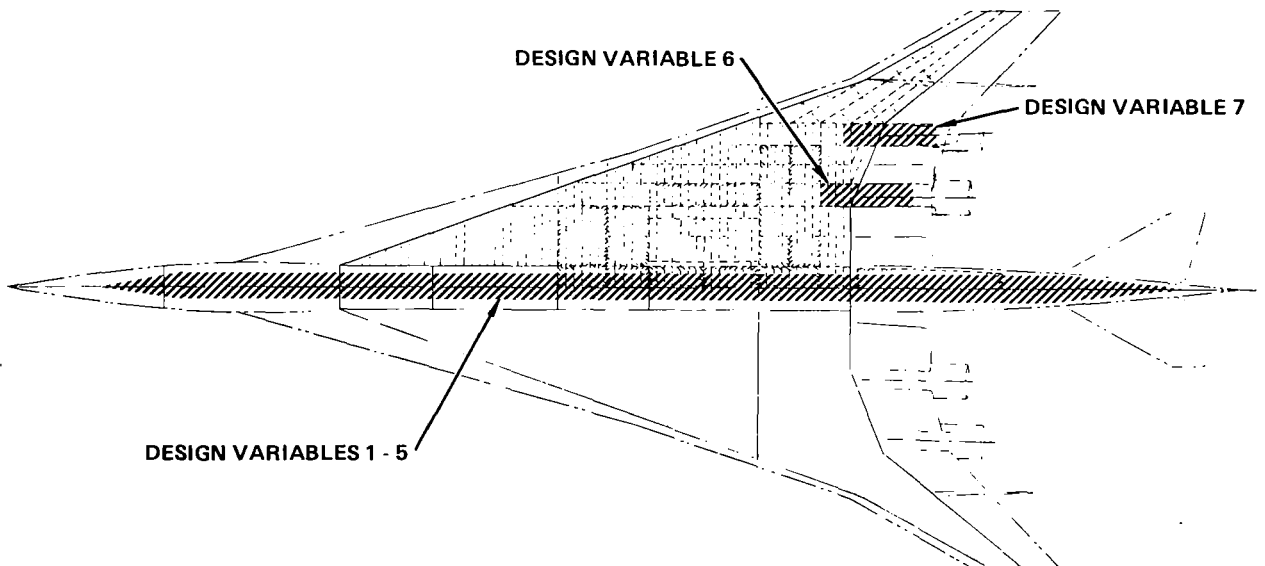
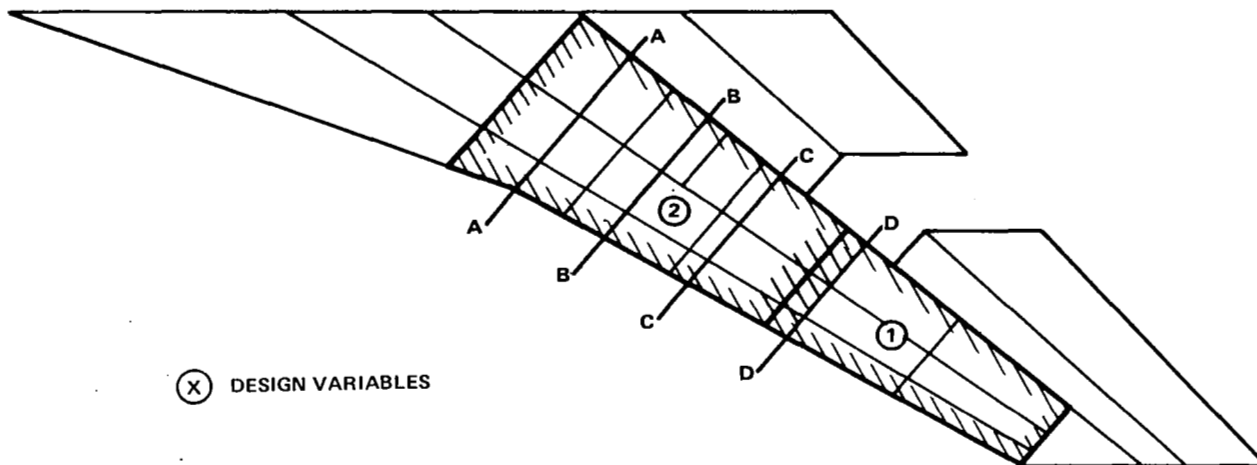
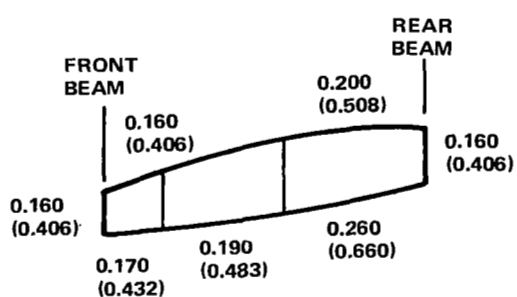


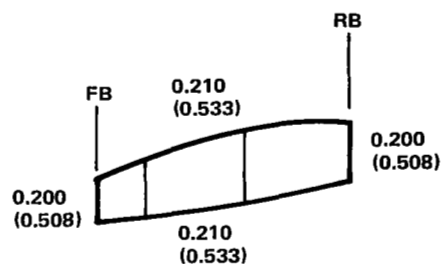
Figure 51. Design Variables for Mach 0.6 Flutter Optimization



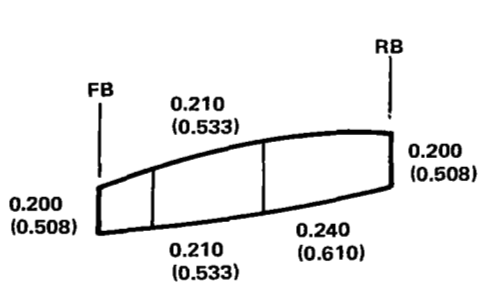
(a). Design Variables



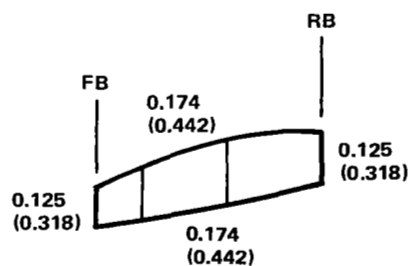
SECTION AA



SECTION CC



SECTION BB



SECTION DD

NOTE: .XXX in (.XXX cm)

(b). Surface Panel and Web Thickness

Figure 52. Mach 1.85 Flutter Optimization

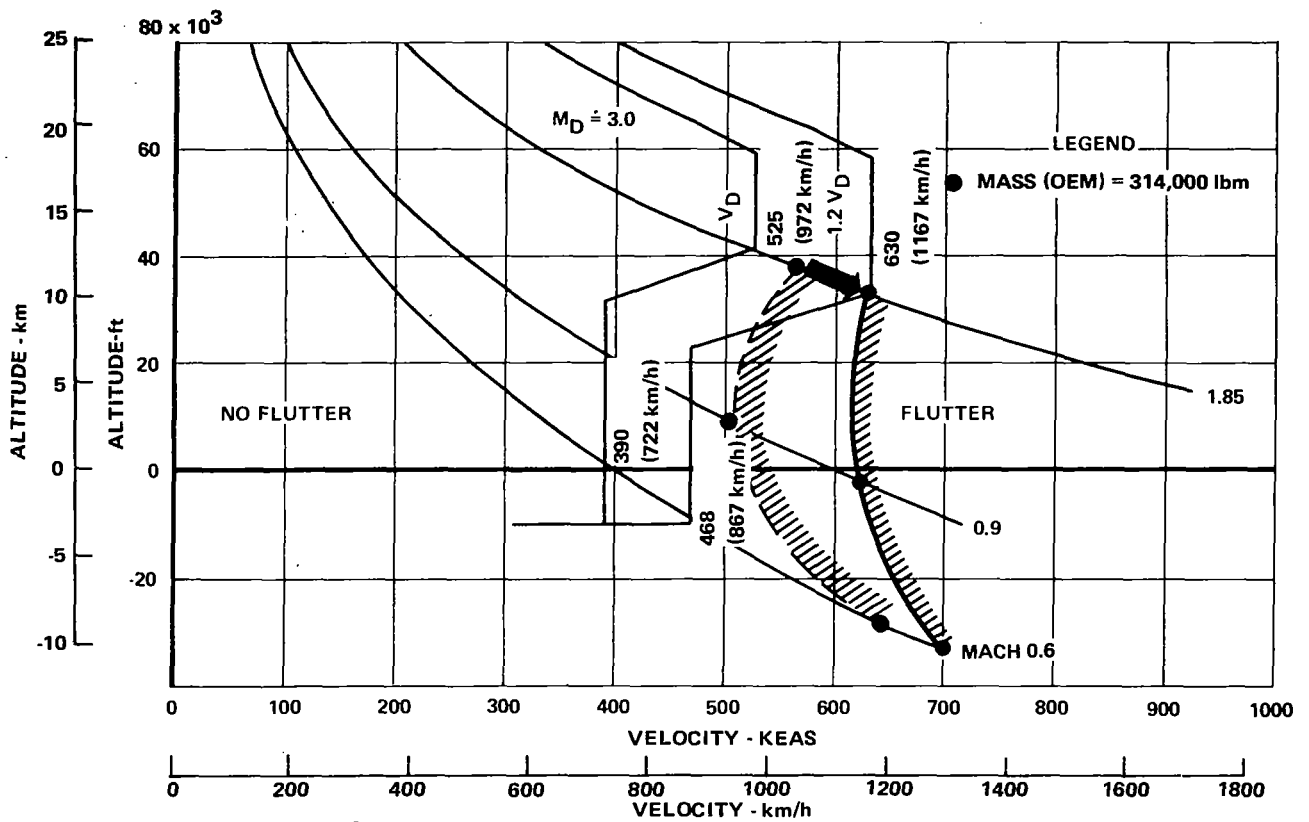


Figure 53. Mach 1.85 Flutter Optimization Results - Bending and Torsion Mode

TABLE 42. SUMMARY OF MASS PENALTIES FOR FLUTTER

MACH NO	CRITICAL COND.		MECHANISM	FLUTTER SPEED	CRITICAL REGION	ADDED MASS PER AIRCRAFT
	MASS	BOUNDARY				
0.60	OEM	SYMM	STABILITY	468-keas 867-km/h	INBOARD ENG RAIL	0.00
0.90	FFFP	SYMM	BENDING AND TORSION	615-keas 1139-km/h	WING TIP	2402-lbm 1190-kg
1.85	OEM	SYMM	BENDING AND TORSION	630-keas 1167-km/h	WING TIP	1198 lbm 544 kg
TOTAL MASS ADDED FOR FLUTTER						3600 lbm 1734 kg

at the various operational Mach numbers for this analysis are shown in Figure 54. The subsonic roll control was obtained by use of the wing trailing edge panels (No. 2 through No. 4) with the low speed aileron locked-out above Mach 0.40 or 260-keas (482-km/h). For supersonic roll control, the spoiler-slot deflector at No. 2 and the inverted spoiler-slot deflector at No. 3 were used. In all cases, the final design airplane exceeded the specified requirement.

Figure 55 presents a measure of roll capability of the final design airplane at supersonic speeds. The results were obtained by executing a one-degree of freedom steady state roll using the spoiler-slot deflector at No. 2 and the inverted spoiler-slot deflector at No. 3. The results indicate a roll-rate capability of 20-degree (.35 rad) per second at supersonic speeds for the flexible supersonic cruise aircraft.

FINAL DESIGN AIRPLANE

The structural arrangement of the resultant final design for the Mach 2.7 arrow-wing supersonic cruise aircraft is illustrated in Figure 56.

Wing Structure Design

A hybrid structural approach was used for the wing design. For the inboard wing, a chordwise-stiffened structural arrangement using low-profile, convex-beaded surface panels of titanium alloy, Ti-6Al-4V, was employed. Submerged titanium spar caps, reinforced with unidirectional boron-polyimide composite, were used in the aft box region and local areas of the forward box (near the main landing gear well). The design details for a typical surface panel and substructure are shown in Figure 57. With the beaded-skin design, wing bending material is concentrated in the spar caps, and the surface panels primarily transmit the shear and chordwise inplane loads and out-of-plane pressure loads. This surface design alleviates thermal stresses and reduces heat transfer to the fuel, in comparison with a flat skin, since only a portion of the fuel is in direct contact with the wing external skin.

Weldbonding was used for joining the inner and outer skins of the surface assembly. The manufacturing limits for the surface panels were held to 15-ft (4.57-m) by 35-ft (10.67-m). The length limit was based on tooling considerations for hot vacuum forming of the skins, while the width limit was based on the postulated size of spotwelding equipment.

In locating wing spars in the chordwise-stiffened wing area, a minimum spacing of 21-in (0.53-m) was maintained between constraints such as fuel tank boundaries. Wing rib spacing was a nominal 60-in (1.52-m) but was modified as required to suit geometrical design constraints. These dimensions define minimum mass conditions which were determined through the studies involving various spar and rib spacing. In the chordwise-stiffened and transition areas, welded truss spars were used except where a spar serves as a fuel tank wall. At such locations, spars have welded

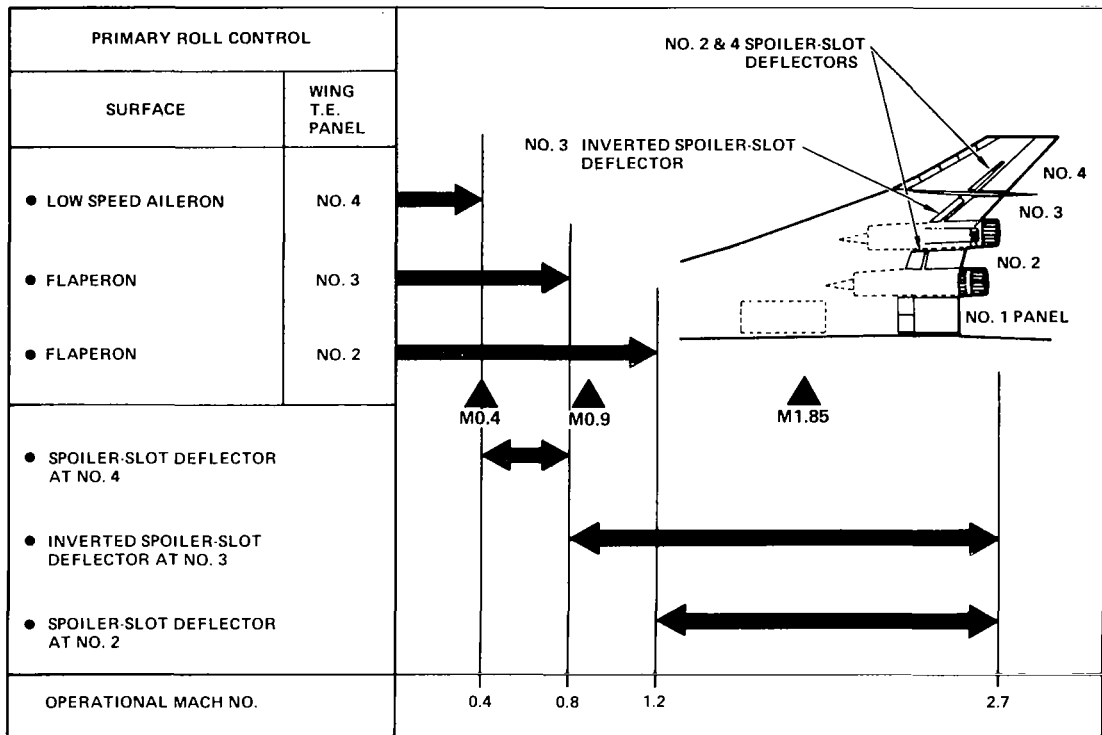


Figure 54. Primary Roll Control Schedule

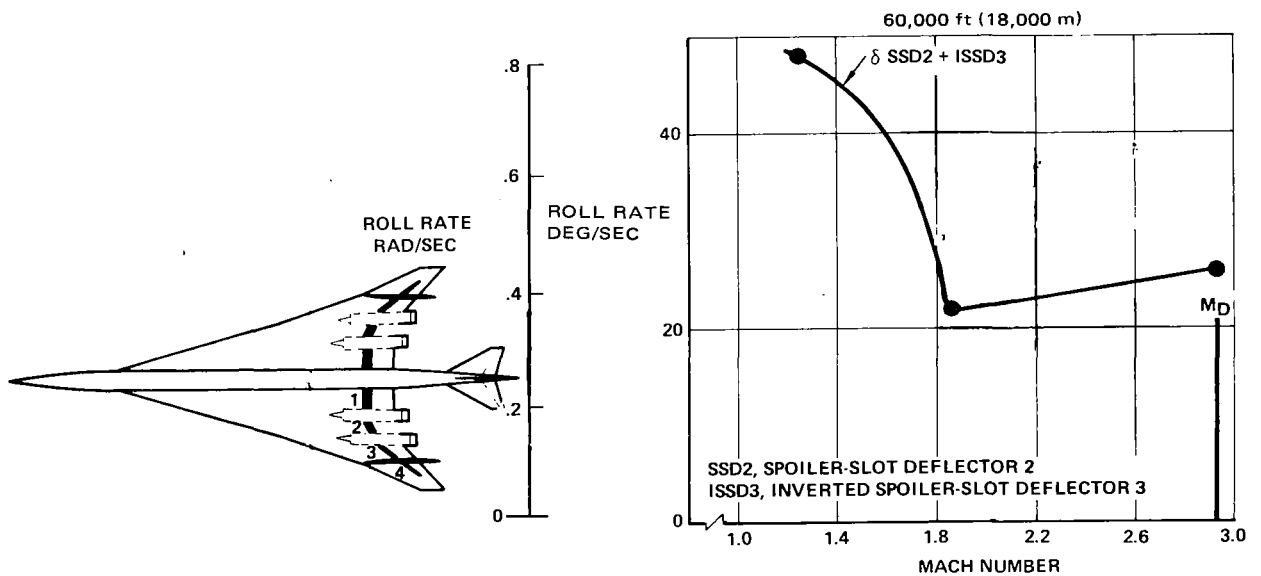


Figure 55. Supersonic Roll Power

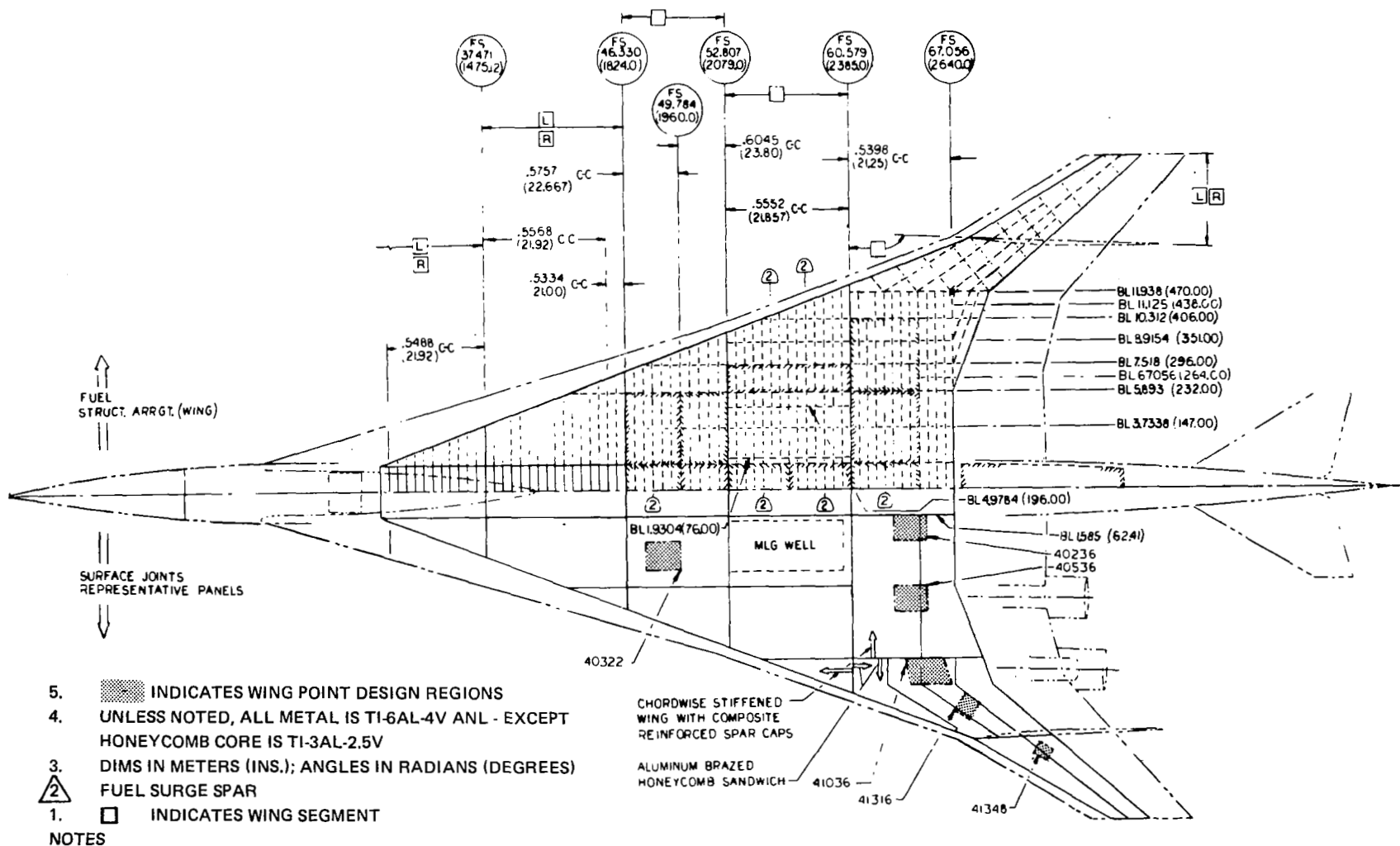


Figure 56. Structural Arrangement of Final Design Airplane

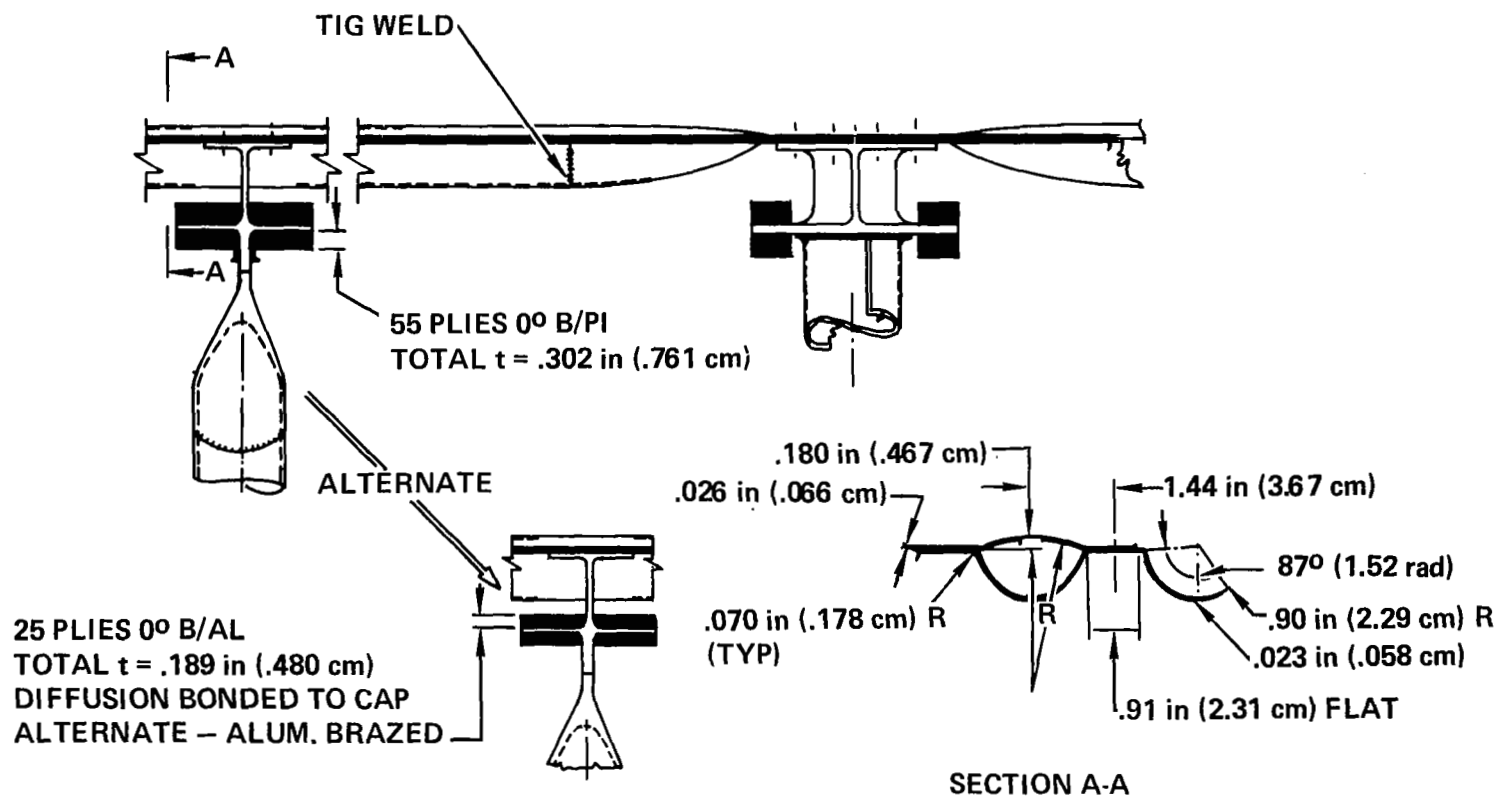


Figure 57. Structural Details for Chordwise-Stiffened Surfaces

circular arc webs with stiffened "I" caps. To facilitate fuel sealing, surface beads do not extend across tank boundaries. Wing spars in the aft wing box were fabricated as continuous subassemblies between BL 470 L and R. Boron-polyimide was selected for the spar cap reinforcement for its structural efficiency and compatibility with titanium. The multielement approach results in damage tolerance capability. Boron-aluminum composite-reinforcement was used for the engine support rails to provide the required stiffness at the higher temperatures associated with this region.

Monocoque surfaces were used in the stiffness critical wing tip box. The sandwich surfaces were brazed together using 3003 aluminum alloy as the brazing material (the "Aeronca" process). Welded circular-arc spars and ribs were used since the minimal need for web penetrations allows the realization of their inherent minimum mass and design simplicity feature. Composite reinforcement was not used in the brazed surfaces or the welded circular arc spars and ribs. A size limit of 68-in (1.73-m) by 40-ft (12.19-m) for brazed surfaces was postulated as a guide after consultation with Aeronca. The panel configurations were based on the design philosophy that all or some panels of the upper surface are attached with screws and are removable for inspection and maintenance purposes.

The flexibility of the aluminum braze process was exploited by incorporating crack stoppers and panel edge doublers in the surface panel brazements. Also, the capability of tapering the panel thickness was utilized in the joint between the chordwise-stiffened and monocoque surface areas. In the joint area, where the transition in arrangement was made, the outboard sandwich surfaces were extended inboard so that spanwise components of the outboard surface loads due to wing bending loads are transferred directly to the spar caps of the chordwise-stiffened structure at the interface rib.

Fuselage Structure Design

The fuselage shell has a closed-hat stiffened design with supporting frames. Design details for a typical frame are shown in Figure 58. The arrangement includes machines extrusion stringers, crack stoppers between frames, and floating zee frames with shear clips. The closed hat-section extruded stringers are machined to provide for crack stoppers and to vary stringer thickness. The floating zee frames with shear clips are preferable, from a fatigue standpoint rather than full depth frames having notches for stringers.

Weldbonding was used for attaching frames, stringers and crack stoppers to the skin because of economy, minimum mass, good fatigue characteristics, and the avoidance of sealing problems. Satisfactory weld-bonding of three thicknesses, as encountered at some locations, may require further development. Weldbrazing was considered as a possible backup to weldbonding. Where fasteners were used at shear clips and frame/stringer attachments, fastener-bonding was utilized in lieu of fasteners alone to obtain enhanced fatigue properties. The size of fuselage skin panel assemblies has been limited to 15-ft (4.57-m) by 50-ft (15.24-m); the

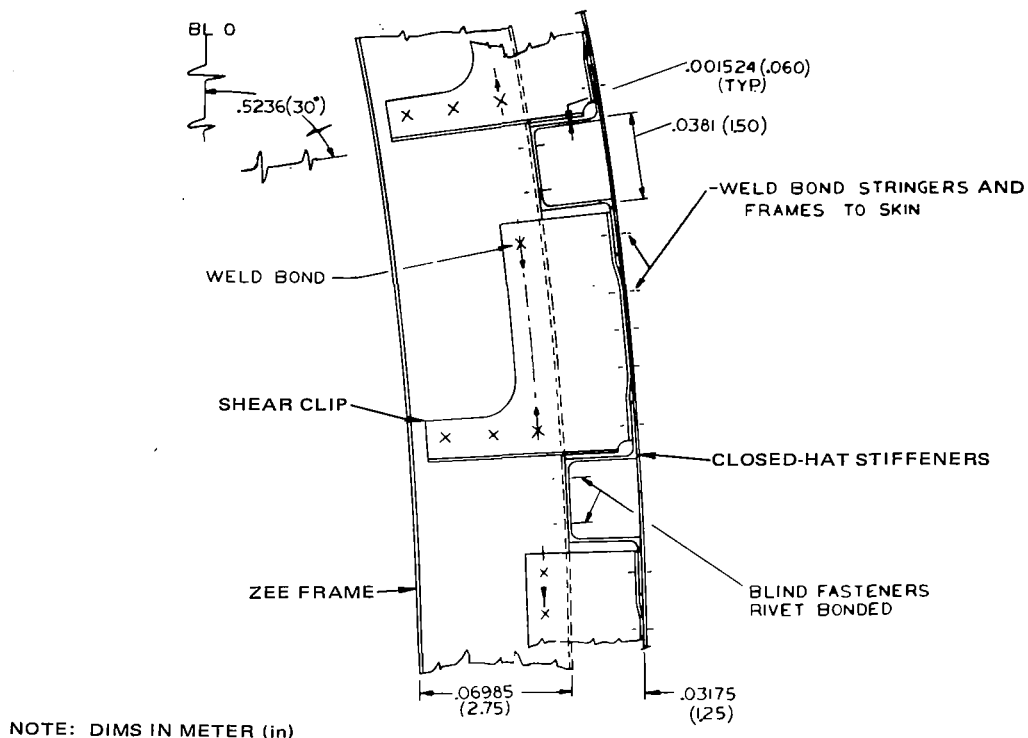


Figure 58. Structural Details for Fuselage Shell

former is based on the postulated size of spotwelding equipment, the latter on the postulated length of the adhesive curing ovens.

Longitudinal shell splices were located only at the top and bottom centerlines of the fuselage, and at the floor to shell intersections fore and aft of the wing carry-through area. These longitudinal splices utilize external and internal splice plates in conjunction with fastener-bonding to achieve a double-shear splice having damage tolerance capabilities and good fatigue properties. Suitable combinations of fastener size and external splice-plate thickness were utilized to avoid feather edges at countersinks for flush fasteners. At circumferential panel splices, and other locations as required, feather edges were avoided by incorporating thickened pads in the external skin in a manner similar to that for wing skins. Chemical milling was used to vary fuselage skin thickness in accordance with load requirements.

Critical Design Conditions and Requirements

The design requirements that sized various portions of the wing structure are shown in Figure 59. The upper and lower surfaces of the wing are divided into three general zones as dictated by their design requirements. The tip structure was stiffness critical and sized to meet the flutter requirements. The aft box and selected regions of the forward box were strength-designed to transmit the wing spanwise and chordwise bending

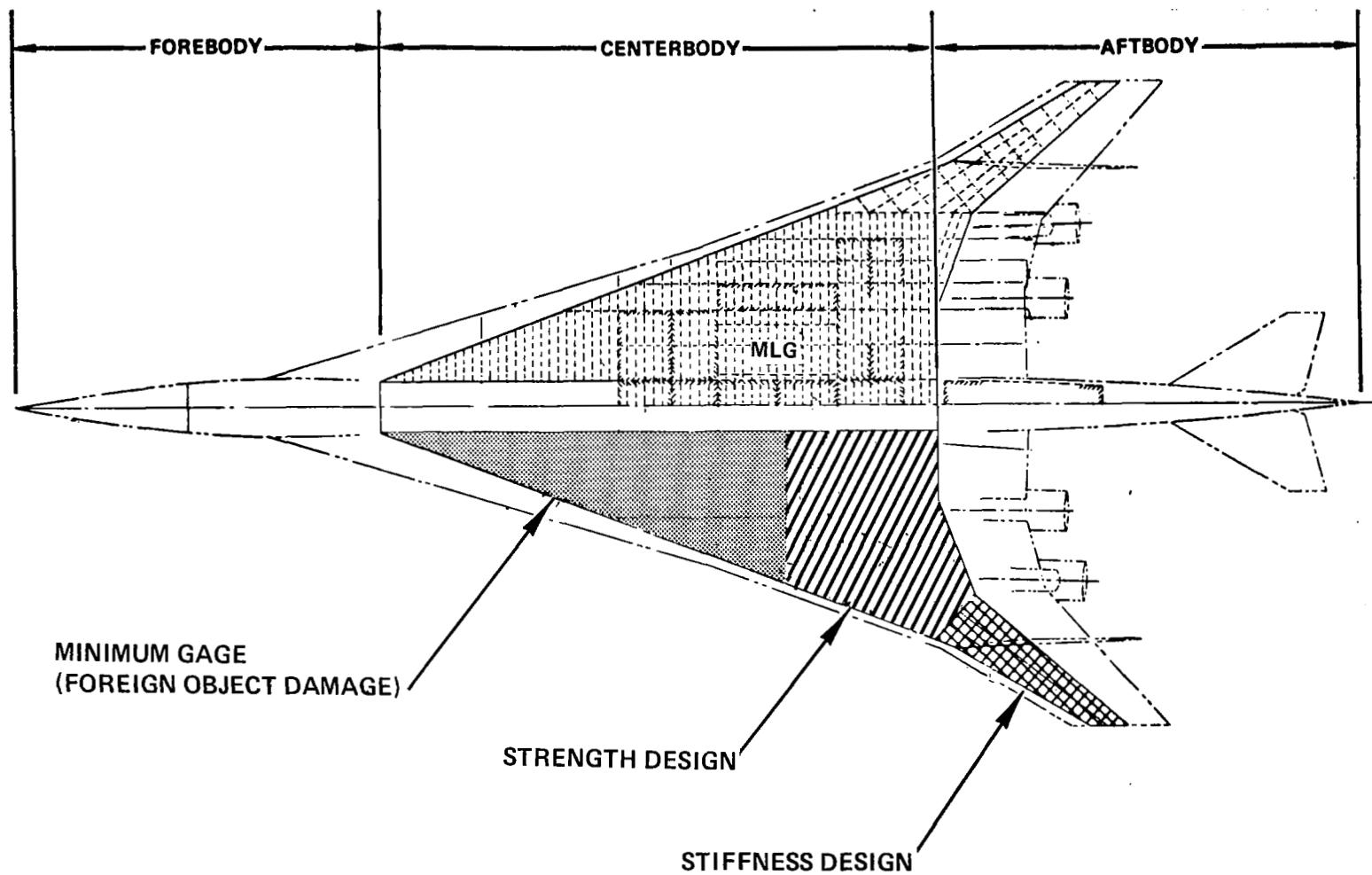


Figure 59. Critical Design Requirements for the Wing Structure

moments and shears. In general the forward box structural-sizing resulted in surface panels and substructure components with active minimum gage constraints. Foreign objective damage was the governing criterion for selection of minimum gage. The fuselage structure was designed by ultimate strength and fatigue requirements.

The critical design conditions for the wing and fuselage structure are presented in Figure 60. In general, the wing critical design conditions correspond to those conditions which produced the maximum surface-panel loadings. The exception being the wing-tip structure which needed additional material to meet the stiffness requirement dictated by the Mach 1.85 flutter condition. The Mach 1.25 symmetric-maneuver condition was the predominate design condition for the highly loaded aft-box region and portions of the forward box on both upper and lower surfaces. Conversely, the design condition for the wing forward box was associated with the elevated temperature condition at Mach 2.7. Minimum-gage constraints were active for major portions of this region.

The fuselage design was influenced by the high temperature environment for a major portion of the fuselage upper shell, and for the pressure critical forebody region. The forebody shell was loaded principally by fuselage pressurization, and therefore was critical for the combined operational load and temperature environment at Mach 2.7. The constant amplitude-type fatigue loadings imposed upon this structure required reduced allowable tension stresses to achieve the service life requirements. As indicated in the figure, the remainder of the fuselage was bending critical. The lower forebody and aftbody structure were critical for dynamic landing; the upper forebody for gusts. The centerbody and upper aftbody were critical for combined load and temperature effects.

Final Design Airplane Mass Estimates

Detailed mass descriptions of the wing and fuselage are presented in Tables 43 and 44, respectively. The wing mass description includes fail-safe provisions, allowance for flutter prevention, and panel thickness changes for manufacturing/design constraints. The fixed mass consists of those items invariant with box structural concept, such as control surfaces, engine support beams, leading and trailing edge structure.

The fuselage mass was also divided into two major categories: shell mass and fixed mass. Here again the shell mass was dependent upon structural concept while the fixed mass such as doors, windows, flight station and fairing were invariant. The fuselage mass shown reflects the use of the conventional skin-stringer-frame construction for the shell, although epoxy resin composites were employed in selected areas of the interior (i.e., floors, floor beams, and trim).

The study focused on the two largest structural mass items; the wing and the fuselage, which amounts to 90,584-lbm (41,088-kg) and 42,122-lbm

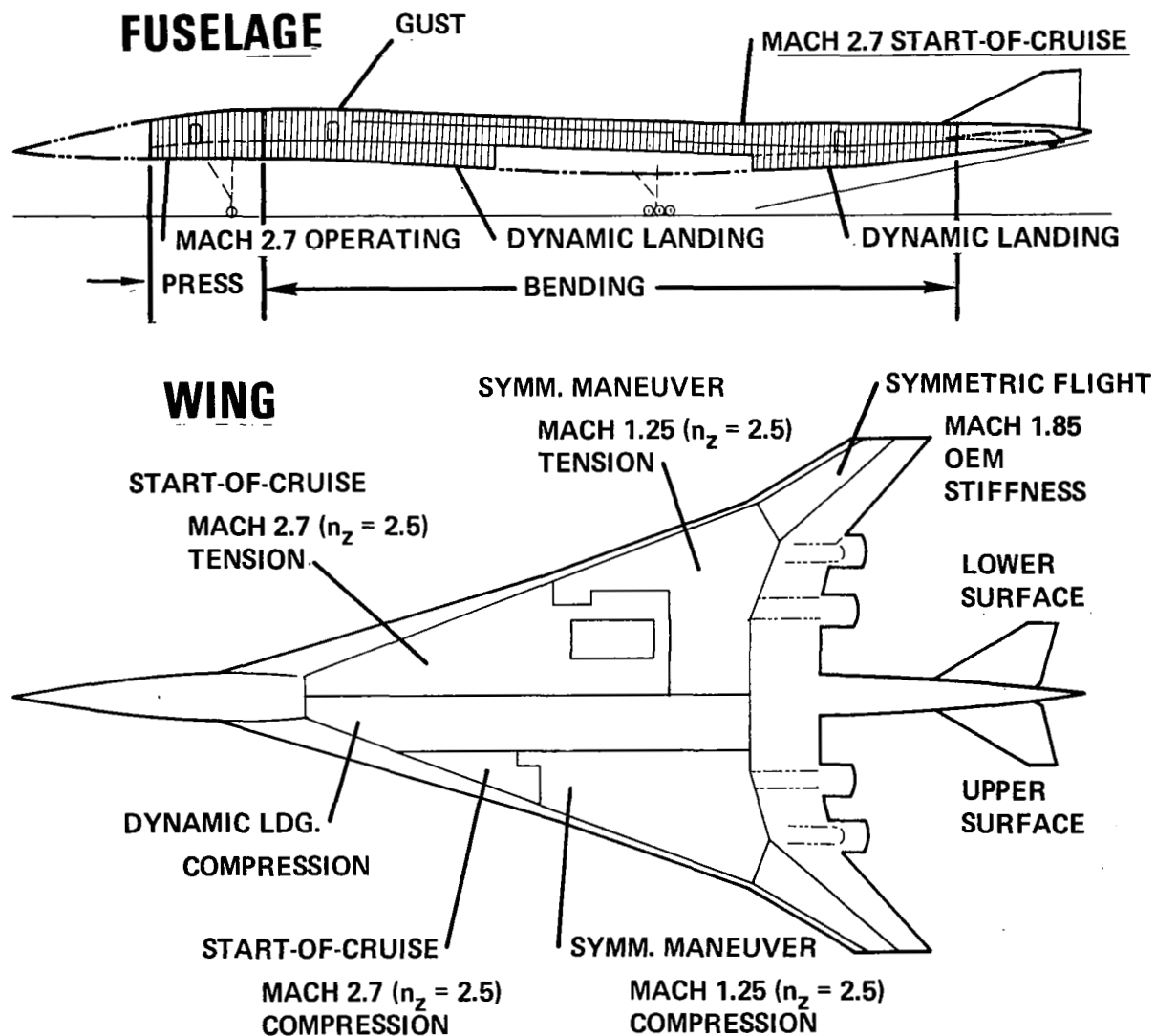


Figure 60. Critical Design Conditions

TABLE 43. MASS ESTIMATES FOR FINAL DESIGN WING

ITEM	PLANFORM AREA		MASS	
	ft ²	m ²	lbm	kg
<u>VARIABLE MASS</u>			50,432^(A)	22,876^(A)
FORWARD BOX	4136.6	384.3	(20,580)	(9,335)
• SURFACES ~ CONVEX BEADED, CHORDWISE STIFFENED			9,452	4,287
• SPARS ~ INCLUDING 522 lbm (237 kg) COMPOSITES			8,558	3,882
• RIBS			2,570	1,166
AFT BOX	2132.4	198.1	(17,384)	(7,885)
• SURFACES ~ CONVEX BEADED, CHORDWISE STIFFENED			7,302	3,312
• SPARS ~ INCLUDING 3,762 lbm (1706 kg) COMPOSITES			8,568	3,886
• RIBS			1,514	687
TRANSITION ~ AFT BOX TO TIP BOX			(1,380)	(626)
TIP BOX	947	88.0	(11,088)	(5,030)
• SURFACES ~ BRAZED HONEYCOMB SAND., MECH. FAST.			9,435	4,280
• SPARS			1,336	606
• RIBS			317	144
<u>FIXED MASS</u>			40,152	18,213
LEADING EDGE	1047	97	5,235	2,375
TRAILING EDGE	1941	180	4,888	2,217
WING/BODY FAIRING	800	74	1,600	726
LEADING EDGE FLAPS/SLATS	133	12	1,130	513
TRAILING EDGE FLAPS/ FLAPERONS	553	51	5,890	2,672
AILERONS	250	23	1,250	567
SPOILERS	225	21	1,360	617
MAIN LANDING				
GEAR ~ DOORS	484	45	2,904	1,317
SUP'T. STRUCTURE			3,750	1,701
B.L. 62 RIBS			1,430	649
B.L. 470 RIBS			700	318
FIN ATTACH RIBS (B.L. 602)			435	197
REAR SPAR			3,400	1,542
ENGINE SUPPORT STRUCTURE			2,380	1,080
FUEL BULKHEADS			3,800	1,724
TOTAL WING MASS			90,584	41,088
(A) INCLUDES FAIL-SAFE PENALTY OF 822 lbm (373 kg)				

TABLE 44. MASS ESTIMATES FOR FINAL DESIGN FUSELAGE

ITEM	MASS	
	lbm	kg
SHELL STRUCTURE	22,582^(A)	10,243^(A)
SKIN	11,144	5,055
STIFFENERS	7,921	3,593
FRAMES	3,517	1,595
FIXED MASS (B)	19,540^(B)	8,863^(B)
NOSE AND FLIGHT STATION	2,500	1,134
NOSE LANDING GEAR WELL	900	408
WINDSHIELD AND WINDOWS	1,680	762
FLOORING AND SUPPORTS	3,820	1,733
DOORS AND MECHANISM	4,170	1,891
UNDERWING FAIRING	1,870	848
CARGO COMPARTMENT PROV.	1,060	481
WING TO BODY FRAMES AND FITTINGS	1,500	680
TAIL TO BODY FRAMES AND FITTINGS	600	272
PROV. FOR SYSTEMS	740	336
FINISH AND SEALANT	700	318
TOTAL FUSELAGE MASS	42,122	19,106
(A) INCLUDES FAIL-SAFE PENALTY OF 1,432 lbm (650 kg)		
(B) INCLUDES COMPOSITE MATERIAL WEIGHT OF 1120 lbm (508 kg)		

(19,106-kg), respectively. These mass items represent 66-percent of the total structural mass and about 17.7-percent of the aircraft taxi mass. A more detailed look at the mass distribution of the largest component, the wing, indicates that 50,432-lbm (22,876-kg) is attributed to the primary structural box (i.e., forward, aft, tip and transition structure). The major ribs, rear spar, fuel bulkheads, and engine support structure accounts for 12,145-lbm (5,509-kg). The leading-edge and trailing-edge structure, spoilers, wing/body fairing, and main landing gear doors and support structure accounts for the remaining 28,007-lbm (12,704-kg).

The mass properties for the final design airplane are summarized in Table 45 as an estimated group mass statement. The data reflect a fixed size aircraft with a takeoff gross mass of 750,000-lbm (340,000-kg) and payload of 49,000-lbm (22,000-kg).

CONCLUSIONS

The objective of the study described in this report was to evaluate advanced structural concepts suitable for high performance supersonic cruise aircraft, and to determine the best structural approach for the design of the primary wing and fuselage structure of a Mach 2.7 arrow-wing configured aircraft. The study encompassed an in-depth structural design of the NASA-defined baseline configuration, based on the specified design criteria and objectives, and consistent with the premise of near-term start-of-design using 1980 technology.

TABLE 45. ESTIMATED GROUP MASS STATEMENT FINAL DESIGN AIRPLANE

ITEM	MASS	
	(lbm)	(kg)
WING	90,584	41,088
TAIL - FIN ON WING	2,800	1,270
TAIL - FIN ON BODY	2,600	1,179
TAIL - HORIZONTAL	7,950	3,606
BODY	42,122	19,106
LANDING GEAR - NOSE	3,000	1,361
LANDING GEAR - MAIN	27,400	12,428
AIR INDUCTION	19,760	8,963
NACELLES	5,137	2,330
PROPULSION - T/F ENGINE INBD.	25,562	11,595
PROPULSION - T/F ENGINE OUTBD.	25,562	11,595
PROPULSION - SYSTEMS	7,007	3,178
SURFACE CONTROLS	8,500	3,856
INSTRUMENTS	1,230	558
HYDRAULICS	5,700	2,585
ELECTRICAL	4,550	2,064
AVIONICS	1,900	862
FURNISHING & EQUIPMENT	11,500	5,216
ECS	8,300	3,765
TOLERANCE & OPTIONS	1,980	898
MEW	303,144	137,504
STD & OPER. EQ.	10,700	4,853
OEW	313,844	142,357
PAYLOAD	49,000	22,226
ZFW	362,844	164,583
FUEL	387,156	175,611
TAXI MASS	750,000	340,194
LEMAC = FS 1548.2 MAC = 1351.06 in. (34.32 m) X ARM = DISTANCE FROM FUSELAGE STATION (F.S.) 0 FUS. NOSE AT F.S. 279		

The resultant final design airplane satisfies all of the design criteria and constraints, and meets all of the design objectives, including a design payload of 49,000-lbm (22,000-kg), a design service life of 50,000 flight hours, and a design range of 4200-nmi (7800-km). Minimizing the structural mass required a hybrid design configuration using titanium alloy 6Al-4V and selected composite material reinforcement. Chordwise-stiffened convex-beaded skin with boron-polyimide reinforced spar caps were selected for the basic wing structure. Monocoque honeycomb sandwich was used for the wing tip. Conventional stringer-stiffened skin with supporting frames was used for the fuselage.

The study illustrated that the design analysis of large, flexible aircraft requires realistic aeroelastic evaluation, based on detailed finite-element analyses and steady and unsteady aerodynamic loading determination. Static aeroelastic and flutter characteristics are important design considerations, and should be investigated early in the design cycle. Significant additional structure, over and above that required for strength, was required in the wing tip and the engine support rails to eliminate initial flutter deficiencies.

The design analyses performed in this study required the use of multi-discipline computer-aided design methods. The study showed that the use of

automated modeling techniques and interactive computer graphics can greatly decrease manpower expenditures and design calendar time.

The design analyses described in the body of the report, and the supplementary studies conducted in support of these analyses (e.g., Appendices A, B and C), resulted in the identification of a number of technology areas with the potential and need for further development to meet the anticipated requirements for a far-term (1990) design aircraft competitive environment. These include advanced composite materials, aircraft configuration improvement, active controls, and advanced design analysis methods.

RECOMMENDATIONS

In addition to making an in-depth structural design analysis of the baseline Mach 2.7 arrow-wing supersonic cruise aircraft, the objectives of the study included the identification of opportunities for structural mass reduction, and the recommendation of needed research and technology.

A major potential source for structural mass reduction is the increased use of advanced composite materials, particularly when the cascading effects on aircraft size and cost are considered (see Appendix A). Continued development of composite materials is recommended in several areas. Further development of high-temperature polyimides is needed if significant application of composites in the Mach 2.7 temperature environment is to be achieved. On the other hand, if lower cruise speed designs, e.g., Mach 2.2 (see Appendix B), are considered, addition-type polyimides are a potential solution. Finally, metal matrix composites offer mass savings for local "hot spots," e.g., engine support structure, and for stiffness critical areas like the wing tip (see Appendix C).

Further improvements in aircraft configuration are also needed. For example, the over-under engine installation concept needs further exploration. This concept offers improved directional control by reducing two-engine failed requirements, and by increasing the amount of trailing edge available for flaperons for increased roll control power. In addition, research and development of high-speed roll control devices is needed. Low-speed lift improvement is also needed; both, powered lift and increased wing span offer potential solutions here.

As a part of the aircraft performance investigations, the use of active controls was postulated. Further studies are needed concerning their use for pitch, roll and yaw augmentation, ride quality improvement, increased fatigue life, flutter suppression and other aeroelastic applications.

A number of needed improvements in advanced design analysis methods were identified during the study. These included transonic loads prediction methods, better flutter optimization techniques, and improved computer-aided design capabilities. Included in the latter were automated data generation, integration of the design analysis system and the associated data management system, and interactive design analysis. Finally, there is a need for cost prediction methods for composite structures.

APPENDIX A

ADVANCED TECHNOLOGY ASSESSMENT

Introduction

Previous studies of advanced technology application to future transport performance and economics identified major technological advances that could reasonably be available during the 1990-time period (Reference 12). The trends indicated that the greatest structural mass payoff was in the area of composite materials and fabrication technology. Furthermore, the most significant mass reduction resulted from resizing the airplane to reflect the lower structural mass achieved through advanced materials application.

The impact of advanced technologies on supersonic cruise aircraft design were identified in the early tasks of the systems integration studies (Reference 4). Technology improvements in composite materials, new structural concepts, and active controls were collectively forecasted. Projected composite development trends postulated the availability of improved stable high temperature resin systems such as thermoplastic polyimides or high temperature polyaromatics; large numerically controlled tape laying equipment, filament winding and pultrusion equipment; and larger autoclaves. The studies indicated that, with the aggressive application of composite materials and fabrication technology, the takeoff gross mass of the near-term aircraft design reported in the body of this report could be reduced by approximately 100,000-lbm (45,400-kg), or the range increased by 500-nmi (926-km).

Approach

To arrive at projections for airframe structural mass for the assessment of the impact of advanced composite materials technology on the supersonic cruise aircraft design, the results of the design concept evaluation for the reference configuration were used to size specific point design regions. The sizing data included the internal loads and stiffness requirements of the appropriate airframe arrangements (i.e., chordwise-stiffened and monocoque designs). A comparison was then made with the minimum mass titanium design to similar designs in graphite or boron composites. Reduction factors for secondary and other structural components were obtained from the results of Reference 12. The basic section mass was taken as the basis of comparison since nonoptimum factors resulting from advanced manufacturing techniques used for the near-term aircraft assembly (e.g., welded design) were offset by a bonded composite structure having approximately equal utilization of mechanical fasteners.

Considering the 1990-time period, adjustments were made in the material properties to reflect improvements anticipated for these materials. In making the adjustments, no major breakthroughs have been forecasted. Rather, it was postulated that as a minimum, current inconsistencies in the material properties would diminish through refined processing.

It was recognized that composite materials require provisions for protection beyond that of their all-metal counterparts. In particular it was necessary to protect against degradation by aggressive environments such as electrical hazards, erosion, impact, and weathering. For this study all exterior surfaces were assumed to be covered with 200 x 200 aluminum mesh, except at the leading edge sections where 120 x 120 mesh was used. The 120 x 120 mesh was selected for the leading edge to improve heat dissipation for this area. Additional composite protection was provided by an electrical insulating barrier consisting of one ply of 120 glass laminated between the laminate and the aluminum wire mesh. The 120 glass barrier ply and the aluminum wire mesh were cocured with the resin from the 120 glass, bonding the mesh to the composite. The wire mesh was connected to metallic substructure to provide a path for electrical discharge. Other protective measures include coating all surfaces with a polyurethane system (more desirable, higher service temperature systems are anticipated by 1985), sealing all cut edges, and wet installation of fasteners.

Design Concepts

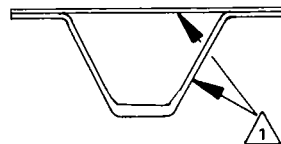
The composite design concepts that were examined were variations of those evaluated for the metal design, and included both biaxially and uniaxially stiffened surface panels. All the wing surface panel concepts (Figure 61) were smooth-skin designs which exploited the low coefficient of thermal expansion characteristics inherent in the graphite-polyimide system. For the fuselage, the more conventional skin-stringer and frame designs were evaluated.

Manufacturing Concept

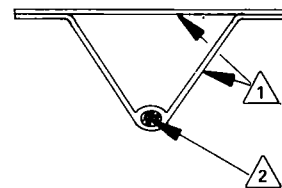
The principal premise for producing the 1990 advanced technology aircraft was that polyimide resin systems would have been developed to a point such that processing could be accomplished with ease. Thus, the low cost manufacturing methods now being developed for epoxy processing were taken as feasible for polyimides. Restrictions on such factors as laminated thickness, bond pressure, etc., were neglected for this study.

Fabrication of ribs and spar caps as well as truss webs was accomplished by closed mold processing with elastomeric tooling as a pressure generator. Single-stage molding and attachment of caps to truss or corrugated webs were performed by similar techniques.

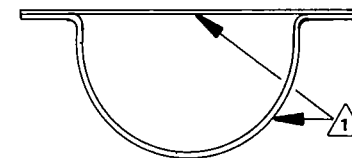
Wing skin panels, honeycomb or hat-stiffened, would be produced with large sheets of material laminated by automated machines. Unit panels having dimensions of 10-feet x 20-feet (3.0-m x 6.1-m) were assumed. Since, for the most part, the wing skin gages were small, the hat-stiffeners were first produced as trapezoidal corrugations molded from a flat sheet. The hats were then cocured to the skins using removable expansion mandrels. Because of contour complexity, flexible elastomeric tooling was used extensively.



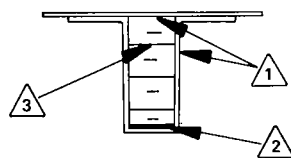
CONCEPT A
CORRUGATED HAT STIFFENER



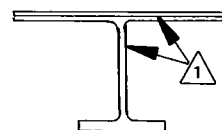
CONCEPT B
POINTED HAT STIFFENER



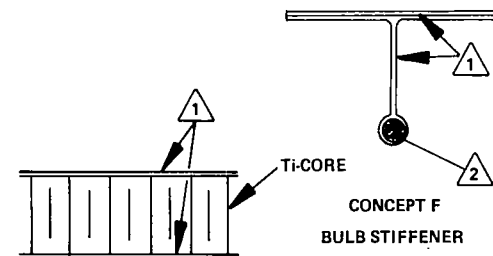
CONCEPT C
ROUNDED HAT STIFFENER



CONCEPT D
HONEYCOMB STABILIZED HAT STIFFENER



CONCEPT E
TEE STIFFENER



CONCEPT F
BULB STIFFENER

CONCEPT G
HONEYCOMB CORE SANDWICH

LEGEND:

- 1 MULTI-DIRECTIONAL COMPOSITE LAMINATES B/PI OR GR/PI
- 2 UNIDIRECTIONAL COMPOSITE ELEMENTS B/PI OR GR/PI
- 3 GR/PI HONEYCOMB CORE

Figure 61. Composite Material Wing Design Concepts

Point Design Regions

Selected point design regions used in the metallic concept evaluations were used to establish unit mass data for estimating the total airplane mass of the composite designs. Representative structures were defined and analyzed at these locations, including consideration of the associated non-optimum factors. In the wing, these included upper and lower surface panels, and typical rib and spar structure.

Design Loads

The internal loads and surface pressures for the critical load conditions from the metallic concept evaluation were used in the analyses of the composite designs; load reduction based on the reduced airframe mass potential of composites application was not included. In addition, the stiffness of the composite shell structure was maintained at least equivalent to the titanium shell design.

Concept Analyses







Wing concept analyses were performed for both the chordwise-stiffened and the monocoque arrangements. Screening of the potential all-composite design concepts of Figure 61 were performed both on a qualitative and quantitative basis. The results of this assessment identified the corrugated hat-stiffener (Concept A) and the tee-stiffener (Concept E) as the leading candidates for the all-composite design. The former provides good compression efficiency and excellent torsional rigidity. For the more lightly loaded, pressure critical forward wing box structure, the tee-stiffener concept was also evaluated.

For the monocoque design only the honeycomb sandwich panel with laminated face skins of boron-polyimide or graphite-polyimide composites and a titanium alloy core was evaluated.

Table 46 presents a comparison of unit wing mass for the three point design regions for the chordwise-stiffened hat section design, and the monocoque honeycomb sandwich design. The unit mass data for the surface panels and individual substructure components are shown. The minimum mass design for each point design region is identified by the shading. Trends similar to the metallic design are noted, with the chordwise-stiffened design being minimum-mass for the lightly loaded forward box region (40322) and the honeycomb design being minimum-mass for the highly loaded aft box and the stiffness critical wing tip structure. These unit mass data were applied to establish the total wing mass for the advanced technology aircraft.

The assessment to identify the potential payoff for composite technology application to the fuselage shell structure was made observing practical constraints for passenger accommodation. The two major factors included: (1) the need for passenger windows and (2) the requirement for ingress and emergency egress. To obtain the design trends for this study,

TABLE 46. WING MASS COMPARISON FOR COMPOSITE DESIGNS

POINT DESIGN REGION	40322				40536				41348			
STR. ARRANGEMENT	CHORDWISE		MONOCOQUE		CHORDWISE		MONOCOQUE		CHORDWISE		MONOCOQUE	
COMPOSITE MATERIAL	B/PI	GR/PI	B/PI	GR/PI	B/PI	GR/PI	B/PI	GR/PI	B/PI	GR/PI	B/PI	GR/PI
PANEL CONCEPT												
UPPER SURFACE	0.998 (4.87)	0.988 (4.82)	1.044 (5.09)	1.037 (5.06)	1.694 (8.27)	1.674 (8.17)	2.255 (11.01)	2.228 (10.87)	1.457 (7.11)	1.443 (7.04)	2.125 (10.37)	2.115 (10.34)
LOWER SURFACE	0.998 (4.87)	0.988 (4.82)	0.957 (4.67)	0.950 (4.63)	1.412 (6.89)	1.394 (6.80)	2.623 (12.81)	2.584 (12.62)	1.003 (4.90)	0.993 (4.85)	1.993 (9.73)	1.983 (9.70)
TRUSS SPAR	0.336 (1.64)	0.338 (1.65)	0.265 (1.29)	0.267 (1.30)	0.656 (3.20)	0.663 (3.24)	0.517 (2.52)	0.523 (2.55)	—	—	—	—
CORRUGA. SPAR	0.540 (2.64)	0.535 (2.61)	0.773 (3.77)	0.763 (3.72)	0.716 (3.49)	0.711 (3.47)	0.735 (3.59)	0.725 (3.54)	0.545 (2.66)	0.541 (2.64)	0.227 (1.11)	0.220 (1.10)
TRUSS RIB	0.102 (0.50)	0.095 (0.46)	0.359 (1.75)	0.362 (1.77)	0.099 (0.48)	0.100 (0.49)	0.349 (1.70)	0.354 (1.72)	—	—	—	—
CORRUGA. RIB	0.584 (2.85)	0.579 (2.83)	0.428 (2.08)	0.422 (2.06)	0.798 (3.90)	0.792 (3.87)	0.365 (1.78)	0.360 (1.76)	0.402 (1.96)	0.399 (1.95)	0.076 (0.37)	0.070 (0.34)
SPAR CAP	0.337 (1.64)	0.334 (1.63)	0.178 (0.87)	0.177 (0.86)	3.795 (18.53)	3.761 (18.36)	0.252 (1.23)	0.249 (1.22)	3.584 (17.50)	3.552 (17.34)	0.181 (0.88)	0.179 (0.87)
RIB CAP	0.099 (0.48)	0.098 (0.48)	0.138 (0.67)	0.137 (0.67)	0.118 (0.58)	0.117 (0.57)	0.130 (0.63)	0.129 (0.63)	0.118 (0.58)	0.117 (0.57)	0.131 (0.64)	0.129 (0.63)
ΣTOTAL	3.994 (19.50)	3.955 (19.30)	4.142 (20.22)	4.115 (20.09)	9.288 (45.35)	9.212 (44.98)	7.226 (35.28)	7.150 (34.91)	7.109 (34.71)	7.045 (34.40)	4.733 (23.11)	4.713 (23.01)

NOTE: SPAR SPACING = 30 in (0.76 m)

UNIT MASS: X.XXX = lbm/ft²; (X.XXX) = kg/m²

constraints on frame spacing of 20-in (0.51-m) and frame height of 3.0-in (7.6-cm) were observed. Furthermore, the aforementioned constraints were consistent with the titanium skin-stringer and frame design and thus a direct comparison can be made to relate more directly the impact of composite utilization on the primary shell structure design.

The fuselage of the supersonic cruise aircraft was bending critical over most of its length, with internal pressure dictating requirements for the shell structure design forward of FS 1000. The tee-stiffener design was adopted for the lightly loaded, pressure critical forebody structure. For the bending critical regions both the tee-stiffener and corrugated hat-stiffener designs were evaluated.

The results of the fuselage skin panel and frame analysis are summarized in Table 47. The resulting mass trends for both boron-polyimide and graphite-polyimide composites are displayed for the panel concepts analyzed. Similar trends as observed for the metallic design are indicated, with the tee-stiffener being minimum-mass in the forebody and the hat-stringer design being minimum-mass in the centerbody and aftbody structure. The data include an estimate for the protection system mass of 0.045-lbm/ft² (.22-kg/m²). Also shown on the table is a summary of frame mass for the point design regions. The frame mass at FS 750 was conservatively taken as being equal to the requirements at FS 2000 and FS 3000.

Mass Assessment



The relative mass of the wing box structure was based on three wing point design regions. The total variable box mass is presented in Table 48 for the individual boxes (i.e., forward, aft, tip). These results are compared with the near-term hybrid arrangement (Table 25) of the detail concept evaluation study.

Evaluation of the wing box mass data for the near-term and far-term designs indicate the mass advantage of the minimum gage titanium alloy beaded panels of the forward box as compared to an equivalent stiffness composite design of either boron-polyimide or graphite-polyimide. For the stiffness critical tip structure, however, the application of composites affords a significant mass saving.

The relative mass of the shell structure was based on the four point design regions defined at FS 750, FS 2000, FS 2500 and FS 3000. Table 49 presents the shell unit mass for each point design region and resulting total shell mass. Both boron-polyimide and graphite-polyimide material system data are shown along with corresponding mass for the all-titanium shell. A decrease in shell unit mass was reflected at all point design regions; the magnitude varies from a 4-percent to a 21-percent mass saving potential. A mass savings for the total shell when employing advanced composites was 14-percent.

The mass reduction factors for the secondary components were obtained from Reference 12. The secondary components for the wing and fuselage total in excess of 60,000-lbm (27,000-kg). The application of the reduction

TABLE 47. FUSELAGE MASS COMPARISON FOR COMPOSITE DESIGNS

FUSELAGE SKIN PANELS					
MATERIAL SYSTEM	REFERENCE TITANIUM	BORON-POLYIMIDE	GRAPHITE-POLYIMIDE	BORON-POLYIMIDE	GRAPHITE-POLYIMIDE
w, UNIT MASS	lb/ft ² (kg/m ²)				
F.S. 750	1.29 (6.30)	—	—	1.134 (5.54)	1.118 (5.46)
F.S. 2000	2.74 (13.38)	2.363 (11.54)	2.349 (11.47)	2.579 (12.59)	2.565 (12.52)
F.S. 2500	3.02 (14.74)	2.839 (13.86)	2.810 (13.72)	2.925 (14.28)	2.954 (14.42)
F.S. 3000	2.90 (14.16)	2.363 (11.54)	2.349 (11.47)	2.579 (12.59)	2.565 (12.52)




FRAMES			
MATERIAL SYSTEM	REFERENCE TITANIUM	BORON-POLYIMIDE	GRAPHITE-POLYIMIDE
w, UNIT MASS	lb/ft ² (kg/m ²)		
F.S. 750	0.25 (1.22)	0.365 (1.78)	0.362 (1.77)
F.S. 2000	0.53 (2.59)	0.365 (1.78)	0.362 (1.77)
F.S. 2500	0.58 (2.81)	0.457 (2.23)	0.452 (2.21)
F.S. 3000	0.53 (2.59)	0.365 (1.78)	0.362 (1.77)

TABLE 48. WING BOX STRUCTURE MASS COMPARISON

ITEM	NEAR-TERM TECHNOLOGY		ADVANCED TECHNOLOGY			
	HYBRID(A)		B/PI		Gr/PI	
START-OF-DESIGN	NEAR-TERM (1980)		FAR-TERM (1990)			
POINT DESIGN REGION						
40322 lbm/ft ² (kg/m ²)	3.80(B)	(18.55)	3.99	(19.48)	3.96	(19.33)
40536 lbm/ft ² (kg/m ²)	7.27	(35.99)	7.23	(35.30)	7.15	(34.91)
41348 lbm/ft ² (kg/m ²)	5.50	(26.85)	4.73	(23.09)	4.71	(23.00)
WING BOX						
FORWARD lbm (kg)	20 580(B)	(9 335)	21 609	(9,802)	21 446	(9,728)
AFT lbm (kg)	17 384	(7 885)	17 288	(7,842)	17 097	(7 755)
TIP lbm (kg)	6 964	(3 159)	5 989	(2,716)	5 963	(2 705)
FLUTTER INCR lbm (kg)	2 340(C)	(1 061)	829(C)	(376)	773(C)	(351)
ΣTOTAL lbm (kg)	47 268	(21 440)	45 715	(20 736)	45 279	(20 538)

- NOTES: (A) COMPOSITE REINFORCED SPAR CAPS; BEADED PANELS EXCEPT H/C SANDWICH TIP BOX.
- (B) SIGNIFICANT ADVANTAGE OF METAL SURFACE PANELS AND COMPOSITE REINFORCED SPAR CAPS.
- (C) SIGNIFICANT ADVANTAGE OF COMPOSITE SANDWICH APPLICATION TO THE TIP STRUCTURE; FLUTTER INCREMENT BASED ON G/ρ RELATIONSHIP ASSUMING ±45° LAYUP.

TABLE 49. FUSELAGE SHELL STRUCTURE MASS COMPARISON

MATERIAL SYSTEM:		NEAR-TERM		FAR-TERM				PERCENT CHANGE OVER NEAR-TERM
POINT DESIGN REGION	UNITS	TITANIUM 6Al-4V		BORON POLYIMIDE		GRAPHITE POLYIMIDE		
F.S. 750	lbm/ft ² (kg/m ²)	1.54	(7.52)	1.50	(7.32)	1.48	(7.22)	-3.9
F.S. 2000	lbm/ft ² (kg/m ²)	3.27	(15.96)	2.73	(13.33)	2.71	(13.23)	-17.1
F.S. 2500	lbm/ft ² (kg/m ²)	3.53	(17.23)	3.30	(16.11)	3.26	(15.91)	-7.6
F.S. 3000	lbm/ft ² (kg/m ²)	3.43	(16.74)	2.73	(13.33)	2.71	(13.23)	-21.0
WSHELL	lbm (kg)	23,148	(10,500)	20,178	(9152)	19,981	(9063)	-13.7

factors to the design results in a potential structural mass savings of approximately 10,000-lbm (4540-kg). These items alone offer significant mass payoff and improve aircraft performance for the supersonic cruise aircraft design.

A comparison of total mass trends for the far-term advanced technology supersonic cruise aircraft and the near-term aircraft is presented in Table 50. A significant improvement in the fuel fraction for the fixed-size and -takeoff mass airplane is shown for the all-composite design. The range is increased from 4183-nmi (7747-km) to an excess of 4600-nmi (8519-km), while holding the payload constant at 49,000-lbm (22,000-kg).

Another approach to exploit the mass advantages of composite application to the far-term design was to resize the airplanes to maintain a range of 4200-nmi (7778-km) with a payload of 49,000-lbm (22,000-kg). The wing loading, takeoff thrust-to-mass ratio and fuel fraction were essentially held constant. For this case, the takeoff mass is 641,500-lbm (291,000-kg) for the composite hybrid design. The wing area was reduced to approximately 9300-ft² (864-m²). As indicated in the table, the zero fuel mass was reduced to 306,046-lbm (138,800-kg) for the resized hybrid aircraft. This reduction of approximately 15-percent would result in a commensurate reduction in flyaway cost.

Advanced Technology Airplane

The final design resulting from this advanced technology assessment was a hybrid structural approach shown in Figure 62. The design makes extensive use of graphite-polyimide material system with a protective system of aluminum wire fabric and 120 glass. The chordwise-stiffened structural arrangement with the convex-beaded surface panel concept of titanium alloy Ti-6Al-4V resulted in minimum mass for the lightly loaded forward wing box structure. For the strength critical wing-aft box and stiffness designed wing-tip structure, the honeycomb-core sandwich using graphite-polyimide face skin was found to be minimum-mass. The fuselage structural arrangement is a skin-stringer-frame approach employing closed trapezoidal hat stiffeners in the centerbody and aftbody, with tee-stiffeners used in the pressure critical forebody design.

The results of this assessment have identified the potential benefits of the composite materials and fabrication technology for application to a 1990-plus start-of-design Mach 2.7 supersonic cruise transport. The impact on the airplane size and mass are significant but require further in-depth analytical and experimental studies for validation, including damage tolerance analysis.

TABLE 50. AIRPLANE MASS AND PERFORMANCE COMPARISON - ADVANCED TECHNOLOGY AIRCRAFT

TECHNOLOGY EVALUATION DATA		ADVANCED TECHNOLOGY	CONCEPT	NEAR-TERM TECHNOLOGY
		FIXED TAKEOFF WEIGHT		FIXED TAKEOFF WEIGHT
START-OF-DESIGN		FAR-TERM (1990)		NEAR-TERM (1980)
PRIMARY MATERIAL SYSTEM		Ti-6Al-4V B/PI REINF GRAPHITE/POLYIMIDE	Ti-6Al-4V B/PI REINF. GRAPHITE/ POLYIMIDE	Ti-6Al-4V B/PI REINF.
WING	STRUCTURAL ARRANGEMENT	HYBRID: CHORDWISE STIFFENED AND MONOCOQUE		
	SURFACE PANEL CONCEPT	TRAPEZOIDAL CORRUGATION AND HONEYCOMB CORE SANDWICH	CONVEX BEADED AND MC SANDWICH	
	STRUCTURAL BOX MASS lbm (kg)	45,279 (20,538)	39,316 (17,833)	47,268 (21,440)
	"FIXED" MASS (L.E., T.E., ETC.) lbm (kg)	33,041 (14,987)	28,261 (12,819)	41,352 (18,757)
	TOTAL MASS lbm (kg)	78,320 (35,525)	67,577 (30,652)	88,620 (40,197)
FUSELAGE	STRUCTURAL ARRANGEMENT	SKIN-STRINGER FRAME		MONOCOQUE
	SURFACE PANEL CONCEPT	TRAPEZOIDAL HAT STIFFENED	CLOSED HAT STIFFENED	
	SHELL MASS lbm (kg)	19,981 (9,063)	19,981 (9,063)	23,148 (10,500)
	"FIXED" MASS (FLT. STA., FAIRING, ETC.)	16,740 (7,593)	16,740 (7,593)	19,540 (8,863)
	TOTAL MASS lbm (kg)	36,721 (16,656)	36,721 (16,656)	42,688 (19,363)
ZFM, ZERO FUEL MASS lbm (kg)		334,610 (151,776)	306,046 (138,820)	361,322 (163,893)
GTM, GROSS TAXI MASS lbm (kg)		750,000 (340,194)	641,500 (290,979)	750,000 (340,194)
AIRPLANE RANGE nmi (km)		4,630 (8,575)	4,200 (7,778)	4,183 (7,747)

- NOTE: 1. ALL AIRCRAFT HAVE SAME FUSELAGE LENGTH AND DIAMETER
2. NEAR-TERM TECHNOLOGY REPRESENTS THE HYBRID ARRANGEMENT RESULTING FROM THE DESIGN CONCEPTS EVALUATION STUDY.

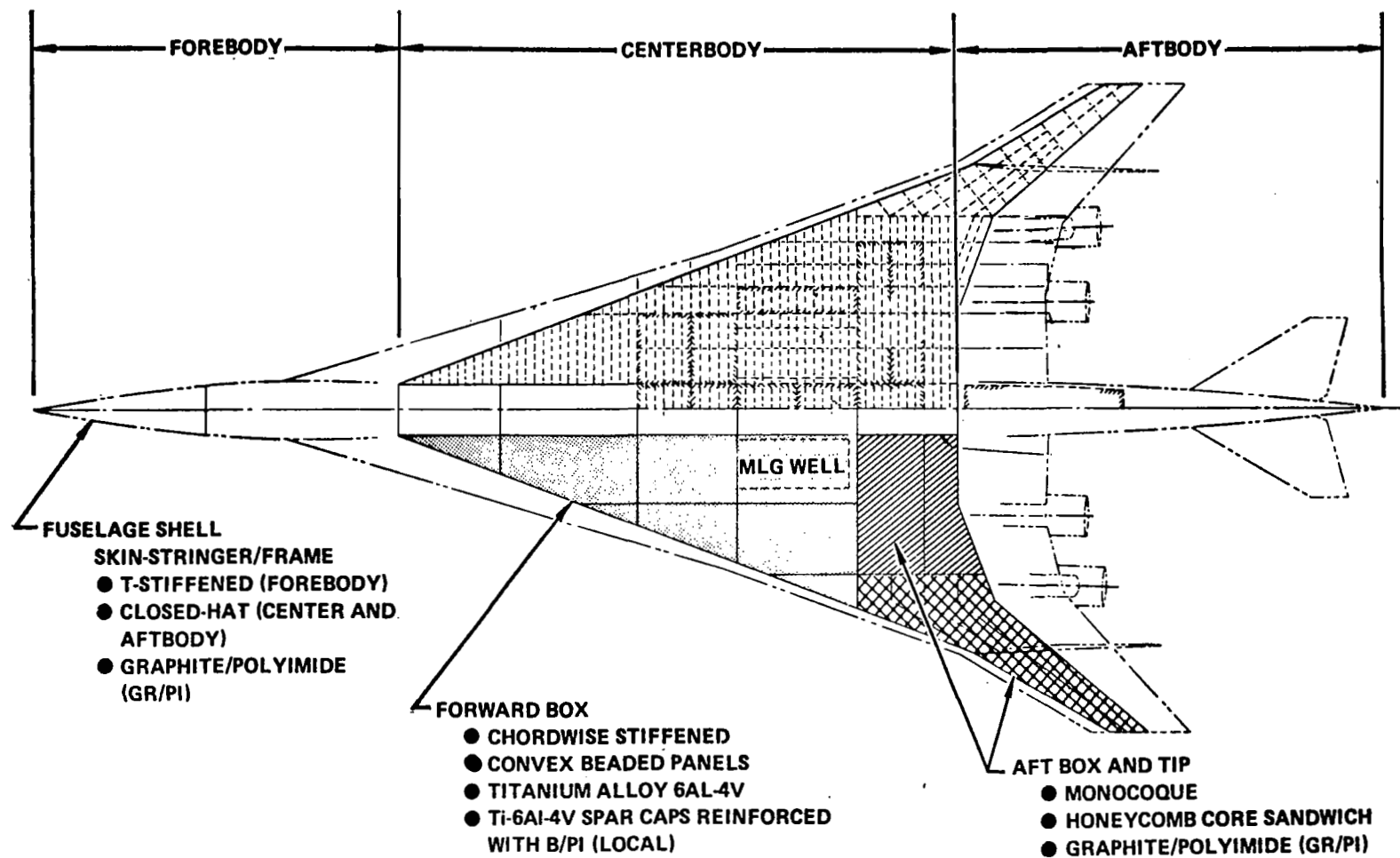


Figure 62. Advanced Technology Hybrid Structural Approach - 1990 Start-of-Design (Far-Term)

APPENDIX B

MACH 2.2 CRUISE SPEED ASSESSMENT

Introduction

Cruise speed selection is a fundamental design consideration for a supersonic cruise aircraft. To provide additional guidance to its selection for future supersonic cruise aircraft designs, an assessment was made to establish the changes to the final design airplane dictated by temperatures associated with a cruise Mach number of Mach 2.2. Final cruise speed selection is an involved process requiring an assessment of not only airplane performance, but also the technology advances required to achieve this performance, and the development costs and risk associated with these advances in the state-of-the-art. This study provided further insight into the design concept and material trends related to the reduced thermal environment at Mach 2.2, and mass estimates for modifying previous findings.

The performance attainable by operating the Mach 2.7 design aircraft at an off-design cruise Mach number of 2.2 without any physical modification to the airplane was determined. The resulting changes in operating drag levels and engine performance dictated the following design flight profile:

Dispatch mass	750,000-lbm (340,000-kg)
Block fuel	320,600-lbm (145,400-kg)
Landing mass	429,600-lbm (194,800-kg)
Reserve fuel	64,300-lbm (29,200-kg)
Zero fuel mass	365,300-lbm (165,700-kg)
Mission range	3,640-nmi (6,730-km)
Mission time	3.5-hrs
Time-at-cruise	2.6-hrs
Cruise altitude	59,750-ft (18,200-m)

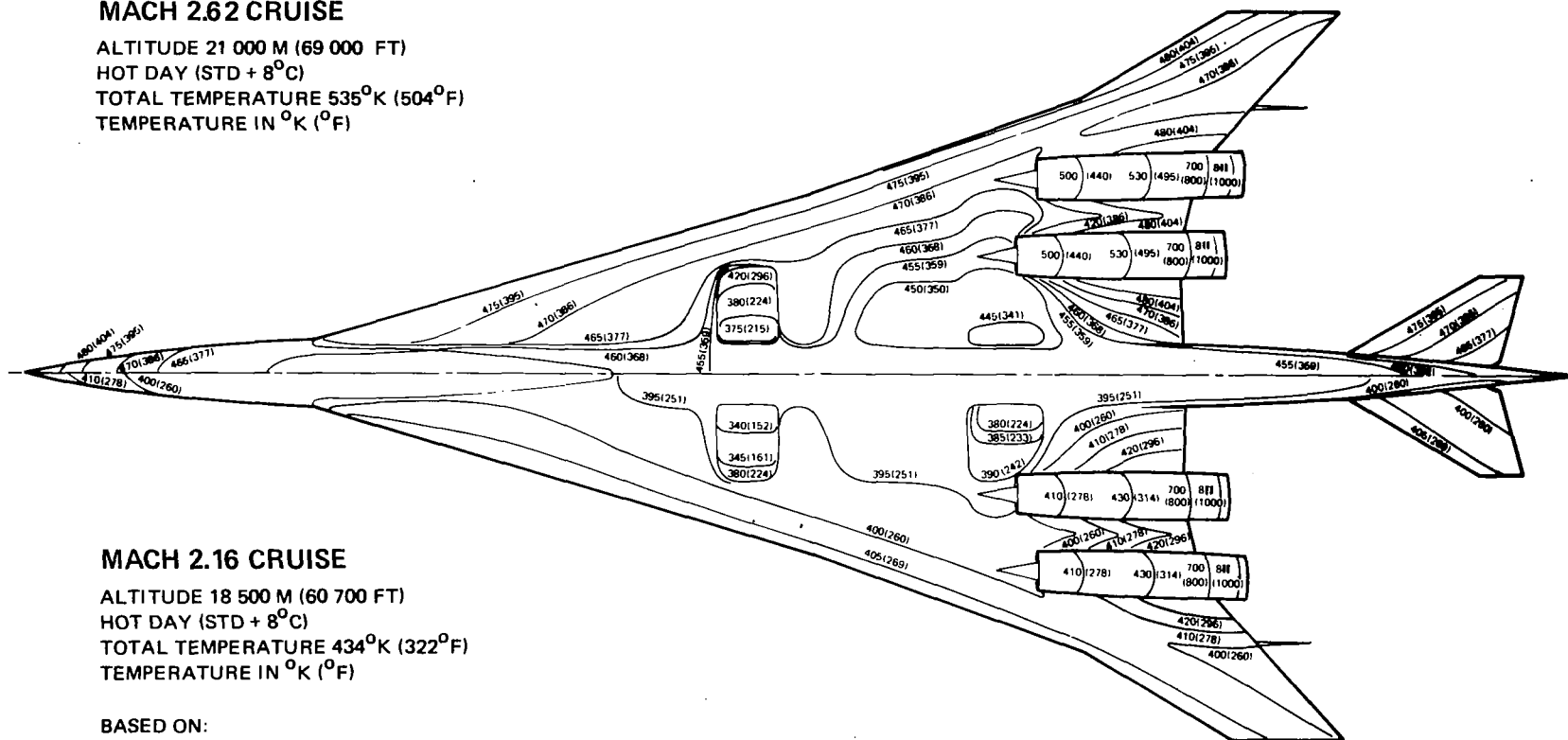
Structural Temperatures

Reducing the cruise speed from Mach 2.7 (Mach 2.62 Hot Day) to Mach 2.2 (Mach 2.16 Hot Day) provided the temperature relief indicated in Figure 63. The external surface isotherms for the airplane lower surface at both Mach 2.62 and Mach 2.16 Hot Day cruise conditions are shown.

Wing and fuselage structure temperatures were determined for selected point design regions at the following flights conditions: Mach 0.90 climb, Mach 1.25 climb, Mach 2.2 start-of-cruise, Mach 2.2 mid-cruise, and Mach 1.25 descent. The structural temperatures were used to determine the effect of a reduced thermal environment on the final design airplane structural arrangement, design concepts, materials and aircraft mass.

MACH 2.62 CRUISE

ALTITUDE 21 000 M (69 000 FT)
HOT DAY (STD + 8°C)
TOTAL TEMPERATURE 535°K (504°F)
TEMPERATURE IN °K (°F)



MACH 2.16 CRUISE

ALTITUDE 18 500 M (60 700 FT)
HOT DAY (STD + 8°C)
TOTAL TEMPERATURE 434°K (322°F)
TEMPERATURE IN °K (°F)

BASED ON:

- FINAL CONFIGURATION
- TIME = 100 MINUTES (MID-CRUISE) IN INTERNATIONAL FLIGHT PROFILE
- ALL SURFACES PAINTED
- INCLUDE FUEL, MLG COOLING EFFECTS

Figure 63. Lower Surface Isotherms - Mach 2.16 and 2.62 Hot Day Cruise

Airframe Mass Trends

The reduced temperatures at Mach 2.2 would permit the use of aluminum material. For this assessment, the use of material properties for aluminum alloy 2024-T81 was specified; the properties of this alloy are similar to aluminum alloy 2618, which is an equivalent to the British alloy RR58 used on the Anglo-French Concorde.

Analyses were made of the impact of the reduced cruise speed on the estimated mass of the final design airplane. The results of the mass analyses are summarized in Figure 64. The baseline Mach 2.7 airframe was 85-percent titanium, 5-percent aluminum, 4-percent composites, and 6-percent other materials, including steel. At a cruise speed of Mach 2.2 a significant amount of aluminum could be used, particularly in the wing and tail structure. However, as indicated in the figure, the increased use of aluminum results in an increase in structural mass.

Assuming that both the Mach 2.7 and Mach 2.2 aircraft would have the same productivity on scheduled trans-Atlantic service, then the Mach 2.2 airplane would realize higher values of utilization. To permit a fair comparison between these two airplane designs, the higher utilization airplane must be designed to have added fatigue-life so as to reflect a longer airframe-life. Specifically, since the Mach 2.7 design was designed for 50,000 hours, the higher utilization Mach 2.2 airplane must be made good for 58,000 hours. Approximately 24 percent of the baseline airframe mass was dependent upon fatigue allowables, and as a result the airframe mass increases slightly when designing to higher values of service life.

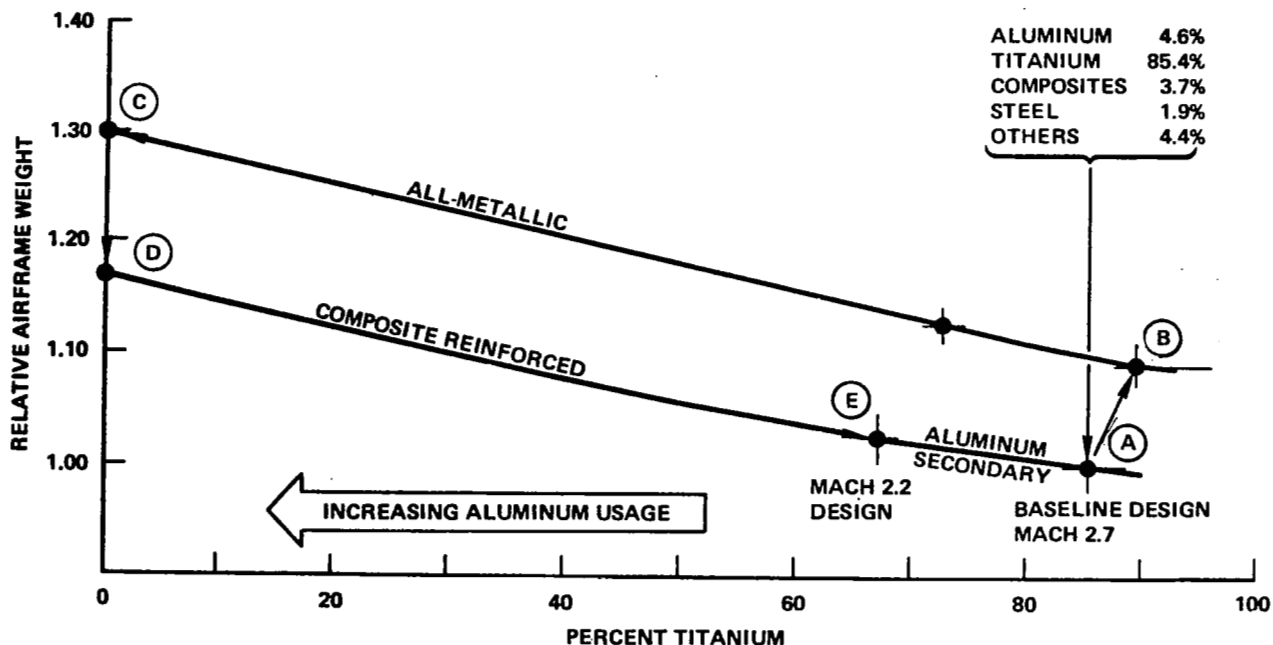


Figure 64. Airframe Mass Trends

Conclusions

The impact of using a larger percentage of aluminum and designing the airframe for a longer fatigue life was an increase in operating empty mass and takeoff gross mass. The increase in airplane design gross mass was 25,000-lbm (11,000-kg) for constant payload-range. The associated impact on airplane size and cost dictates extensive use of titanium, and of composite reinforcement of the titanium substrate. The cost effective regions for application of aluminum are in the secondary components such as the lifting surface leading and trailing edge structures. The results of the study indicated that the amount of aluminum used could be increased to 25-percent, and the amount of titanium reduced to 68-percent. With this limited use of aluminum, there is actually a slight decrease in flyaway and operating costs (2-percent). This is because of the lower material and fabrication costs for aluminum. However, this is an insignificant effect in relative cost, and indicates that there is little to be gained by reducing the cruise speed to Mach 2.2.

APPENDIX C

WING TIP THICKNESS ASSESSMENT

The wing tip of the final design airplane described in the body of this report required additional stiffening over and above that provided for strength design to meet the flutter speed requirements. This stiffening was provided primarily by increasing the thickness of the surface structure in the wing tip region, and resulted in a significant mass penalty. An alternate approach to improving the aeroelastic behavior of the wing tip, and thereby reducing the mass penalty, is to increase the depth of the wing tip structural box; with due consideration to the associated aerodynamic performance degradation due to increased wave drag.

For this assessment the wing tip box depth was increased 25- and 50-percent over the baseline design, and the resultant mass and drag increments, and their impact on range evaluated. A smooth transition was maintained with the unmodified structure inboard of BL 470. A variable thickness-to-chord ratio increase was also evaluated, from 50-percent at the tip, to 25-percent near the wing vertical (BL 600), to zero at BL 470.

The results of this study are summarized in Figure 65. The figure shows the impact of increasing the wing tip thickness on airplane range. Both the increase in range due to the reduced mass penalty, and the decrease in range due to increased drag, are indicated. The results show that if the baseline use of titanium for the wing tip structure is retained, an increase in wing tip thickness affords no significant benefits since the wave drag penalties offset the savings resulting from the reduced surface panel thickness.

Another approach to improving the aeroelastic behavior is to change the structural material. With this in mind, the use of boron-aluminum composite material for the surface panels of the wing tip, with and without increasing the box depth, was evaluated. The results of this assessment are also indicated on Figure 65 with the potential payoff highlighted by shading. The most significant improvement in performance was achieved with the application of boron-aluminum composite material on the unmodified baseline wing tip.

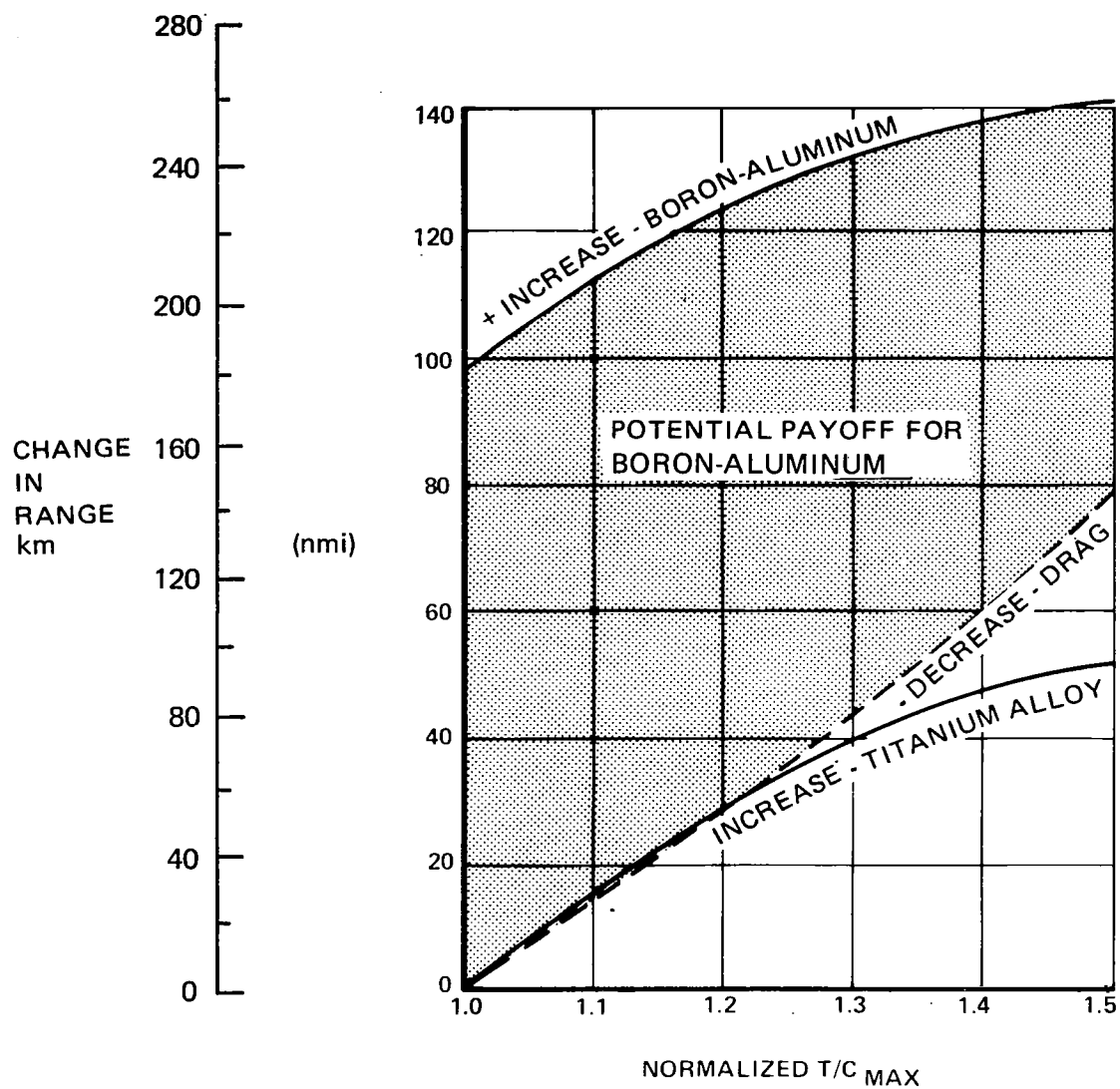


Figure 65. Impact of Wing Tip Thickness Increase on Range

REFERENCES

1. Sakata, I. F.; and Davis, G. W.: Substantiating Data for Arrow-Wing Supersonic Transport Configuration Structural Design Concepts Evaluation. NASA CR-132575-1, -2, -3, -4, October 1976.
2. Sakata, I. F.; Davis, G. W.; Robinson, J. C.; and Yates, E. C. Jr.: Design Study of Structural Concepts for an Arrow-Wing Supersonic-Cruise Aircraft. AIAA Paper No. 75-1037, AIAA 1975 Aircraft Systems and Technology Meeting, Los Angeles, California, August 4-7, 1975.
3. Van Hammersveld, John: Producibility Technology Studies - Supersonic Cruise Aircraft. 21st National SAMPE Symposium and Exhibition, Los Angeles, California, April 6-8, 1976.
4. Foss, R. L.; Zalesky, R. E.: Studies of the Impact of Advanced Technologies Applied to Supersonic Transport Aircraft. NASA CR-132618, April 1975.
5. McCulloch, A. J.; Melcon, M. A.; and Young, L.: Fatigue Behavior of Sheet Material for the Supersonic Transport. AFML-TR-64-399, Volume I, Lockheed-California Company, January 1965.
6. "Equations, Tables, and Charts for Compressible Flow," NACA Report 1135, 1953.
7. "U.S. Standard Atmosphere, 1962," U.S. Government Printing Office, Washington, D.C., December 1962.
8. Albano, E. and Rodden, W. P.: A Doublet-Lattice Method for Calculating Lift Distributions on Oscillating Surfaces in Subsonic Flows. AIAA Journal, Volume 7, February 1969, pp. 270-285; Errata, AIAA Journal, Volume 7, November 1969, p. 2192.
9. Pines, S., Dugundji, J., and Neuringer, J.: Aerodynamic Flutter Derivatives for a Flexible Wing with Supersonic and Subsonic Edges. Journal of Aeronautical Science, Vol. 22, 1955, pp. 693-700.
10. Hassig, H. J.: An Approximate True Damping Solution of the Flutter Equation by Determinate Iteration. Journal of Aircraft, Volume 8, November 1971, pp. 885-889.
11. R. F. O'Connell, H. J. Hassig; and N. A. Radovcich: Study of Flutter Related Computational Procedures for Minimum Weight Structural Sizing of Advanced Aircraft. NASA CR-2607, March 1976.
12. Lange, R. H.; Sturgeon, R. F.; Adams, W. E.; Bradley E. S.; Cahill, J. F.; Eudaily, R. R.; Hancock, J. P.; and Moore, J. W.: Study of the Application of Advanced Technologies to Long-Range Transport Aircraft. NASA CR-112088 (C), April 1971.